EXPERIMENTAL APPROACH TO OVEREXPRESS PITUATARY ADENYLATE CYCLASE ACTIVATING POLYPEPTIDE (PACAP) SPECIFICALLY IN THE HYPOTHALAMUS

by

Yamna Rahim
BSc, University of Sharjah (2014)

THESIS SUBMITTED IN PARTIAL FULFILLMENT OF
THE REQUIREMENT FOR THE DEGREE OF
MASTER OF SCIENCE IN
BIOCHEMISTRY

UNIVERSITY OF NORTHERN BRITISH COLUMBIA
February 2021

Abstract

Obesity is a detrimental health condition that occurs when energy intake, exceeds energy expenditure. Pituitary adenylate cyclase-activating polypeptide (PACAP) regulates energy expenditure, including adaptive thermogenesis, through the hypothalamic-sympathetic nervous system-brown adipose tissue axis. We hypothesize that PACAP expression in the ventromedial nucleus (VMN) is required for adaptive thermogenesis. To assess this, our goal is to develop an animal model that expresses PACAP specifically in the VMN of the hypothalamus. As a first step to achieving this goal, we established a protocol to deliver an adeno-associated virus (AAV) expressing the visible protein eGFP under the control of a VMN-specific promoter, steroidogenic factor 1 (SF1) using stereotaxic surgery. A second step was to develop a protocol to detect PACAP mRNA in the brain using *in situ* hybridization. Our results showed that the stereotaxic protocol was successful and provides significant progress towards achieving PACAP-specific expression in the VMN.

Table of Contents

List of Tables

List of Figures

List of Abbreviations

AAV	Adeno-associated virus
AgRP	Agouti-related peptide
ATP	Adenosine triphosphate
ARC	Arcuate nucleus
BAT	Brown adipose tissue
α-MSH	Alpha melanocyte-stimulating hormone
ANS	Autonomic nervous system
CMV	Cyromegalovirus
CNS	Central nervous system
CRP	Cryptic peptide
DIG	Digoxigenin
DMN	Dorsomedial nucleus
eGFP	Enhanced green fluorescent protein
FFA	Free fatty acid
GPCR	G-coupled protein receptor
HPA	Hypothalamic-pituitary adrenal axis
ICV	Intracerebroventricular
ISH	*In situ* hybridization
LHA	Lateral hypothalamic area
PACAP	Pituitary adenylate cyclase-activating polypeptide
PACAP -/-	PACAP knockout
PACAP +/+	PACAP wildtype
PBS	Phosphate-buffered saline
PC	Pro-hormone convertase
PI3K	Phosphoinositide 3-kinase
POMC	Pro-opiomelanocortin
PNS	Parasympathetic nervous system

PRP	PACAP-related peptide
PVN	Paraventricular nucleus
scAAV9	Self-complimentary adeno-associated virus serotype 9
SF1	Steroidogenic factor 1
SP	Signal peptide
SNA	Sympathetic nervous system
UCP1	Uncoupling protein 1
UTR	Untranslated region
VMN	Ventromedial nucleus

Acknowledgement

I would to like to first and foremost sincerely thank my supervisor Dr. Sarah Gray for her unwavering support throughout my studies, and for helping me academically and professionally develop myself. I am eternally grateful for the opportunity to complete my masters under her mentorship. Working in the Gray lab has been one of the most rewarding experiences of my life. She has fostered a caring environment in the lab, catered to allowing her students to focus on the development of their research skills.

I thank my committee members, Dr. Ranjana Bird and Dr. Chow Lee, for being amazing professors and being a part of my educational journey. Their constrictive feedback, guidance, and knowledge has been very helpful and supportive of my master's work. I am really appreciative of having the opportunity to hear their perspective on my research work.

I thank Sianne Vautour for taking such amazing care of the mice. I would like to thank Natalie de Brun for helping me learn how to comfortably handle the animals, and dedicating the time to practice stereotaxic surgeries with me. I thank Shelly Mcerlane from UBC for teaching me how to perform stereotaxic surgeries and understanding anaesthesia management in mice.

Finally, I would like to acknowledge my fellow Gray lab members. I thank Landon for helping me learn lab techniques. I thank Ekaterina for helping me with optimizing my antibodies and sharing her expertise in Western blot analysis. I would also like to thank Parleen, Katie, and Judy. It has been a pleasure working everyone.

Dedication

I would like to dedicate my work to family. My achievements are the result of all of their consistent support, and for that I am eternally grateful.

First and foremost, I would like to acknowledge my parents Shazia and Shahab. I would like to thank you for always helping me strive and achieve my goals, and for teaching me to never limit my dreams. I truly would not be where I am without your support. I would also like to thank my siblings Tooba, Omer, and Raed, for being my cheerleaders in life, no matter what I journey I embarked on.

I would like to thank my grandmother Zeenat. You have always been my role model. Thank you for instilling in me the value of education and self development. You always emphasize on using one's time in a productive manner, and you keep pushing me to strive for better things, and for that I am truly grateful.

I would like to acknowledge and thank my husband Moiz. Thank you being my rock throughout this journey. I am incredibly blessed to have your unwavering support through it all. You cheered me on and supported me through the ups and downs, so I thank you for believing in me and helping me stay motivated. I could not have done this without you and our son Yusuf, who is a consistent source of joy and makes everything worth it.

Chapter 1

General Introduction: PACAP and energy metabolism.

1.1 Development of obesity and its effects

Over 650 million people globally are now classified as obese, based on their height and weight, which is used to calculate body mass index (BMI) ("Obesity and overweight," n.d.). A BMI greater than 25 kg/m^2 is classified as overweight, and over 30 kg/m^2 is classified as obese. In Canada, the prevalence of obesity increased by over 6 percent between 2014 and 2018, around 7.3 million Canadian adults are now classified as obese ("Overweight and obese adults, 2018," 2019) ("Overweight and obese adults (self-reported), 2014," n.d.). An imbalance in energy metabolism causes obesity. The imbalance in energy metabolism occurs when energy intake, through caloric intake, exceeds energy expenditure, which occurs via basal metabolic rate, physical activity, and thermogenesis (Figure 1.1) (Lowell & Spiegelman, 2000a). This imbalance results in the accumulation of stored energy in the form of triglycerides in white fat, also known as white adipose tissue.

Adipose tissue is a heterogeneous organ found throughout the body. The tissue itself is composed of adipocytes, fibroblasts, macrophages, stromal cells, and preadipocytes (Vázquez-Vela, Torres, & Tovar, 2008) and is highly vascularized. There are two types of adipose tissue that play distinct roles in energy metabolism. White adipose tissue stores excess energy as triglycerides, providing a pool of stored energy released as free fatty acid (FFA) in fasting times and acts as an essential endocrine organ, producing and secreting signalling molecules that regulate energy metabolism. Brown adipose tissue (BAT) is the site of adaptive thermogenesis (Lowell & Spiegelman, 2000b) and plays a pivotal role in energy expenditure in response to cold stress and overeating. Adaptive thermogenesis is a form of biochemical thermogenesis that is activated in brown and beige adipose tissues in response to chronic cold exposure and/or overeating.

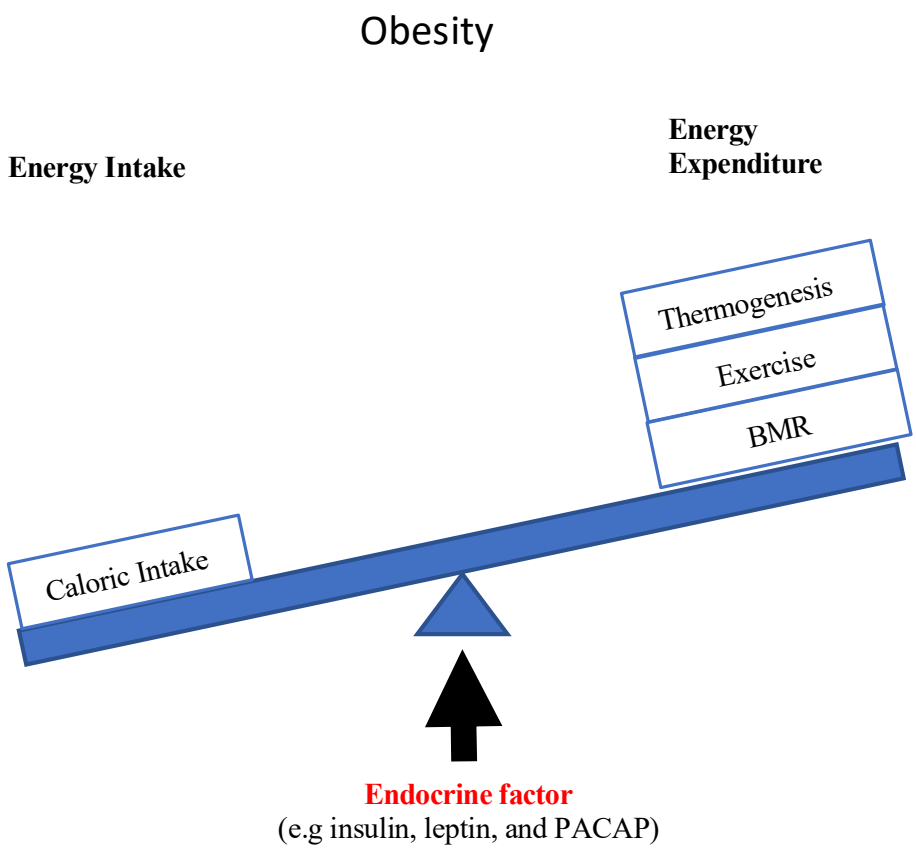

Figure 1.1. Obesity occurs due to an imbalance in energy homeostasis. When energy intake (caloric intake), exceeds energy expenditure (occurring through basal metabolic rate (BMR), exercise, and thermogenesis) it results in the development of positive energy balance, overweight or obesity. Energy homeostasis is influenced by various endocrine factors such as, insulin, leptin and pituitary adenylate cyclase activating polypeptide (PACAP).

Endocrine factors are crucial in the regulation of energy metabolism. A classic hormone involved in energy regulation is insulin. In a fed state, insulin is released by β-cells of the pancreas. Insulin travels via the portal system to bind tyrosine kinase receptors on the adipose tissue, muscle, liver and many other tissues involved in metabolism. In the adipose tissue, binding to and activation of the insulin receptors results in the activation of many signal transduction pathways, including the phosphatidylinositol 3-kinase (PI3K) pathway, for which one of the downstream effects is lipogenesis in adipose tissue. Alternately, in a fasted state, a drop in circulating insulin results in the removal of insulin's inhibition of lipolysis in adipose tissue, with an overall net effect of inhibiting lipid storage.

As mentioned previously, the adipose tissue is itself an essential endocrine organ regulating the synthesis of crucial hormones required in energy metabolism, such as leptin (Hu et al., 2018). Leptin is an adipokine released by white adipose tissues in proportion to their abundance, acting as a sensor of peripheral energy stores, through regulation of both energy intake (appetite) and energy expenditure (thermogenesis) at the level of the hypothalamus and peripherally. Leptin has potent effects on appetite regulation, and the neuronal pathways by which leptin imposes these actions are well characterized (Klok, Jakobsdottir, & Drent, 2007). Leptin binds to leptin receptors present on orexigenic neurons (neuropeptide Y (NPY) and agouti-related peptide (AgRP) expressing neurons), and anorexigenic neurons; (Pro-opiomelanocortin (POMC)) neural populations in the hypothalamus of the brain (Cone, 2005), this results in a myriad effect on energy metabolism. It results in an increased expression of anorexigenic neuropeptides; melanocortin stimulating hormone (α-MSH) derived from POMC,

and an inhibition of orexigenic neuropeptides; NPY and AgRP. Therefore, in a state of energy deprivation, leptin increases food consumption and decreases energy expenditure. Mice lacking leptin (*ob/ob* mice) or leptin receptors (*db/db* mice) are genetically predisposed to develop morbid obesity (Cohen et al., 2001; Pelleymounter et al., 1995). Leptin-deficient obese mice (*ob/ob*) present an anabolic phenotype; not only do they display increased energy intake, but they also have reduced energy expenditure in part due to dysfunctional adaptive thermogenesis in brown and beige adipose tissue (Scarpace & Matheny, 1998; Trayhurn & James, 1978).

The development of obesity is a significant risk factor for various health conditions such as cardiovascular disease, type 2 diabetes, and certain types of cancers (Van Gaal, Mertens, & De Block, 2006). Understanding the pathophysiology of obesity is therefore essential for the development of safe and effective therapies. In the past two decades, many other endocrine factors have shown to interact with and regulate sympathetic control of adaptive thermogenesis. One such neuropeptide is Pituitary adenylate cyclase-activating polypeptide (PACAP).

1.2 Discovery of PACAP

Miyata et al. discovered PACAP-38 (38 amino acid residues) in 1989. The peptide was isolated from ovine hypothalamus and was shown to regulate the synthesis of cyclic adenosine monophosphate (Miyata et al., 1989). A truncated isoform of the peptide was later discovered by the same group through fractionation as PACAP-27 (27 amino acid residues), which is generated by posttranslational processing. Both the isoforms of PACAP are encoded by the Adcyap1 gene (Oride, Kanasaki, & Kyo, 2018), and have been shown to have similar adenylate cyclase stimulating activity (Miyata et al., 1990). PACAP-38, however, is more abundantly expressed (Miyata et al., 1990). PACAP belongs to the glucagon/vasoactive intestinal (VIP) superfamily. PACAP structure has been highly conserved over the past 700 million years, sharing high

structural homology with other superfamily members, predominantly with VIP (68% homology) (McRory, Krueckl, & Sherwood, 2000). The primary structure of PACAP has been tightly conserved throughout evolution. For example, human PACAP-27 shares 100% homology with ovine and mice PACAP, and 97% homology with chicken and salmon PACA27, due to the variation of just a single amino acid (McRory et al., 2000). This high conservation across species suggests it plays a fundamental role in biological processes required for survival.

1.3 PACAP synthesis

PACAP is encoded by the Adcyap1 gene. The gene is composed of 5 exons. It consists of a 5'untranslated region (5'UTR), a signal peptide (SP), a PACAP related peptide (PRP), PACAP and a 3'UTR (McRory et al., 2000). The gene is transcribed and translated to form preproPACAP consisting of 176 amino acids in humans and 175 amino acids in mice and rats. The gene encodes four peptide sequences (Figure 1.2) (Okazaki et al., 1995). The PACAP precursor has proteolytic cleavage sites required for the post-translational modification of the precursor peptide. Signal proteases initially process preproPACAP to generate a signal peptide and pro-PACAP sequence (Hirabayashi, Nakamachi, & Shioda, 2018). The pro-PACAP sequence is then processed to PACAP-38/PACAP-27, by proteolytic cleavage proteins; prohormone convertase 1 (PC1) and prohormones convertase 2 (PC2), as is confirmed by RP-HPLC and radioimmunoassay analysis of pituitary cell extracts that were co-transfected with proPACAP and proteolytic cleavage proteases (Min et al., 1999).

1.4 PACAP receptors

Once PACAP undergoes posttranslational modifications, it mediates its effect on the target tissue through G-protein coupled receptors (GPCRs). Structurally the receptors, constitute an N-terminal extracellular domain, seven-transmembrane protein, and C terminal intracellular

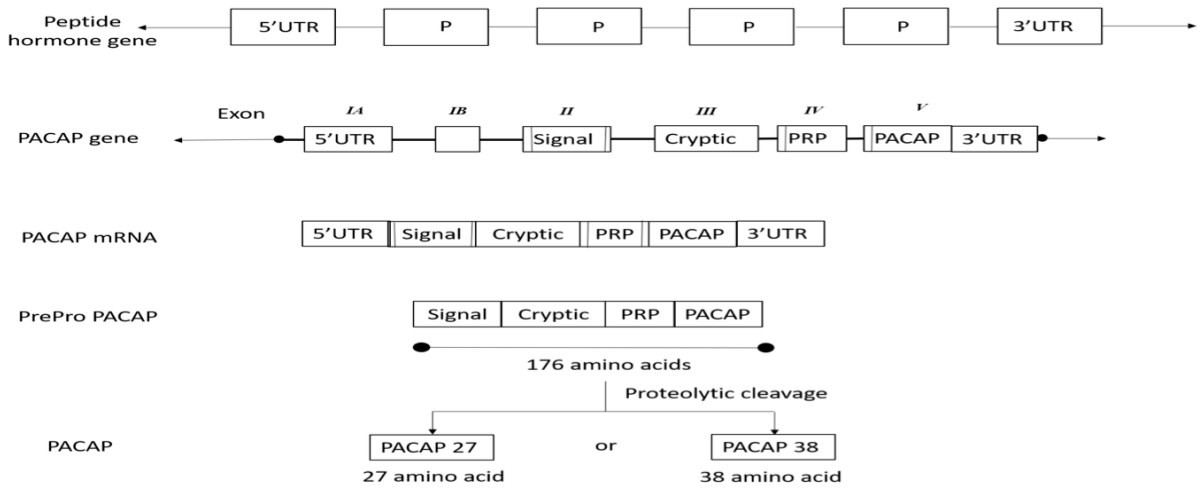

Figure 1.2:Genes encoding peptide hormones, code for single or multiple bioactive peptides (P). The gene for pituitary adenylate cyclase-activating polypeptide (PACAP), like other peptide hormone genes, encodes for multiple peptides. The PACAP gene has 5 exons consisting of; the 5' untranslated region (5'UTR), signal peptide, cryptic peptide, PACAP-related peptide (PRP), PACAP, and 3'UTR. PACAP mRNA is transcribed to a pre-proPACAP (176 amino acids). The prepro peptide is cleaved through various proteolytic enzymes to generate functional peptide; PACAP27 (27 amino acids) or PACAP 38 (38 amino acids).

domain. PACAP binds to three receptors within the GPCRs; PAC-1R, which is a PACAP specific receptor, VPAC-1R, and VPAC-2R, which have equal affinity for PACAP and VIP due to their high structural homology (Harmar et al., 2012).

PACAP receptors are coupled with Gαs and Gαq stimulatory protein. Stimulation of Gαs results in activation of adenylate cyclase, whereas stimulation of Gαq results in activation of phospholipase C. The downstream effect of both the pathways is the activation of protein kinases. In the case of Gαs, protein kinase A (PKA) is stimulated, and Gαq stimulates protein kinase C (PKC). Protein kinases are essential in the activation of various metabolic pathways through phosphorylation of target proteins. PKA, for instance, phosphorylates hormone-sensitive lipase, resulting in lipolysis (Dickson & Finlayson, 2009; Furness et al., 2012; Gray & Cline, 2019).

PACAP specific, PAC1 receptor is a highly spliced receptor. Within the receptor N-terminal and the intracellular domain of the receptor is highly spliced. The receptor's splicing is determined by the presence/absence of 28 aa cassette 'hip' and 'hop' in the intracellular domain. The splice variant of the PAC1 receptor expressed on different tissues determines the PAC1 receptor's downstream effect (Dickson & Finlayson, 2009).

1.5 PACAP and PACAP receptor expression in the hypothalamus

PACAP receptors are abundantly expressed throughout the central nervous system (CNS) and in most peripheral tissues. Research with rodents has shown that PACAP and its receptors are highly expressed in various nuclei of the hypothalamus (Hannibal, 2002; Hashimoto et al., 1996) such as the; paraventricular nuclei (PVN)(Hannibal et al., 1995), arcuate nuclei (ARC) (Segal et al., 2005), dorsomedial nucleus (DMN) (Segal et al., 2005) and the ventromedial

nucleus (VMN) of the hypothalamus (Hannibal, 2002; Segal et al., 2005) (Figure 1.3). Laser capture microdissection and cDNA analysis of gene expression in the VMN and the adjacent nuclei of the hypothalamus, such as the ARC and DMN, has shown that PACAP is highly expressed in the VMN (Segal et al., 2005).

1.6 Biological role of PACAP in regulating stress

Stress pathways are centrally regulated in order to restore homeostasis within the body when external and internal stressors disrupt or threaten to disrupt physiological balance. Stressors can be psychogenic (requiring cognitive processing, e.g. restraint stress) or physiological/metabolic (stressors which do not require cognitive processing, eg, cold, hypoglycemia) in nature (Gray & Cline, 2019).

Stressors, such as cold exposure, are detected peripherally by afferent sensory neurons, which bring information about the outside world either directly or via other regions of the central nervous system to the hypothalamus, where the information is integrated. Complex pathways extending from the hypothalamus to other areas of the central nervous system activate efferent sympathetic neurons to "turn-on" adaptive thermogenesis in BAT. The two major stress axes which respond to stress stimulation are the hypothalamic-pituitary axis (HPA) and the autonomic nervous system (ANS) (Figure 1.4). PACAP is an integral part of the regulation of both stress axes; the HPA and the SNS (Figure 1.4). Given that the sympathetic nervous system (SNS) is crucial in regulating adaptive thermogenesis in the context of energy homeostasis I will focus on PACAP's role in the SNS.

The autonomic nervous system is composed of the SNS and the parasympathetic nervous system (PNS). The parasympathetic branch of ANS deals with 'rest and digest' response,

Figure 1.3: Pituitary adenylate cyclase-activating polypeptide (P), is highly expressed in the various nuclei of the hypothalamus. The hypothalamic nuclei expressing (P) include the ventromedial nucleus (VMN), paraventricular nuclei (PVN), dorsomedial nuclei (DMH), arcuate nuclei (ARC).

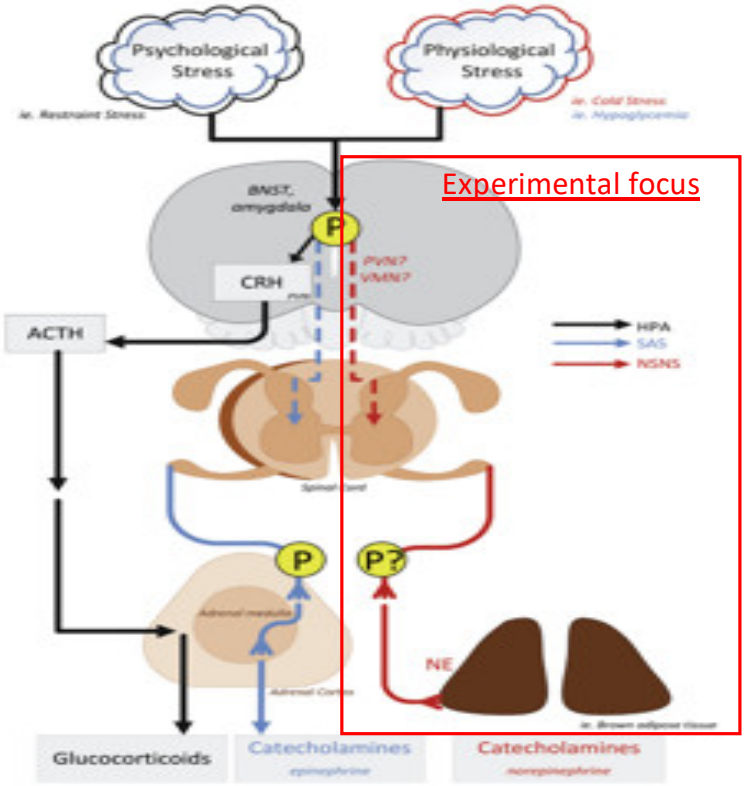

Figure 1.4: Pituitary adenylate cyclase-activating polypeptide (P) is integral in the regulation of both the hypothalamic pituitary axis (HPA), and the sympathetic nervous (SNS). In our research we focused on the role of (P) expression in the hypothalamic-SNS-brown adipose tissue axis (highlighted in red). Norepinephrine (NE) is released from post ganglionic nerve fibers in the SNS and binds to the β_3-andrenergic receptors on the brown adipose tissue inducing thermogenesis. Modified from (Gray & Cline 2019).

whereas the sympathetic nervous system responds to physiological stressors, requiring a 'flight or fight' response. Stimuli transmitted through afferent neurons are transmitted to the hypothalamus. The signals are innervated at the hypothalamus and transmitted through efferent neurons to effector organs. The SNS, for example, plays a crucial role in the activation of adaptive thermogenesis in response to cold stress, through the hypothalamic–SNS–BAT axis, where norepinephrine released from postganglionic nerves of the SNS, binds to β-adrenergic receptors on BAT (Cannon & Nedergaard, 2004) and activates lipolysis through hormone-sensitive lipase. Fatty acid released undergo β-oxidation, and uncoupling protein 1 (UCP1), a specialized protein present in the inner mitochondrial membrane of brown adipocytes, promotes uncoupling of ATP synthesis and generation of heat (Figure 1.4) (Fenzl & Kiefer, 2014; Hraton et al., 1978).

PACAP is an integral part of the regulation of both stress axes; the HPA and the SNS (Figure 1.4). The sympathetic nervous system is crucial in regulating adaptive thermogenesis. Pups lacking PACAP gene (PACAP -/-) have been shown to have lower levels of norepinephrine in BAT (Gray et al., 2002), which as discussed is required for adaptive thermogenesis at β-adrenergic receptors on BAT. The exogenous administration of norepinephrine in the absence of PACAP expression has been shown to be unsuccessful in inducing adaptive thermogenesis, associated with a decrease in expression of β-adrenergic receptors (Diané et al., 2014). As such, it is speculated that PACAP acts at both the level of the hypothalamus and within the SNS to maintain sympathetic tone and mediate β-adrenergic receptor expression in BAT in response to cold. In my thesis, I am going to focus on the effect of PACAP expression in the VMN of the hypothalamus on thermogenesis.

1.7 Role of hypothalamic PACAP in regulating energy metabolism upstream of the SNS and BAT

PACAP regulates energy metabolism downstream of leptin. Research has shown that administration of leptin in the presence of a PACAP receptor antagonist decreases the magnitude of the anorexigenic effect of leptin. In addition to this, there was a decrease in energy expenditure through thermogenesis, as measured by a reduction in core body temperature (Bechtold et al., 2006).

To decipher the central effect of PACAP in regulating adaptive thermogenesis, pharmacological studies have been conducted by independent groups working in the field of energy metabolism (Banki et al., 2014; Pataki et al., 2000; Resch et al., 2011, 2013)

Intracerebroventricular (ICV) administration of PACAP in wildtype rats (Pataki et al., 2000), and knockout mice (Banki et al., 2014), have shown that PACAP causes an increase in core body temperature in the animals in a dose-dependent manner (Banki et al., 2014; Pataki et al., 2000). In contrast, when PACAP-38 is administered intravenously, the effect on thermogenesis was negligible (Masuo et al., 1995). This work suggests the effect of PACAP is regulated at a central level rather than locally at the adipose tissue.

The VMN in the hypothalamus has a high expression of PACAP, and its receptors (Hannibal, 2002; Hashimoto et al., 1996; Segal et al., 2005). Electrical stimulation of the VMN has been shown to induce thermogenesis in interscapular BAT (Perkins et al., 1981). Administration of PACAP-38 peptide specifically into the VMN has shown to induce thermogenesis as was measured by an increase in core body temperature and increased expression of UCP1 in BAT in PACAP -/- (Resch et al., 2011, 2013) and PACAP +/+ mice (Hawke et al., 2009). Administration PACAP specific receptor antagonist PACAP-38

ameliorated the thermogenic effect of PACAP, suggesting that PACAP mediates an effect in the VMN through PAC-1R (Hawke et al., 2009).

1.8 Evidence that PACAP regulates whole animal energy balance via thermogenesis

PACAP has been shown to be involved in the maintenance of energy homeostasis. PACAP's role in regulating energy metabolism and specifically energy expenditure via thermogenesis was first observed when reserpine-induced hypothermic mice recovered from hypothermia upon intracerebroventricular (ICV) administration of PACAP-38 (Masuo et al., 1995). In 2001, genetic evidence for PACAP's role in energy metabolism and thermoregulation was shown with the observation that PACAP -/- mice survival was dependent on housing temperature (Gray et al., 2001; Gray et al., 2002). PACAP -/- pups raised at 21°C die prematurely, accompanied by a loss in core body temperature compared to wildtype mice expressing PACAP (Gray et al., 2002). When housing temperature was raised, PACAP -/- mouse survival increased (Gray et al., 2002), indicating an essential role for PACAP in cold adaptation and the maintenance of core temperature in response to cold environmental stress. Later it was confirmed that PACAP -/- mice had impaired norepinephrine-induced adaptive thermogenesis (Diané et al., 2014).

1.9 Significance of the research design and hypothesis

As discussed above, a role for PACAP in regulating adaptive thermogenesis is established. Given that thermogenesis occurring in BAT contributes to 20% of the total energy expenditure (Cypess et al., 2009; Lee, Swarbrick, & Ho, 2013), characterizing the biological mechanism regulating energy expenditure through thermogenesis is therefore essential to our understanding of energy metabolism and has the potential to identify novel therapeutic targets to combat obesity. The mechanism by which PACAP, that is abundantly expressed in the

hypothalamus, induces adaptive thermogenesis in BAT is yet to be fully elucidated. In order to better understand the role of hypothalamic PACAP in energy metabolism, the Gray lab aims to utilize their PACAP -/- mouse line to generate a transgenic mouse line that only expresses PACAP in the VMN the hypothalamus (Gray et al., 2001).

I hypothesize that PACAP expression in the VMN of the hypothalamus is required for adaptive thermogenesis. To study the overarching hypothesis, it is essential to develop a tool to express PACAP exclusively in the VMN of the hypothalamus and robustly detect this expression using sensitive and specific molecular techniques in order to provide an experimental approach for generation of the above described transgenic mouse, with the goal of rescuing the cold sensitive phenotype of PACAP -/- mice.

My research aims were:

1. Use adeno-associated virus AAV9 as a delivery tool for transgenic overexpression of PACAP or eGFP (control) specifically in the VMN of the hypothalamus.
2. Develop an *in situ* hybridization (ISH) protocol to detect transgenic overexpression of PACAP.

The research aims are divided into my thesis chapters and will be discussed in detail in Chapter 2 and 3. The results from the preliminary data of these chapters will contribute to future physiological studies conducted in the lab, to decipher the effect of PACAP expression in the VMN on thermogenesis.

Chapter 2

Delivery protocol of adeno-associated virus 9 (AAV9) for transgenic overexpression of PACAP or eGFP specifically in the ventromedial nucleus of the hypothalamus

2.1 Introduction

The hypothalamus is a critical regulatory center within the brain that controls many endocrine regulated processes such as reproduction, growth, stress response, and energy metabolism. The hypothalamus is a small yet complex structure; it is organized into nuclei that are made up of a collection of neurons. Broadly the hypothalamus is divided into three major regions; the anterior (prechiasmatic region), medial (tuberal area), and posterior region (Gabriela et al., 2018). The anterior hypothalamus is involved in reproduction and cardiovascular control. The medial region is involved in energy metabolism through regulation of appetite and energy expenditure, including thermogenesis and activity. The posterior hypothalamus regulates various functions such as memory, learning, and blood pressure (Gabriela Pop et al., 2018). In this chapter, I will focus on the medial hypothalamus.

The medial hypothalamus is composed of various nuclei that are integral in restoring homeostasis, such as the arcuate nuclei (ARC), lateral hypothalamus (LH), paraventricular nuclei (PVN), and ventromedial nuclei (VMN) (Figure 1.3). The nuclei function in a coordinated manner and have overlapping roles. Our current understanding of the function of the different nuclei in energy metabolism comes from studies, where the effect of disruption of an entire nucleus within the hypothalamus, through lesioning or pharmacological and genetic manipulation, is used to decipher the function of said nuclei in regulating energy expenditure.

Historically crude lesioning of the VMN was done, which provided strong evidence for the role of VMN in energy metabolism (Monda, Sullo, & De Luca, 1997). Studies have shown that impaired VMN function in rodents due to physical lesioning of the VMN (Monda et al., 1997), or via the use of neurotoxin, colchicine (Choi & Dallman, 1999) results in morbid obesity compared to control rats with a functional VMN (Choi & Dallman, 1999; Monda et al., 1997).

The increase in body weight is approximately eight times more than in control rats due to decreased sympathetic nerve stimulation of the BAT and an increase in appetite (Monda et al., 1997). Additionally, the VMN nuclei is integral in lipid handling in the adipose tissues, as VMN lesioned rats undergo lipolysis at a much lower rate, as measured by a low level of serum-free fatty acid compared to control rats (Nishizawa & Bray, 1978). Conversely, electrical stimulation of the VMN, as discussed in Chapter 1, has shown to induce adaptive thermogenesis in interscapular BAT (Perkins et al., 1981). These studies have highlighted a role for the VMN in regulating thermogenesis in response to cold stress, which results in SNS activation of lipolysis in BAT to fuel adaptive thermogenesis via uncoupling protein 1 (UCP1).

The results from these studies have been integral in our understanding of the role of VMN in energy metabolism. However, the specific mechanisms, including the neuroendocrine factors involved in VMN regulation of adaptive thermogenesis, is complex and not well understood. There are various endocrine factors within the VMN that are essential in regulating energy metabolism, such as leptin and PACAP. The VMN has abundant expression of leptin and PACAP and their receptors (Bingham et al., 2008; Hannibal, 2002; Segal et al., 2005). As discussed in Chapter 1, leptin is a well-established endocrine factor involved in regulating appetite and energy expenditure. Deletion of leptin receptors in the VMN is associated with a significant increase in body weight in response to a high fat diet, in comparison to wildtype mice that retain leptin receptor expression, due to impaired adaptive thermogenesis in the mice lacking leptin receptors in the VMN (Bingham et al., 2008). Central administration of leptin, in rats with a lesioned VMN, does not alleviate the impairment in adaptive thermogenesis, as validated by BAT, UCP1 expression, which doesn't increase in response to leptin treatment (Choi et al., 1999). This suggests that the VMN is required for leptin-induced effect on adaptive

thermogenesis. Other studies suggest there are neuropeptides that function downstream of leptin to modulate the VMN-SNS-BAT axis. One such peptide that has been shown to be highly expressed in VMN and able to contribute to SNS activation via the hypothalamus is PACAP (Hawke et al., 2009; Tanida et al., 2013). Administration of leptin in the VMN in the presence of PACAP receptor antagonist, which when applied to VMN prior to VMN-specific injection of leptin prevented leptin from inducing adaptive thermogenesis in BAT (Hawke et al., 2009). These pharmacological studies (Hawke et al., 2009; Tanida et al., 2013) suggest PACAP functions downstream of leptin to regulate adaptive thermogenesis and is an essential peptide required for normal adaptive thermogenesis (Diane et al., 2014).

As detailed in Chapter 1, PACAP is crucial in regulating energy expenditure (Diané et al., 2014; Gray et al., 2002). PACAP -/- mice have a temperature sensitive phenotype in response to cold stress (Gray et al., 2002). In the sympathoadrenal synapse of the sympathetic nervous system, PACAP is known to regulate the SNS which is hypothesized to occur in other areas of the nervous system. PACAP is expressed in various nuclei of the hypothalamus in compliance with its role in the regulation of energy expenditure. The nuclei that have a high expression of PACAP include the ARC, PVN, and VMN. However, the VMN has a marginally high expression of PACAP compared to other nuclei (Hannibal, 2002; Hashimoto et al., 1996; Segal et al., 2005). Pharmacological studies have shown that overexpression of PACAP specifically in the VMN results in an increase in core body temperature due to adaptive thermogenesis as verified by an increase in UCP1 expression (Resch et al., 2011, 2013).

Pharmacological studies involve delivering PACAP peptides to induce and confirm the effect of PACAP on thermogenesis. These studies are critical in our understanding of the neurocirculatory effect of PACAP in inducing thermogenesis in BAT. However, these studies

rely on pharmacological doses of PACAP to induce a response which may not be reflective of normal physiology, where the endogenous expression PACAP will produce nanomolar concentrations of PACAP, released very specifically at the neuronal synapse of select neurons. Endogenously, the half-life of the PACAP peptide is short as the peptide is degraded by proteases, such as dipeptidyl peptidase IV (Zhu et al., 2003). Pharmacological studies, show that the effect of PACAP peptide delivered centrally on thermogenesis does not persist over 18 hrs (Hawke et al., 2009; Resch et al., 2011). In pharmacological studies, the delivery of peptide at high concentrations or as a single dose, do not accurately reflect the half-life kinetics of PACAP and thus also impact the translatability of results to normal physiology. For instance, in mice it takes three to five weeks of acclimatization to cold stress to fully 'turn on' adaptive thermogenesis (Virtue & Vidal-Puig, 2013). As such, pharmacological studies are limited in their ability to provide a regulated and persistent peptide presence. To overcome these challenges, we propose an alternate approach, using a genetic model of PACAP expression. Genetic approaches of peptide expression aim to induce near the endogenous expression of the peptide, driven by a promotor that will provide a physiological level of expression in a tissue or cell of interest. Additionally, it provides continual, long-term expression of the peptide, which is critical when studying complex physiological processes over time, or in response to a changing environment.

To successfully express peptide hormones using a genetic approach, there are three key factors that need to be taken into consideration for targeting specific expression of the peptide. The factors include; 1. The model used for gene delivery, 2. The promoter used to drive expression of the peptide coding sequence, 3. The delivery technique used to administer the expression vector.

Model for delivery: self complimentary adeno associated viruses

Self complimentary adeno-associated viruses (scAAV) are robust tools for transgenic overexpression of a desired gene as they preferentially infect different tissues, so can be selected to promote tissue specificity of expression and they provide sustained gene expression (Flotte & Carter, 1999; Wang, Tai, & Gao, 2019). The scAAV vector replicates independently of the host genome (Naso et al., 2017). Different serotypes of the AAV exist, which supports targeted delivery. To date, 13 serotypes of AAV have been identified, defined by variation in the capsid structure, which influences binding affinity of the virus to endogenous receptors in a tissue-specific manner (Samulski & Muzyczka, 2014). AAV serotype 9 (AAV9) binds to N-terminal galactose on neuronal tissues, it is used for targeted delivery and gene expression in the central nervous system (CNS) as it is able to cross the blood brain barrier (Lukashchuk et al., 2016; Murlidharan, Samulski, & Asokan, 2014), and relative to other serotypes, it is more efficiently expressed in neuronal tissues (Dayton, Wang, & Klein, 2012).

Promoter: Targeted expression in the VMN using the steroidogenic factor 1 promoter

The AAV9 vector can accommodate 5 kb of genome (Wang et al., 2019). The genome contains a promoter sequence, coding sequence for the gene of interest, additionally the genome contains ampicillin resistant gene and an origin of replication. Selection of the promoter region is critical to successfully achieving desired expression of the gene of interest, which may include tissue-specific expression. My goal is to induce PACAP expression only in neurons of the VMN in mice lacking PACAP in all cells of the body (PACAP-/- mice), and therefore identified a promoter that is uniquely expressed in the VMN in the CNS and developed a protocol for delivery only to the CNS. While peripherally steroidogenic factor 1 (SF1) is expressed in the

adrenal gland and gonads (Ikeda et al., 1995a), within the CNS, it is exclusively expressed in the VMN (Ikeda et al., 1995a).

Mice lacking SF1 (SF1 KO), do not develop a normal VMN due to a disruption in the nuclear organization of the VMN. Other nuclei of the hypothalamus however, develop normally (Ikeda et al., 1995a; Majdic et al., 2002). Due to impaired VMN development, SF1 KO mice develop obesity compared to wildtype mice (Majdic et al., 2002). SF1 neurons express leptin receptors, and deletion of leptin receptors specifically in SF1 neurons (SF1-cre-lepr$^{flox/flox}$), results in obesity, as verified by increased fat mass (Dhillon et al., 2006). SF1 neurons in the VMN are therefore critical in regulating in energy expenditure. SF1-cre-lepr$^{flox/flox}$ mice have significantly lower expression of PACAP in the VMN compared to wildtype mice (Hawke et al., 2009). Compounding evidence suggests that all SF1 neurons in the VMN express PACAP mRNA (Hawke et al., 2009), which is essential for regulating energy metabolism.

Delivery technique: Stereotaxic surgery

Specific delivery of AAV9-SF1-PACAP to the CNS, is achieved through the use of stereotaxic surgery. Stereotaxic injection procedures require meticulous techniques to be developed to deliver very small volumes ($\leq$2ul) of pharmacological agents or expression vectors to a minute region in the brain in anaesthetized animals (Carter & Shieh, 2015). In our study, we aim to deliver AAV9-SF1-PACAP specifically to the VMN, a minute structure within the hypothalamus located deep within the midbrain. To target the VMN, the anatomical landmarks; bregma (intersection between sagittal and coronal sutures) and lambda (intersection between sagittal and lambdoid sutures) on the skull of the rodent is used in conjunction with coordinates suggested from a brain atlas to precisely inject the expression vector in the target nuclei (Carter & Shieh, 2015). The combination of the targeted injection and the VMN-specific promoter, SF1,

is designed to increase the likelihood of achieving VMN-specific expression of PACAP in PACAP-/- mice.

We hypothesize that PACAP expression in the VMN is essential for the induction of adaptive thermogenesis in response to cold stress. As such we propose that overexpression of PACAP specifically in the VMN, using AAV9-SF1-PACAP coupled with VMN-targeted injections is a robust transgenic model to test this hypothesis. As such in this Chapter, I will focus on the following aims:

1. Develop a protocol to deliver adeno-associated virus (AAV9-SF1-PACAP) using stereotaxic surgery and injections targeted at coordinates for the VMN of the hypothalamus. A control expression vector, AA9-SF1-eGFP will be used initially to visually confirm the specificity of expression in the VMN.
2. Develop a sensitive and specific protocol to validate the expression of eGFP induced by AAV9-SF1-eGFP virus in the VMN, using immunohistochemistry targeting eGFP and SF1. Overlap in the expression of eGFP and SF1 protein will validate targeted delivery protocols.

2.2 Material and methods

Animal

An adult (12-week old) PACAP +/+, C57Bl/6 mice was used for the study. The mouse was obtained from a PACAP -/- mice line that was previously generated by (Gray et al., 2001) which were then backcrossed to C57Bl6 mice to source the mouse used. The mouse was housed at the University of Northern British Colombia at room temperature (24°C) on a corn cob bedding. The mouse had free access to chow diet (LabDiet 5001, lab diet, Inc., Brentwood,

Leduc, AB, Canada, metabolized energy 3.02 kcal/g). The animals were kept at a 12-hr light/dark cycle and were weighed twice a week as an assessment of general health. The protocol for this study has been approved by University of Northern British Colombia's Animal Care and Use Committee.

Designing AAV-9-SF1-eGFP plasmid

Self-complementary (sc) scAAV-SF1-eGFP plasmid was developed by previous members in the Gray lab as follows:

scAAV-CMV-eGFP plasmid developed by John T. Gray was obtained from Addgene Plasmid #32396 (Watertown, MA, USA). The plasmid was packaged in *Escherichia coli,* and was received as an agar stab. The plasmid was cultured and isolated. The cytomegalovirus (CMV) promoter in the plasmid backbone was removed using restriction enzyme digestion and was replaced with 3706 - 4095 bp of the SF1 promoter (Figure 2.1) The SF1 promoter fragment was amplified in pGEM-T vector (Promega, Madison, WI). scAAV-SF1-eGFP was packaged into AAV serotype 9 virus (Vigene Biosciences, Inc., Rockville, MD). scAAV9-SF1-eGFP virus received from Vigene was stored at a concentration of 2.14×10^{14} viral genome/ml at -80°C (McMillan, 2017).

Stereotaxic surgery: Delivery of adeno-associated virus, AAV9-SF1-eGFP

The protocol for stereotaxic surgery was adapted and modified as per the recommendation of a previous Gray lab member (Cline, 2020). In this previous work by Cline, the selected stereotaxic coordinates resulted in expression of scAAV9-SF1-eGFP plasmid 0.025 mm anterior to the VMN, in addition the concentration of the virus delivered was high, resulting in leakiness of the virus (2020). As such, I adjusted the depth of the Hamilton syringe needle from the brain surface, and the concentration of the virus. A 1:10 dilution (2.14×10^{13} viral genome/ml) of the virus was administered using stereotaxic surgery as detailed below. Mock

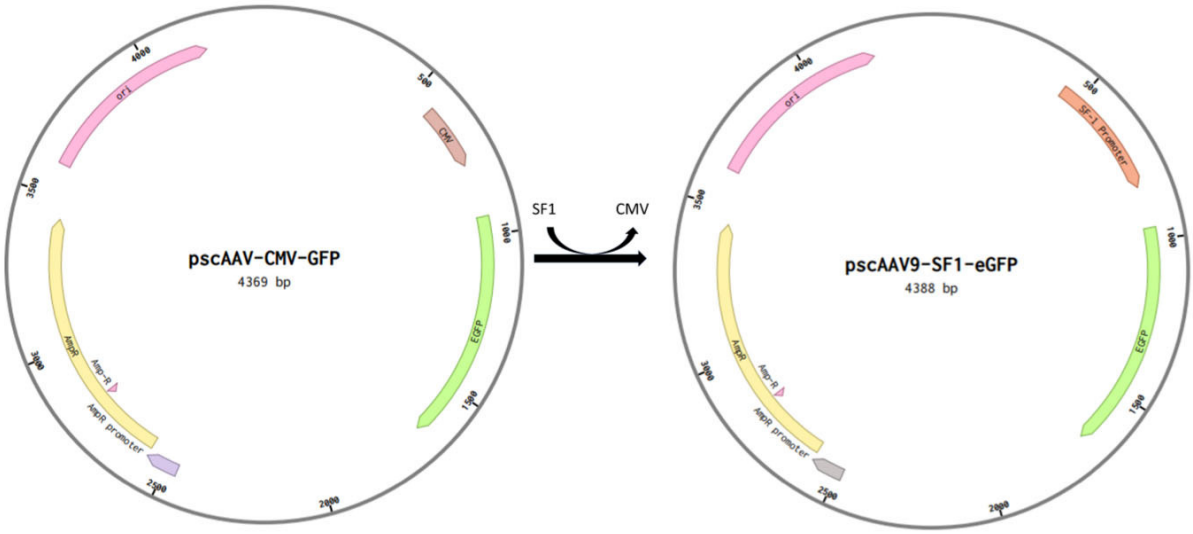

Figure 2.1: Development of adeno-associated virus stereotype 9-steroidogenic factor1-green fluorescent protein (pscAAV9-SF1-eGFP). Cytomegalovirus (CMV) promoter, in self-complimentary pscAAV-CMV-eGFP was removed using restriction enzymes. The promoter was replaced by steroidogenic factor 1 (SF1) promoter. The plasmid was packaged in AAV serotype 9 virus and delivered specifically to the VMN. The diagram has been adapted from (Cline, 2020).

surgeries were performed using PBS dyed with food coloring to establish anesthesia management techniques and to ensure the needle did not penetrate the brain with the new revised coordinates without the virus, which adds biosafety concerns and cost implications. Following the mock surgeries mice were immediately euthanized post stereotaxic procedure using an ultra-high dose of sodium pentabarbital, and brain tissue was collected, and coronal section was cut to assess the brain (Figure 2.2).

The mouse was prepared for surgery by shaving the fur around the head, and the mouse was weighed to calculate the dose of injectable anesthetics. The mouse was anaesthetized under 5% isofluorane, 1.5 L/min O_2. Once the mouse had lost its righting reflex and the breathing had slowed and become regular, the isoflurane delivery was decreased to 3%, 1.5 L/min O_2. The mouse was subcutaneously administered anesthetics; 12.5 mg/kg ketamine, and 0.05 mg/kg dextomatidine. In addition, two analgesics were administered: 0.05 mg/kg buprenorphine, and 2.5 mg/kg meloxicam. Ringer lactate solution (1.6 ml) was administered to maintain hydration.

The mouse was transferred to a stereotaxic framework equipped with a nose cone for administration of inhaled anesthetics. Isoflurane was adjusted to 2% isoflurane, 2.5 L/min O_2 to maintain the mice under surgical plane. Toe pinch was done to ensure loss of pedal reflex, to confirm the mouse was under a surgical plane. Rectal probe and a heating pad were used to assist with monitoring and maintaining body temperature. Ear bars were inserted in the bullae of the mouse's ears; the snout was tapped lightly to ensure the head was unable to move laterally and was secure. The surgical site was cleaned using chlorohexidine and 70% isopropyl alcohol. Prior to making an incision, 8 mg/kg buvipicane, was subcutaneous administered as a local analgesic. The surgical site was disinfected with chlorohexidine and 70% isopropyl alcohol, before making

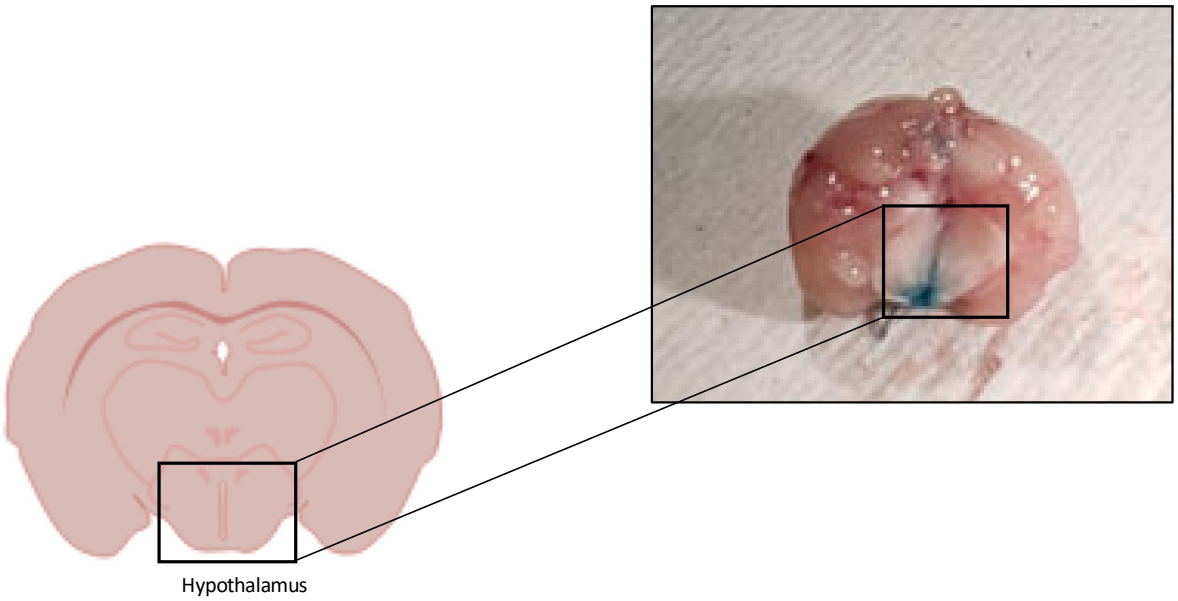

Figure 2.2: Stereotaxic mock surgeries were performed using blue dye. A blue dye was injected in a anaesthetized C57Bl6 mouse using the following coordinates: -1.46 posterior from bregma, 0.39 lateral from lambda. Coronal sections of the brain were used to assess successful delivery of the dye at the base of the hypothalamus. The image on the left is a diagrammatized depiction of a coronal section of the mouse brain. The image on the right is a representative image of a mouse brain injected with blue dye.

a small incision on the center of the head. Throughout the surgery the surgical site was flushed with lactate ringer solution to prevent the skull from drying out.

The skull was leveled using a micro positioner arm on the stereotaxic framework, such that lambda and bregma on the skull were at the same height on the stereotaxic framework (Figure 2.3). Using a 0.039'' drill bit (ball mill carbide) the skull wall drilled using the following coordinates: 1.46 mm posterior from bregma, 0.39 mm lateral from midline. scAAV9-SF1-eGFP virus 2.14 x 10^{13} viral genomes/ml was injected from a 1 µl Hamilton syringe (25 G, 2.75'' needle length, 7000 series) lowered to 5.72 mm from the brain surface. The needle was lowered into the brain at a rate of 1 mm/min and 1 ul of virus (2.14 x 10^{13} viral genomes/ml) was injected over a span of 5 minutes. The needle was held in position in the brain for an additional five minutes following injection to allow for the virus to diffuse, the needle was then withdrawn over a span of 30 seconds.

The surgical site was sutured using a 5-0 polygylcan suture, under a sterile drape created using press n seal food wrap (Glad). The mouse was then withdrawn from the ear bars and was assessed for any damage in the ears. Lidocaine cream was applied over the skull. The mouse was then allowed to recover from anesthesia over a heating pad, until it gained consciousness and was able to walk in a coordinated manner. The mouse was kept on a heated rack (30°C) post-surgery for 3 days to assist with recovery. To manage pain due to the surgical procedure, the mouse was administered 0.05 mg/kg buprenorphine twice a day for 48 hrs post-surgery. The weight (g) of the mouse was measured daily, and activity level and general well-being was visually assessed (using the grimace scale) to evaluate recovery. Sample collection was done two weeks post-surgery to ensure complete expression of viral vector.

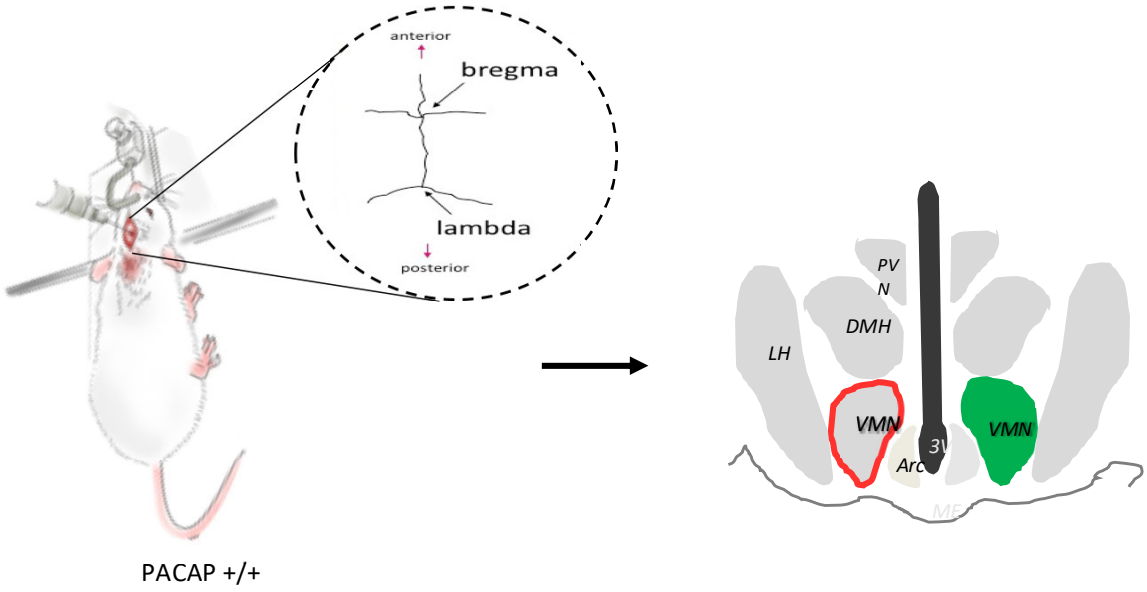

Figure 2.3: Representation of the delivery of adeno-associated virus serotype 9-steroidogenic factor1-green fluorescent protein (scAAV9-SF1-EGFP). The anaesthetized mouse was placed in a stereotaxic framework to conduct the surgery. Bregma and Lambda were used as landmarks to deliver the virus. In order to deliver the virus specifically to the ventromedial nucleus of the hypothalamus (VMN) the virus was delivered 1.46 mm posterior from bregma and 0.39 mm lateral from midline.

Collection of brain tissue

The mouse was anaesthetized under 5% isofluorane, 0.8 L/min O_2. Once the mouse was under a state of surgical plane (as assessed by loss of pedal reflex), the isofluorane was decreased to 3% isofluorane, 0.8 L/min O_2. Before fixing the tissues for sample collection a cardiac perfusion was conducted. The heart was exposed by dissection without damaging any major vessels of the circulatory system. The right atrium of the heart was punctured to disrupt the closed loop of the circulatory system. Then 10 ml 0.5% heparin in 1X PBS was perfused through the circulatory system using ½'' 25G needle into the left ventricle of the heart to remove red blood cells, which could disrupt tissue imaging due to autofluorescence. The heparin prevented clotting. Once the liver turned white, which was indicative of a successful perfusion, the needle was withdrawn from the left ventricle of the heart. To fix the tissues 10 ml of 4% paraformaldehyde (1X PBS, pH 7.2) was perfused through the circulatory system using a ½'' 25G needle, into the left ventricle. Once the fixed brain tissue was collected it was stored in 30 ml of 4% paraformaldehyde overnight at 4°C. The sample was then transferred to 30 ml of 30% sucrose for cryoprotection.

Sample preparation

A fixed brain sample from the wildtype mouse that had undergone stereotaxic surgery was sent for cryosectioning to Wax-It Histology (Vancouver, BC, Canada). Coronal sections (10 μm) of the brain tissue were made in the region that was inclusive of the VMN of the hypothalamus, in addition sections were cut anterior and posterior to the region of interest to ensure there was no off-target expression of scAVV9-SF1-eGFP. All brain sections obtained from this region in the wildtype brain are known to express SF1 (Ikeda et al., 1995a). A total of

30 slides were obtained that were inclusive of the VMN of the hypothalamus. Two brain tissues were mounted per slide and stored at -80°C until it was used for analysis.

To assess expression of eGFP the brain sections were counterstained with DAPI and were incubated at 4°C overnight, prior to imaging. Representative images were taken at 10X magnification on a DAPI filter at an exposure of 109.85 ms, and eGFP filter at an exposure of 3.95 s (Carl Zeiss Microscopy GmbH, Jena, Germany) and the images were tiled and stitched.

Confirmation of SF1 antibody integrity: Immunohistochemistry

Prior to conducting immunohistochemistry, the slides from a wildtype mouse brain containing sections from the hypothalamus were thawed at room temperature (RT) for 20 mins. The slides were then washed in 1X PBS for 10 mins at 450 RPM in a shaking water bath. The tissues were permeabilized using 0.3% Triton X-100 (diluted in 1X PBS). Times of 10 to 20 mins were attempted to optimize tissue permeability. To prevent high background staining, the slides were incubated in a protein block (Dako) for 45 mins to 1 hr 15 mins in a humidity chamber, at RT prior to incubation with the primary antibody. To one of the two brain sections on the slide, 200 µl anti-SF1 antibody was added (1:250 -1:1000 in Dako diluent (catalog number: PA5-41967, Thermofisher scientific, Rockford, USA) at 4°C o/n. The other brain section was used as a control and was incubated in Dako diluent only with no 1°antibody added. The sections were either washed with 0.1% triton X-100 for 10 mins prior to washing then samples in 1XPBS or directly washed thrice in 1X PBS with 450 RPM agitation, for 10 mins each time. Goat anti-rabbit IgG antibody (200 µl) fluor 594 (1:1000 – 1:2000) (Abcam, Burlingame, CA, USA) was added to the samples and the slides were incubated at RT for 1 hr. The slides were then washed thrice in 1X PBS. The sections were counterstained with DAPI nuclear stain and incubated at 4°C o/n, prior to imaging. Representative images were taken at 4X

magnification (Olympus, Richmond Hill, ON, Canada). Images were acquired on the DAPI channel at an exposure of 713.2 ms. Slides were imaged using TEXRED channel to acquire SF1 expression under 7.7 s exposure. At this stage, the experiment was conducted on a brain isolated from wildtype mouse, and thus eGFP expression was not acquired.

Confirmation of SF1 antibody integrity: Western blot

The following tissues were previously isolated from a wildtype mouse in the Gray lab and stored at -80^{o}C; brain, adrenal gland, brown adipose tissue. The specificity of three different antibodies for the SF1 protein was assessed using Western blot analysis. The antibodies used were an SF1 antibody from Thermofisher Scientific (catalog number: PA5-41967, Rockford, USA), an antibody named PCRP-NR5A1-1A4-s from the Developmental Studies Hybridoma Bank (IOWA, USA), and an antibody named NR5A1 from Thermofisher Scientific (catalog number: 434200, Rockford, USA). A standard Western blotting protocol was followed as detailed below. Modifications to the protocol were made with each antibody to achieve optimal signal, as detailed in table 2.1.

For the purpose of this study, protein isolated from the hypothalamus and adrenal glands were used as positive control samples, as these tissues are known to express SF1. The cortex of the brain, brown adipose tissue and liver (for PCRP-NR5A1-1A4-s Ab) were used as negative controls, as SF1 is not expressed in these tissues.

Tissues were chilled in liquid nitrogen, ground using a mortar and pestle and suspended in cocktail RIPA buffer, EDTA, phosphate inhibitor (100:1:1 Catalog no. 89900, Thermo Fisher Scientific, Waltham, USA). The tissues were suspended in RIPA buffer (150 µl – 500 µl).

Table 2.1: Western blot analysis using different steroidogenic factor 1 (SF1) antibodies. Western blot analysis was done using three different antibodies. Protein was isolated from; the hypothalamus, adrenal, interscapular brown adipose tissue (iBAT), cortex, and liver. Various concentrations of protein (µg) were loaded on membrane and blotted with primary antibody o/n at 4^{o}C. The membrane was then blotted with secondary antibody for 2 hrs at room temperature.

SF1 Antibody used	Protein source	Concentration of Protein loaded (µg)	Concentration of primary antibody	Secondary antibody used	Concentration of secondary antibody	Duration of membrane exposure (min)
SF1 antibody*	Hypothalamus	10 - 40	1:5000	Goat-mouse IgG antibody horse radish peroxidase	1:5000	1
	Adrenal	20				
	iBAT	10 - 20				
	Cortex	10 - 40				
PCRP-NR5A1-1A4-s**	Hypothalamus	10 – 40	1:50		1:5000	1
	Adrenal	20				
	iBAT	10 – 20				
	Cortex	10 - 40				
NR5A1***	Hypothalamus	50 -75	1:500		1:10000	1
	Adrenal	50				
	iBAT	50				
	Cortex	50 - 75				
PCRP-NR5A1-1A4-s**	Hypothalamus	50	1: 2000	Goat anti-mouse IgG1 cross-adsorbed secondary antibody	1:1000	0.43
	Adrenal	50				
	iBAT	50				
	Cortex	50				
	Liver	50				

* SF1 antibody (catalog number: PA5-41967, Thermofisher scientific, Rockford, USA)
** PCRP-NR5A1-1A4-s (Developmental studies Hybridoma bank. IOWA, USA)
*** NR5A1 antibody (catalog number: 434200, Thermofisher scientific, Rockford, USA)

The samples were centrifuged for 15 mins at 14 000 RCF (4°C). Protein was isolated from the supernatant using Amicon Ultra 0.5 ml centrifuge 10 kDa filter (Millipore, Ireland) according to manufactures guidelines. A 1:50 dilution of the protein lysate was prepared in milliQ water and was quantified using Pierce BCA protein assay kit (Thermo scientific, Rockford, USA).

An acrylamide gel (12%) composed of a resolving gel (12%, bisacrylamide (40%), 10% Ammonium persulfate, TEMED (1:1000), 0.75 M Tris-HCl, 0.2% SDS, and water) and a stacking gel (4%, bis-acrylamide (40%), 10% ammounium persulfate, 1:500 TEMED, 0.25 M Tris-HCl, 0.2% SDS, and water) was prepared.

Protein, at various concentrations (see Table 2.1), were prepared in loading dye (0.25 M Tris-HCl, 0.2% SDS (2 ml), glycerol (1 ml), 10% SDS (2 ml), bromophenol blue (0.005 g)) and loaded on the gel and run at 150V for 1 hr 10 mins at RT in running buffer. Ladder (250 kDa) (New England biolabs, Ipswich, MA, USA) was loaded to allow the size of the protein target to be assessed. Protein was transferred from the gel to a 0.45 µm 2% PVDF membrane (Millipore, Ireland) through tank transfer using transfer buffer (10X Tris-glycine, 20% methanol, water) for 16 hrs at 20 mA (4°C).

The membrane was blocked in 5% non-fat skim milk (NFSM PBS-T) for 2 hrs at RT prior to incubation with one of the three primary antibodies for SF1 described above at 4°C o/n. The primary antibodies were diluted in NFSM as follows: SF1 antibody (1:5000), PCRP-NR5A1-1A4-s (1:50) (1:2000), NR5A1 antibody (1:500).

The membrane was rinsed thrice for 5 mins in 1X PBS-T (0.1% Tween 20) and then incubated with goat anti-mouse IgG antibody horseradish peroxidase conjugate (BIO-RAD,

Hercules, CA, USA) for 2 hrs at RT at various concentrations. The concentration of secondary antibody ranged from 1:5000-1:10000. A separate membrane probed with PCRP-NR5A1-1A4-s was incubated with goat anti-mouse IgG1 cross adsorbed secondary antibody from Thermofisher scientific (Alexa fluor, 594, catalog number A-21125, Rockford, USA)

The membranes were rinsed thrice for 5 min 1X PBS (0.1% Tween 20) prior to imaging. The membranes were visualized using chemiluminescent reagents (Pierce™ ECL Western Blotting Substrate, Thermofisher Scientific, Waltham, MA, USA). The membranes were imaged (FluorQ system, protein simple, San Jose, Cam, USA) under 1 min exposure to visualize the SF1 antibody, PCRP-NR5A1-1A4-s antibody, and NR5A1 antibody. A 26 sec exposure was additionally used to visualize PCRP-NR5A1-1A4s using (Chemidoc MP imaging system, BIO-RAD, CA, USA) (Table 2.1). The membrane was reprobed with a primary antibody to GAPDH (1:10000) (Abcam, Cambridge, UK) and reimaged after incubation of secondary antibody, goat anti-mouse IgG antibody horseradish peroxidase conjugate (BIO-RAD, Hercules, CA, USA) to confirm the presence of protein on the membrane.

2.3 Results

Assessment of EGFP expression: Morphology

ICV injection of AAV9-SF1-eGFP virus resulted in expression of eGFP in the hypothalamus of the brain as confirmed by anatomical assessment of the region within the brain expressing eGFP (Figure 2.4). Using anatomical landmarks such as the 3rd ventricle, ARC, VMN and DMH and known SF1 mRNA expression patterns established using *in situ* hybridization published in the Allan brain atlas and comparing that to our results we were able to confirm that

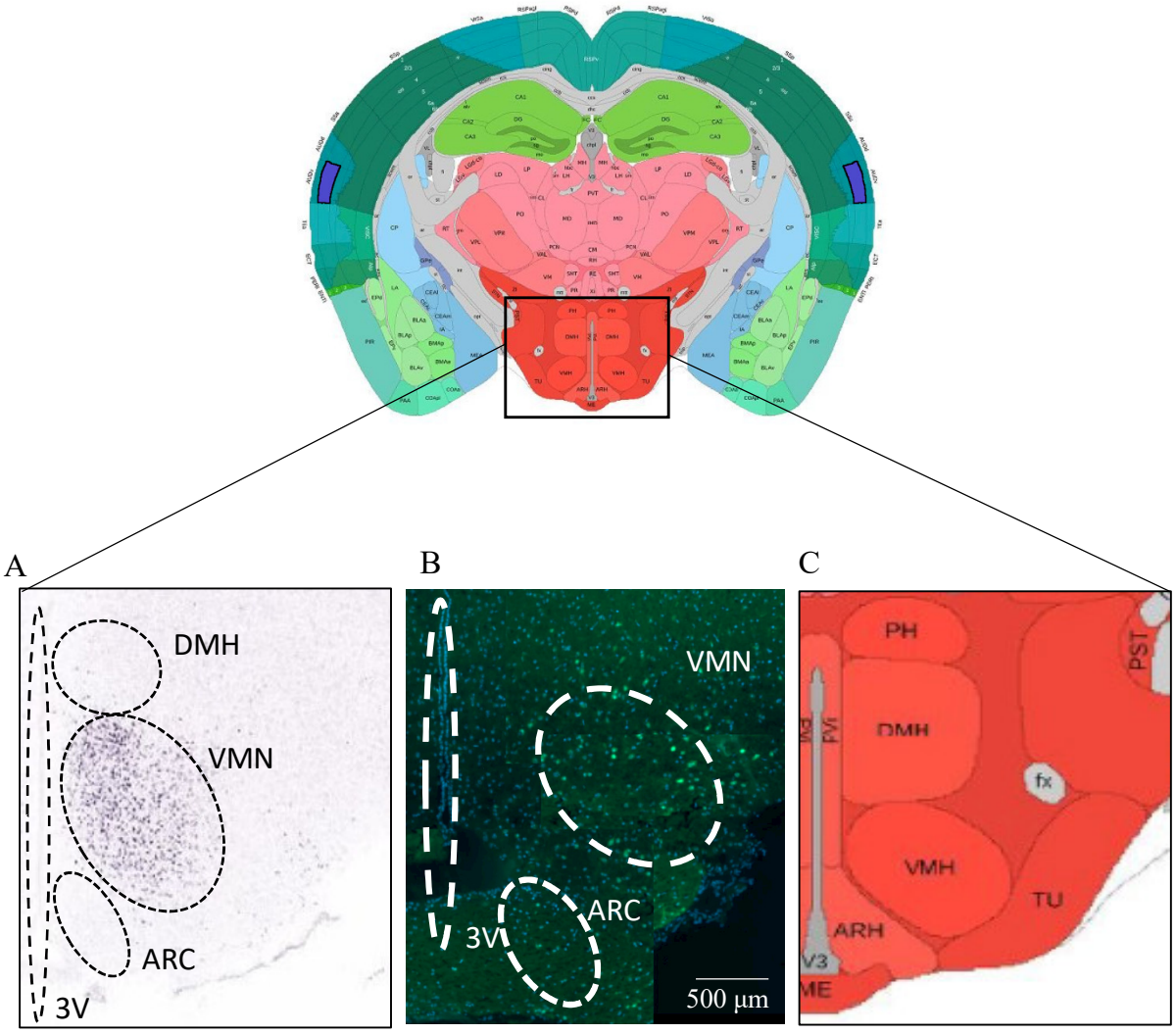

Figure 2.4: Results showing a representative image (10X magnification) tiled and stitched, coronal section of a brain of a C57Bl6 mouse (n =1) injected with adeno-associated virus serotype 9 (AAV9-SF1-eGFP), at a dose of 2.14 x 10^{13} viral genome/ml into the ventromedial nucleus (VMN) of the hypothalamus (**B**). Image B shows distribution of eGFP expression. Image A is a published image of the expression of steroidogenic factor 1 (SF1) mRNA in the VMN of the hypothalamus as deduced by in situ hybridization using riboprobes complimentary to SF1 mRNA (Allen Brain Atlas). The image was used as a reference for anatomical assessment of VMN morphology in the hypothalamus to compare the location of the vector expressing eGFP in our sample. Image (**C**) is a published diagram from the Allen Brain Atlas (image 71) and was used as a reference for comparison of anatomical landmarks: the 3rd ventricle, ventromedial nucleus (VMN), arcuate nucleus (Arc), with our sample.

Allen Institute.© [2004] Allen Institute for Brain Science. Allen Mouse Brain Atlas, Coronal. Available from: atlas.brain-map.org/atlas.

Allen Institute.© [2004] Allen Institute for Brain Science. Allen Mouse Brain ISH Atlas, Coronal. Available from: mouse.brain-map.org/gene/show/1103.

the expression pattern of eGFP in the brain sections appears to occur in the VMN (Figure 2.4 A,B,C).

Confirmation of SF1 antibody integrity: Immunohistochemistry

The SF1 antibody ordered from Thermofisher Scientific (catalog number: PA5-41967, Rockford, USA) did not detect SF1 immunoreactivity in the VMN despite various modifications to the protocol to optimize binding (Figure 2.5).

Confirmation of SF1 antibody integrity: Western blot analysis

Western Analysis revealed no specific binding of the SF1 antibody from Thermofisher Scientific (catalog number: PA5-41967, Rockford, USA) at 52.07 kDa in the separated hypothalamic or adrenal protein samples, suggesting the antibody did not bind to SF1 protein. This antibody did however bind to a 77 kDa protein in the protein isolated from the hypothalamus and the cortex (Figure 2.6 A). There were additional non-specific bands present at 23 KDa in the protein samples isolated from the hypothalamus and the cortex (Figure 2.6 A).

Western Blot analysis were conducted on two additional commercially available antibodies; PCRP-NR5A1-1A4-s, and NR5A1 antibody. NR5A1 antibody bound to protein that was 52.07 kDa in size isolated from protein in the hypothalamus and adrenals, however protein was detected in the cortex and iBAT (negative controls). Additional protein (23 kDa) was observed in all the tissues (Figure 2.6 B).

PCRP-NR5A1-1A4-s antibody bound to protein corresponding to 52.07 kDa in the adrenal gland (20 µg) in addition to a 23kDa protein, similar band size was observed in iBAT (negative control). PCRP-NR5A1-1A4-s did not bind to protein in the hypothalamus and cortex (Figure 2.6 C). Upon analysis with an alternate secondary antibody goat anti-mouse IgG1 cross

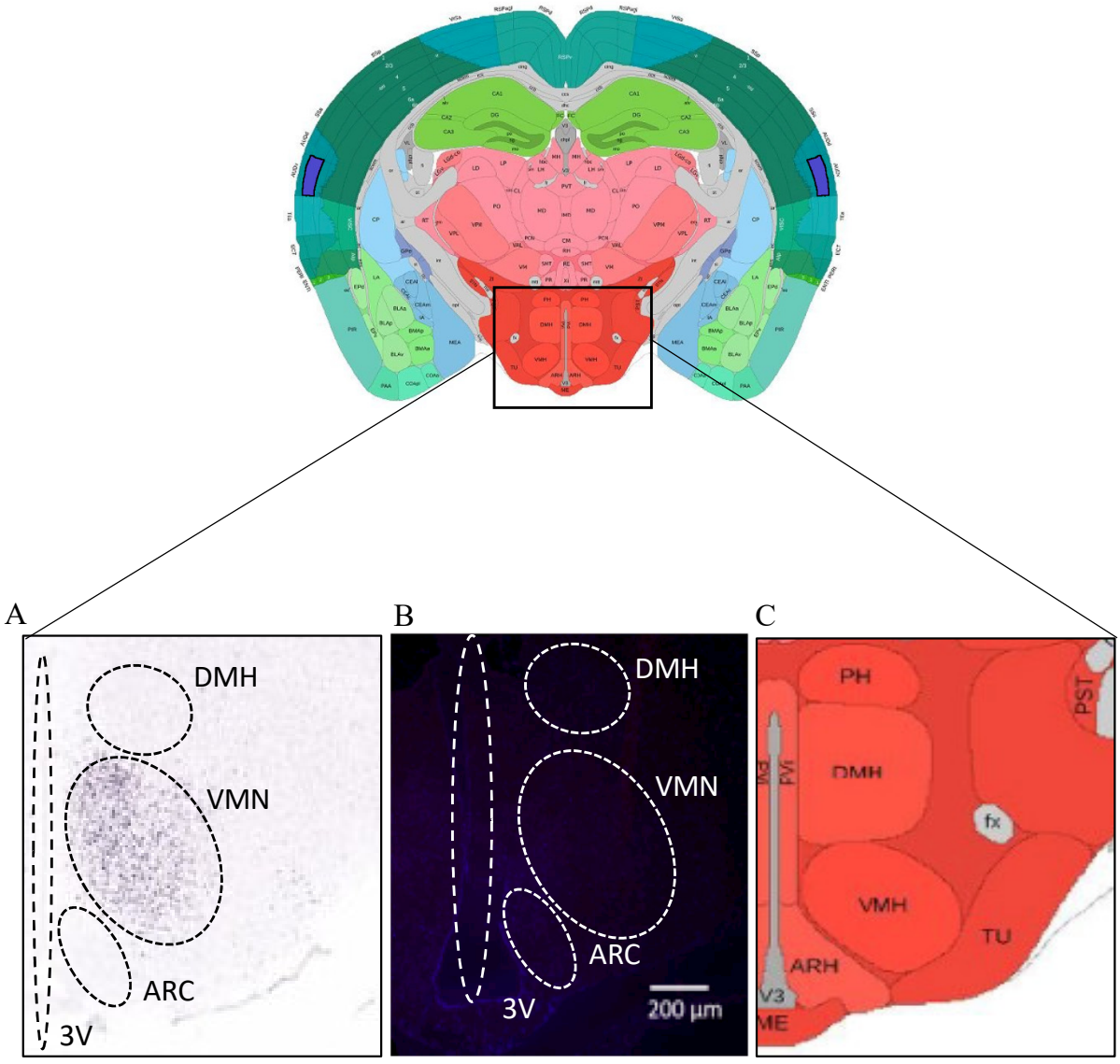

Figure 2.5: Representative image (4X magnification) of immunohistochemical analysis for steroidogenic factor 1 (SF1) conducted in coronal sections obtained from a C57Bl6 mouse brain (n = 1) known to express SF1. (SF1 antibody, catalog number: PA5-41967, Thermofisher Scientific, Rockford, USA) (**B**). Image **A** was obtained from the Allen Brain Atlas as representative image of the expected expression of SF1 in the VMN of the hypothalamus as deduced by in situ hybridization using riboporbes targeting SF1 mRNA. Image (**C**) is a diagram obtained from the Allen Brain Atlas (image 71) used for anatomical landmarks such as: the third ventricle, the arcuate nucleus (ARC), ventromedial nucleus (VMN), and dorsomedial nucleus (DMH).

Allen Institute.© [2004] Allen Institute for Brain Science. Allen Mouse Brain Atlas, Coronal. Available from: atlas.brain-map.org/atlas.

Allen Institute.© [2004] Allen Institute for Brain Science. Allen Mouse Brain ISH Atlas, Coronal. Available from: mouse.brain-map.org/gene/show/1103.

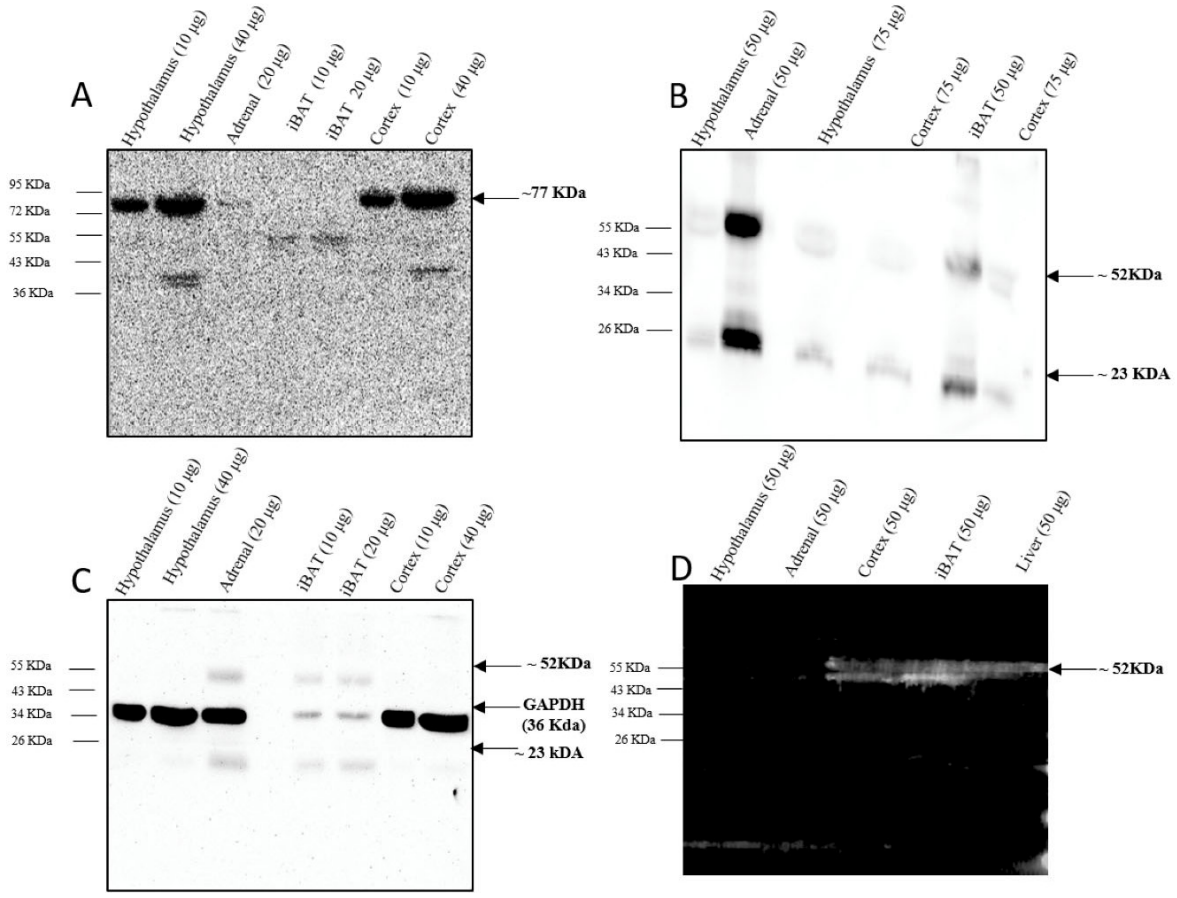

Figure 2.6: Western blot analysis was run to test the specificity three different antibodies against steroidogenic factor 1 (SF1) for detection of SF1 protein (52.1 KDa). Protein isolated from hypothalamus (10µg – 75µg) and adrenal tissues (20µg – 50µg) were loaded as positive controls, protein isolated from interscapular brown adipose tissue (iBAT) (10µg - 50µg), cortex (10µg - 75µg), and liver (50 µg) were loaded as negative controls. The three different primary antibodies were used; SF1 antibody (catalog number: PA5-41967, Thermofisher Scientific, Rockford, USA) (1:5000) (Image **A**), NR5A1 antibody (catalog number: 434200, Thermofisher Scientific, Rockford, USA) (1:500) (Image **B**), and PCRP-NR5A1-1A4s (Developmental Studies Hybridoma Bank, IOWA, USA) (1:50) (Image **C**) and (1:2000) (Image **D**). After incubation with primary antibody, membrane **A – C** were incubated with IgG horseradish peroxidase conjugate secondary antibody (BIO-RAD, Hercules, CA, USA) at various concentration: 1:5000 (**A**), 1:10000 (**B**), 1:5000 (**C**). For membrane **D** goat anti-mouse IgG1 cross-adsorbed secondary antibody was used (Thermofisher Scientific, Rockford, USA). Images were acquired under 1 minute exposure (A), (C); 1 minute exposure (B), 26 second exposure (D). To confirm the presence of protein on membrane **C** the membrane was reblotted with an antibody to GAPDH (1:10000) (Abcam, Cambridge, UK).

adsorbed secondary antibody, the antibody didn't bind to protein isolated from the hypothalamus and adrenal tissues, however a band was observed in the negative tissues; cortex iBAT, and liver (Figure 2.6 D).

2.4 Discussion

This chapter reports results that demonstrate immense progress in the development of the protocol to generate a transgenic mouse expressing PACAP specifically in the VMN of a PACAP-/- mouse. Previous work done in the Gray lab has shown that scAAV9-SF1-eGFP virus is a successful tool to deliver the vector in the brain, and obtain expression of eGFP (Cline, 2020). However, previous attempts to express eGFP using ICV showed expression 0.025 mm superior to the VMN, and expression in non-VMN tissue, which was speculated to result from too high a concentration of virus (Cline, 2020). Previously the Hamilton syringe was injected at a depth of 5.7 mm (Cline, 2020). Here I increased the depth of the injection to 5.72mm from the brain surface and decreased the concentration of the virus by 10-fold. The reduction in concentration was supported by a recent, independent study, which showed successful expression of PACAP protein using an adeno-associated virus in the VMN, using 2×10^{13} viral genome/ml (Nguyen et al., 2020), which is comparable to the dose we delivered (2.14×10^{13}). In conclusion, the combination of using revised coordinates and the reduced concentration of virus outlined in this ICV protocol successfully induced expression of eGFP specifically in the VMN of the hypothalamus (Figure 2.4).

The Allen Brain Atlas was used to navigate the successful delivery of the scAAV9-SF1-eGFP virus into the VMN. Based on the Allen Brain Atlas the height from the top of the brain to the base is around 5.9 mm (Mouse Brain Atlas, 2001.), since the depth of viral delivery is critical to avoiding off-target delivery of the vector, we increased the depth by just 0.02 mm, as

aggressive changes in the depth could potentially result in the leaking of the virus to either a region in the hypothalamus inferior to VMN such as the ARC or leakage from the base of the brain. We compared our samples to images of brain sections with SF1 positive neurons labelled by *in situ* hybridization published in the Allen Brain Atlas. Based on morphological assessment, the expression of eGFP achieved with my protocol for ICV injection using the new coordinates and decreased concentration of virus is within the VMN, in a similar region to the SF1 expressing neurons of the VMN as established by the Allen Brain Atlas (Figure 2.4 A,B) . To validate these results further we attempted to confirm our results using molecular analysis via immunohistochemistry to detect SF1 immunoreactivity within our sections, with the goal of measuring co-stained neurons, positive for both eGFP and SF1 immunoreactivity.

SF1 protein is only expressed in the VMN of the brain (Ikeda et al.,1995b). Therefore, the ability to detect SF1 expression in the VMN of the hypothalamus and detect an overlap in the eGFP expression would be a robust tool to confirm our protocol which aims to utilize localized injection and an AAV9 expression vector containing the SF1 promoter to achieve targeted delivery of the vector into VMN exclusively. Several attempts to detect SF1 immunoreactivity using the SF1 antibody from Thermofisher Scientific (catalog number: PA5-41967, Rockford, USA) were unsuccessful in detecting SF1 expression in the brain sections raising questions about antibody specificity (Figure 2.5). To confirm the specificity of the antibody for SF1 protein we performed Western blot analysis. The SF1 protein is 52.07 kDa in size ("NR5A1 Antibody (434200)," n.d.), the antibody did not bind to SF1 protein rather it bound to a protein that was around 77 kDa in size (Figure 2.6 A). Since SF1 antibody bound to an off-target protein the antibody was deemed non-specific for SF1 protein and therefore not pursued for further analysis.

Two alternate commercial SF1 antibodies were used to support this approach and tested for specificity using Western blot analysis; PCRP-NR5A1-1A4-s, and NR5A1 antibody. Again, neither of these antibodies showed staining patterns compatible with SF1+ immunoreactivity and therefore we could not confirm VMN-specific eGFP expression using molecular analysis (Figure 2.6 A -D). The antibodies bound non-specifically in the negative control tissues could be attributed to the antibodies binding to a protein that shares homology with SF1 such as, nuclear receptor subfamily 5, group A member 2 (NR5a2). SF1 protein and NR5A2 share a 58% homology ("Protein BLAST: Align two or more sequences using BLAST," n.d.). Whilst Nr5A2 is larger in size (61kDa), compared to SF1 protein (52.07 kDa) due to limitation in the Western blot analysis proteins that are that close in size may not separate enough to decern separate binding between the two proteins. The goat-mouse IgG horse radish peroxidase secondary antibody binds to all primary antibodies that belong to IgG class of antibodies regardless of the nature of the IgG isotype. To confirm if the antibodies were non-specifically binding to an alternate protein, we used a different secondary antibody goat anti-mouse IgG1 cross-adsorbed antibody (Alexa fluor 594), we repeated the experiment with primary incubation of PCRP-NR5A1-2A4s antibody. PCRP-NR5A1-1A4-s antibody belongs to an IgG1 isotype, therefore a secondary antibody that is IgG1 specific was used to increase specificity of binding of secondary antibody to primary antibody, to ensure that the non-specific binding of the SF1 antibody observed was in fact due to the non-specific nature of the primary antibody rather than an artifact of secondary antibody binding non-specifically. Using an IgG1 specific secondary antibody we were able replicate our previous results and confirm that the primary antibody was in fact not specific for SF1 protein, as protein was detected in the liver, iBAT and cortical brain tissues which don't express SF1 protein (Figure 2.6 d). Since the antibodies are not specific for SF1

protein as no preferential binding with SF1 protein can be deciphered in the hypothalamus and adrenal tissue compared to negative controls, the antibodies were not used to conduct immunohistochemistry. Despite this, the anatomical analysis of the eGFP suggests that the ICV protocol for VMN-specific delivery of scAAV9-SF1-eGFP virus, does produce VMN-specific expression of eGFP.

The results presented in this chapter provide evidence that the tool (AAV9-SF1-PACAP) and protocol (stereotaxic mediated, VMN -targeted injection) developed to achieve PACAP specific overexpression in the VMN are working as predicted. Specifically, visual assessment of eGFP expression in relation to neuroanatomical landmarks shows promising evidence that the eGFP was being expressed only in the VMN. While we were unable to establish a conclusive immunohistochemistry protocol to detect an overlap in SF1 expression and eGFP expression, we have validated that three commercially available SF1 antibodies are not specific and nor sensitive and therefore not suitable for this purpose and will move to alternate approaches to achieve this molecular evidence.

Future directions

Immunohistochemistry protocol using SF1 antibodies are complex to design as is evident in the results presented. Upon thorough analysis of various SF1 antibodies I would like to make the following recommendations for future experiments:

1. Identify an alternate SF1 antibody to detect SF1 expression: An anti-SF1 antibody designed by Yokoyama et al. 2009) has been used in independent studies using tissues isolated from mice to successfully conduct immunohistochemistry (Wilson et al., 2005) but is not commercially available. Since the three commercially available antibodies

tested here have proven to be non-specific, I would recommend collaborating with this academic lab to acquire the antibody to test by Western blot analysis and subsequent immunohistochemistry, if successful.

2. Use neuroanatomical stain to decern anatomical localization of eGFP expression: Due to the sparsity of commercially available robust SF1 antibodies, and the complexity of developing an immunohistochemistry protocol, I would suggest using a neuroanatomical dye such as luxol blue. Luxol blue is routinely used to visualize myelination ("Luxol® fast blue solution 1% | Sigma-Aldrich," n.d.). Luxol blue binds to phospholipids on myelin, resulting in the white matter (highly myelinated) appearing blue and gray matter appearing white.
3. Establish reproducibility of the stereotaxic surgery technique: Prior to proceeding with delivery of the experimental vector AAV9-SF1-PACAP, the stereotaxic surgery should ideally be repeated using the control vector AAV9-SF1-EGFP to ensure reproducibility of expression in the VMN using the co-ordinates established in this chapter. Physiological studies could be conducted on wildtype mice administered with AAV9-SF1-eGFP virus using the established coordinates, the physiological impact of AAV9-SF1-eGFP virus would be a great control to compare the physiological impact upon administration of AAV9-SF1-PACAP.

In conclusion, we have made immense progress towards developing a protocol to deliver AAV9-SF1-eGFP in the VMN exclusively. Morphological analysis is promising since the vector visually appears to be expressed in the VMN, however in order to confidently state the location of the vector expression the development of immunohistochemistry protocol or alternately using a neuroanatomical dye would add immense value in our study. The work done here is

fundamental in the development of a transgenic animal model to overexpress PACAP exclusively in the VMN, to understand the neurocirculatory effect of PACAP expressed in the VMN on adaptive thermogenesis.

Chapter 3

Development of an *in situ* hybridization protocol to detect PACAP mRNA expression in mouse hypothalamus

3.1 Introduction

To study the effect of PACAP on thermogenesis in the central nervous system, Dr. Gray's lab has utilized a mouse model of PACAP deficiency to study the physiological impact of the absence of PACAP on energy metabolism and showed the model to have impaired adaptive thermogenesis (Diané et al. 2014; Gray et al. 2002; Filatov et al., 2020). The hypothalamus is a region of the brain that has a critical role in regulating energy metabolism (Bechtold et al., 2006; Hawke et al., 2009) . Previous studies, using *in situ* hybridization and other methods have shown that mRNA for PACAP (Hannibal 2002, Segal et al 2005) and its receptors (Hashimoto et al. 1996) are abundantly expressed in various nuclei of the hypothalamus. Regions of hypothalamus with abundant PACAP expression include the; ventromedial nucleus (VMN), paraventricular nucleus (PVN), and the arcuate nucleus (Arc) of the hypothalamus (Hannibal 2002; Hashimoto et al. 1996). A region of the hypothalamus that has particularly high expression of PACAP is the VMN (Hannibal 2002; Hashimoto et al. 1996; Segal et al. 2005).

As detailed in Chapter 2 the VMN is essential in regulating energy expenditure, through thermogenesis and appetite regulation (Sujean Choi & Dallman, 1999; Monda et al., 1997; Nishizawa & Bray, 1978). To understand the functional role of PACAP that is highly expressed in the VMN, pharmacological studies have previously been conducted. Pharmacological administration of PACAP-38 peptide into the VMN of the hypothalamus induced adaptive thermogenesis in a dose dependent manner, as measured by an increase in core body temperature (Resch et al., 2011). Pharmacological studies such as these, rely on the physiological response of peptide hormones that are delivered at a pharmacological dose, which is much higher than endogenous levels of PACAP in the brain. These studies are a promising indication that the

VMN is a site within the brain where PACAP receptors are expressed, and PACAP can act to regulate thermogenesis, however pharmacological studies are not an ideal reflection of the endogenous effect of PACAP expression, as the peptide hormone delivered is not representative of the endogenous levels of PACAP released from neurons into the synaptic clefts.

A novel approach to test the role of PACAP in the VMN in thermoregulation, is to develop a transgenic mouse that will express PACAP only in the ventromedial nucleus of the hypothalamus and assess if the deficits in thermogenesis, observed in animals lacking PACAP are rescued or persist. Unlike pharmacological studies, this approach will focus on a genetic model. The model will utilize an associated adenovirus (AAV) to express PACAP specifically in neurons of the VMN, in PACAP-/- mice (details of the approach discussed in Chapter 2). The peptide with our approach will be expressed at near endogenous levels as the expression of AAV9-SF1-PACAP will be driven by the SF1 promoter.

Confirmation that the AAV has successfully induced expression of PACAP messenger ribonucleic acid (mRNA) specifically in the VMN of the hypothalamus, will be a critical step in the validation of specific expression of PACAP using in this method. Detection of PACAP mRNA expression can be achieved by *in situ* hybridization. *In situ* hybridization is a methodology used to identify a specific ribonucleic acid sequence in a specific type of cell or tissue, using a labelled probe complementary to the mRNA sequence of interest. The tissue in which mRNA is being detected in, *in situ* hybridization are morphologically preserved, which permits the expression site of the target mRNA to be determined (Qian & Lloyd, 2002).

Since the discovery of *in situ* hybridization technique in the 1960's by Gall and Purdue, as a tool to detect nucleic acid (Gall & Pardue, 1969), the technique has been greatly refined with the development of highly sensitive probes and a variety of different labels. Immense advances

have been made using *in situ* hybridization technique, in research and diagnostics. *In situ* hybridization was one of the tools used in the compilation of the human genome project (Lander et al., 2001), probes were designed targeting the bacterial artificial chromosome (BAC), in pilot studies. The information from these studies was integrated with cytogenic landmarks to construct whole genome. Anomalies in chromosomes through multiplex probe hybridization has been used to detect locus specific gene mutation (Bishop, 2010) in the genome. These studies are crucial in cytogenic analysis of diseases. In addition to this *in situ* hybridization is a fundamental technique used to detect the expression of specific genes in a variety of tissues for thousands of experimental questions (Radinsky et al., 1993; Hannibal, 2002). *In situ* hybridization is a highly sensitive technique used in molecular biology to detect localized expression of genes and its transcripts.

It is for this reason, we felt *in situ* hybridization was the most appropriate technique to confirm the expression of PACAP mRNA in the VMN and I present here my work to develop an *in situ* hybridization protocol to detect PACAP mRNA in the hypothalamus of mice. PACAP, like other peptide hormones, is encoded by a gene (Adcypa 1 in the case of PACAP) which is transcribed to mRNA and translated to a pre-propeptide, which is processed to produce functional proteins. PACAP mRNA consists of the 5' untranslated region (5'UTR), signal peptide (SP), cryptic peptide (CRP), PACAP related peptide (PRP), PACAP and a 3'UTR (McRory et al., 2000). The mRNA is translated to pre-proPACAP, that is processed through proteolytic cleavage by various proteolytic enzymes as discussed in chapter 1, to generate functional PACAP 27/PACAP-38 (Hirabayashi et al., 2018; Okazaki et al., 1995)(Figure 1.2). PACAP mRNA is an exceptionally challenging sequence to target, as PACAP sequence is highly conserved. It is considered to be the ancestor molecule in the glucagon/secretin/vasoactive

intestinal polypeptide superfamily (McRory et al., 2000). It therefore, shares structural homology with other hormones in the PACAP/glucagon superfamily. The *in situ* hybridization protocol therefore requires extreme caution in designing a probe that will specifically detect expression of PACAP mRNA only.

The procedure for *in situ* hybridization procedure has five major steps, each which must be tailored to one's own experimental goals and paradigm. First, to preserve the integrity of nucleic acid in the tissue sample, surgically isolated tissues are fixed and/or embedded. This is followed by permeabilizing the tissue sample to allow for the nucleic acid probe to access the target nucleic acid sequence present within the cytoplasm of the cells during the hybridization reaction, where the nucleic acid probe, which has been generated in vitro to be complementary to the native mRNA sequence, binds to the target sequence *in vivo* through the formation of hydrogen bond between complementary base pairs. Following hybridization, non-specific binding of the probe is removed through a series of wash steps that are stringent enough to preserve specific binding but will loosen and remove non-specific binding, that contain unstable bonds that can be easily dissociated. Non-specific binding occurs due to hybridization of a small portion of the nucleotides on the probe with that of the target sequence. Since the entire probe doesn't bind to the target sequence, thorough washing the samples with salt solution at a certain temperature, which is tailored for each *in situ* hybridization experiment depending on the probe used, these bonds can be dissociated. The post-hybridization step is critical to ensure non-specific binding of probe is dissociated without the disruption of specific probe binding which could lead to a decreased sensitivity of the *in situ* hybridization reaction. This is followed by detection of probe binding, through visualization of the label within the sample using microscopy, to confirm the presence of the target sequence. The outcomes of *in situ*

hybridization are greatly influenced by tissue preparation, the choice of probe and label used and must be carefully designed and optimized for each mRNA target chosen. In this chapter I will discuss critical decisions involved in the experimental design of the *in situ* hybridization protocol I designed to detect PACAP mRNA in the hypothalamus of mice.

Tissue Processing

Tissue sections for *in situ* hybridization are either prepared using cryostat sections of tissues that have been fixed in paraformaldehyde or by fixing the tissues in formalin and embedding it in paraffin.

For molecular analysis involving nucleic acid it is preferable to use cryostat embedded samples, in comparison to embedding sample in paraffin as frozen cryostat samples preserve the epitope and native nucleic acid integrity as the sample is immediately frozen which prevents degradation of nucleic acid ("The Pros and Cons of FFPE vs Frozen Tissue Samples," n.d.).

Cryostat samples are fixed in paraformaldehyde, to ensure morphology is preserved. In paraformaldehyde fixed tissues, cross linkages do not form between nucleic acid and protein which could potentially compromise the mRNA quality, as is the case with the formalin fixed samples (Grigorev & Korzhevskii, 2018) and thus for *in situ* hybridization, in which mRNA is the target, the nucleic acid post fixation is very critical. Formalin causes the formation of methylene crosslinks within amino acids, and nucleic acids, as well as between nucleic acid and amino acids, this can disrupt the integrity of the nucleic acid and the cellular morphology that is to be studied (Grigorev & Korzhevskii, 2018). Additionally, washing steps that utilize xylene, to eradicate cross links in formalin fixed samples, can degrade nucleic acid and thus are not favored.

Probe design

The choice of probe used, and its sequence are essential in the detection of specific mRNA expression. As discussed earlier, PACAP is a complex sequence to target. Therefore, designing a probe sequence that will specifically target PACAP and not bind to other related peptide hormone mRNAs, was crucial in our experimental design.

We tried two experimental approaches to detect PACAP mRNA expression, approaches that utilized two different types of probes; oligonucleotide probes and a RNA probe (riboprobe).

Oligonucleotide probes, consist of short artificially synthesized nucleotide sequences (approximately 50 nucleotides in length). Oligonucleotide probes were selected in my first attempt for development of a protocol because they are short in length and therefore it is easier to penetrate the tissues. In addition to this, these probes are relatively easy to synthesize in comparison to riboprobes, as no cloning is required (Kumar, 2009). Oligonucleotide probes are synthetically made using deoxyribose, in order to produce a single stranded sequence that has a sequence complimentary to the target mRNA (Lewis, Sherman, & Watson, 1985). However, designing oligonucleotide probes, requires extreme caution in terms of selecting the region of hybridization in the target sequence. Due to its small size, the sequence of mRNA selected must not be homologous with isomers of a given mRNA (Stahl, Eakin, & Baskin, 1993). In this first approach, two oligonucleotide probes were designed that were homologous to PACAP.

An alternate approach to oligonucleotide probe, is the use of a riboprobe. Riboprobes are RNA based probes, that are approximately 500 to 800 base pairs long, and the increased length requires more stringent permeabilization conditions to allow the probe to penetrate into the cytoplasm in order to hybridize with the native mRNA sequence. The increased length of

riboprobes increases sensitivity compared to oligonucleotide probes because of the incorporation of multiple labels in the riboprobe sequence. In comparison, oligonucleotide probes have a single label on the 3' end. Riboprobe alternately are labelled through the incorporation of the label within every 20-25 nucleotide along the entire length of the probe (~ 700 base pair), due to the short length of the oligonucleotide probes (50nt) incorporation of multiple labels within the probe is not possible. (SIGMA-ALDRICH, 2008).In addition, riboprobes have the highest binding affinity to RNA compared to other types of probes, such as DNA probes. RNA-RNA hybrids are highly thermostable, which facilitates in the removal of excess probe in post hybridization wash steps using RNase, to decrease background noise (Robert E.FArrell, 2010). RNA probe synthesis is however more time consuming than oligonucleotide probes, as it requires sub cloning using plasmids containing promoters for SP6, T7 RNA polymerase and a target cDNA are required to generate RNA probes via transcription reactions (Robert E.FArrell, 2010).

Probe Label

Labelling of the probe is essential to elucidate if the probe has bound to the mRNA of interest. There are two main ways of labelling; radiolabeling or non-radiolabeled. Although radiolabeled probes are highly sensitive, there are safety risks associated with the use of isotopes. Radioisotopes have potential health hazards, are expensive to purchase and require facilities for storage and appropriate disposal of isotopes (Kumar, 2009). Due to this, non-radiolabeled probes are routinely used to conduct *in situ* hybridization.

Non-radioactively labelled probes are either visualized directly using fluorophores or indirectly via hapten incorporation using a colorimetric label such as, digoxigenin (DIG). Fluorescent *in situ* hybridization (FISH) involves directly labelling the probe with fluorophores,

which are detected by fluorescence microscopy upon hybridization with the target mRNA sequence. The technique is thus quick and is easily quantifiable. Despite the benefits of direct labelling, is not as sensitive as indirect labelling methods, using a secondary reporter molecule (Chevalier, Yi, Michel, & Tang, 1997).

Hapten-labelled probes are more sensitive than direct fluorescence labelling. RNA and oligonucleotide probes are labelled with a colorimetric label such as, digoxigenin through an enzymatic or chemical reaction. The method of label incorporation does not influence the hybridization reaction or it's sensitivity. DIG is linked to the probe via a spacer arm. Spacer arm increases the affinity of binding affinity of bases during hybridization, by avoiding steric hinderance (Chevalier et al., 1997). Post hybridization, the binding of the probe to the target mRNA can be detected using bright field microscopy (Zimmerman, Peters, Altaras, & Berg, 2013).

Digoxigenin is a commonly used label, it is derived from Digitilis plant, D.lanata and D.purpurea (Farrell, 2010). To visualize the hybridization of the probe to the mRNA, anti-dig antibody conjugated alkaline phosphate is used. Binding of riboprobe to target sequence results in unquenching of alkaline phosphate which hydrolyses 5-bromo-4-chloro-3-indole (BCIP), in the presence of nitroblue tetrazolium (NBT), this results in a colorimetric reaction, that is detected using microscopy. Digoxigenin label provides a high signal to noise ratio relative to other labelling methods, such as fluorescent labels, therefore it provides a high cellular resolution (Schaeren-Wiemers & Gerfin-Moser, 1994).

We hypothesize that *in situ* hybridization is the best approach to detect PACAP mRNA expression in the VMN of the hypothalamus. As such, the experimental aim of this chapter was to develop a sensitive protocol to detect PACAP mRNA expression in brain samples derived

from a wildtype C57Bl6 mouse using *in situ* hybridization. In consideration of the advantages and disadvantages of the different strategies involved in the design of the various steps of an *in situ* hybridization protocol, this chapter focuses on the critical decisions made in the experimental design. In Summary, key decisions regarding sample preparation, conditions involved in; pre hybridization, hybridization, post-hybridization, and imaging were made to generate and test two experimental protocols, one utilizing oligonucleotide probes and another utilizing a riboprobe.

3.2 Material and methods

Animals

PACAP+/+ and PACAP-/- mice were generated from a breeding colony of the PACAP null mouse line at the University of Northern British Colombia. The PACAP -/- mouse line was previously generated by Briefly, using Lox-P recombination a 4 kb region of the PACAP gene was removed, consisting of the cryptic peptide (CRP), PACAP related peptide (PRP) and PACAP (Figure 3.1). The mice were housed up to 4 mice/cage and were maintained with 12:12 light/dark hr cycle, at 24°C with free access to water and food (standard rodent Chow diet, LabDiet 5001, Lab diet, Inc., Brentwood, Leduc, AB, Canada, metabolizable energy 3.02kcal/g). The mice were weighed twice a week to monitor health. The experiments were conducted in accordance with Canadian Council on Animal Care and approved by the University of Northern British Colombia's (UNBC) Animal Care and Use Committee (ACUC).

Sample preparation for protocol development

Brain tissue from a PACAP +/+ and a PACAP -/- mice were isolated by dissection, fixed in 4% paraformaldehyde in PBS, overnight. The samples were transferred into 30% sucrose and cryo-sectioned (Wax-It histology, Vancouver, BC, Canada), as discussed in chapter 2. Sections

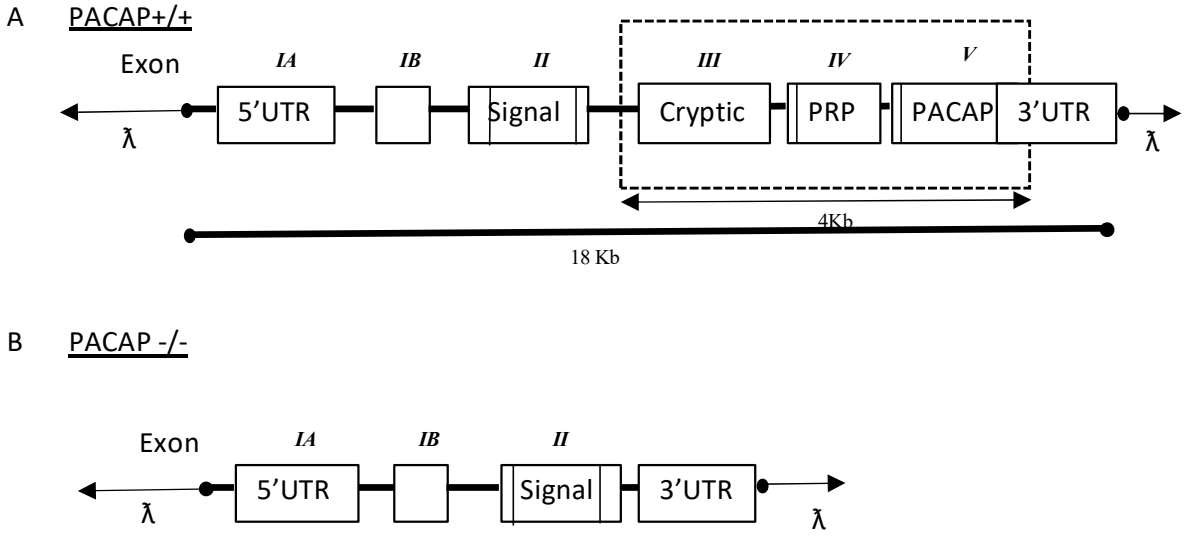

Figure 3.1: Pituitary adenylate cyclase-activating polypeptide (PACAP), wildtype (+/+) and Knockout (-/-) mice on a C57Bl/6 background were initially generated by Gray et al. 2001. The PACAP gene consists of 5 exons encoding a 5'untranslated region (5'UTR), signal peptide, cryptic peptide, PACAP-related peptide (PRP), PACAP and a 3'UTR. Using Cre-LoxP recombination an approximately 4 kb region within the PACAP coding sequence was removed. The genotyping protocol for PACAP KO mice thus amplifies a truncated DNA sequence (**B**) in comparison to PACAP WT mice (**A**).

(10 μm) were cut in the region of the hypothalamus inclusive of the 3rd ventricle, the VMN, PVN and the ARC. This was done in order to target regions of the hypothalamus with high expression of PACAP in the PACAP +/+ brain (Hashimoto et al.1996; Segal et al. 2005). All brain sections obtained from the PACAP +/+ mouse used for these experiments are expected to express PACAP endogenously and thus serve as an appropriate tissue to troubleshoot our protocol for *in situ* hybridization. Two brain sections were mounted per slide. A total of 23 PACAP +/+ slides were analyzed with various *in situ* hybridization conditions detailed below.

For each run, to one of the two sections an antisense probe was added as it is complementary to the PACAP mRNA, the other section was used as a technical negative control to which a sense probe was added which has the same sequence as the PACAP mRNA to decern specific binding of the antisense probe. When signals were obtained from binding of the probes a PACAP -/- brain sample, which doesn't express PACAP, was used as a biological negative control to confirm the specificity of the probe.

Oligonucleotide probe design

Oligonucleotide probes were 50 nucleotides in length and were designed using the National Center for Biotechnology Information (NCBI) basic alignment ("BLAST: Basic Local Alignment Search Tool," n.d.) tool. Sequence homology and alignment of various oligonucleotide sequences, complementary to the PACAP mRNA were analyzed. Since PACAP is highly conserved and has homology with sequences of various peptides in the glucagon superfamily of peptide hormones (McRory et al., 2000), probe selection criteria were set such that the probe of interest had 50% or less homology with other off-target sequences, and 100% alignment with the PACAP mRNA sequence.

In consideration of the selection criteria listed above, two oligonucleotide probes sequences were designed (Figure 3.2); a 50-nucleotide sequence targeting the nucleic acid sequence of the cryptic peptide (Reference number NM_009625.3; 648 – 697), and a 50-nucleotide targeting the nucleic acid sequence of PACAP related peptide (Reference number: NM_009625.3; 697 to 746). For each of the two oligonucleotide probes, an antisense probe complementary to the targeted mRNA sequences was designed, in addition to a sense probe that is identical to the targeted mRNA sequences, that will not bind and thus serve as a negative control, to confirm specific binding of the antisense probes. These oligonucleotide probes labelled with 3' Digoxigenin were obtained from a commercial supplier (integrated DNA technologies (IDT), Coralville, Iowa).

Oligonucleotide Probe: *In situ* hybridization

An *in situ* hybridization protocol was adapted from, DIG Application Manual for Non-radioactive *in situ* Hybridization (SIGMA-ALDRICH, 2008). The general protocol used is described in detail below, noting critical reagents that were manipulated in attempts to produce a successful protocol (Table 3.1). Critical steps within the *in situ* hybridization protocol were subcategorized into pre-hybridization, hybridization, post hybridization, and imaging. All solutions were prepared using DEPC treated water, to remove contaminating RNases. Slides were either immersed in reagents in coplin jars, or sections were bathed in solution after placing a hydrophobic barrier around the section. Antisense probes and sense probes were tested in each run (Table 3.2).

Pre-hybridization

Prior to conducting *in situ* hybridization, the slides were thawed at 40°C for 2 hrs. The sections were incubated twice in 1X PBS for 5 mins. The sections were then transferred into

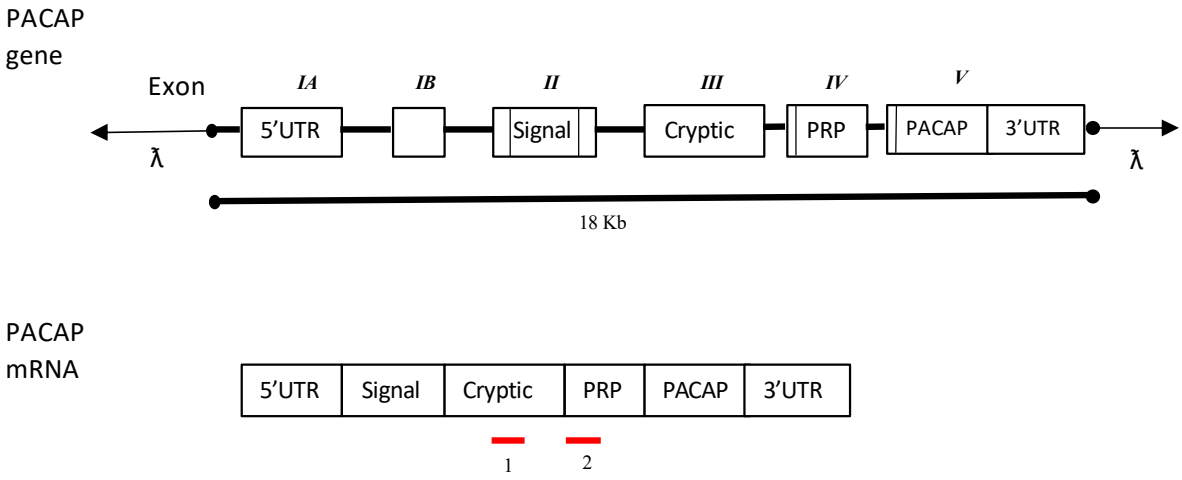

Figure 3.2: Two oligonucleotide probes were designed targeting the pituitary adenylate cyclase-activating polypeptide (PACAP) messenger ribonucleic acid (mRNA). The PACAP gene consists of a 5' untranslated region (5'UTR), signal peptide, cryptic peptide, PACAP related peptide (PRP), PACAP and a 3'UTR. The designed probes were complementary to the cryptic peptide (1) (NM_009625.3, 647-967) and PACAP-related peptide (PRP) (2) (NM_009625.3, 697 – 747) (NCBI, Blast: Basic Local Alignment Search tool).

Table 3.1. Reagents used in *in situ*-hybridization.

Experiment conditions	Purpose
Pre-hybridization	
Proteinase K conc.	Permeabilize tissue
Hybridization	
Denharts solution	Blocking solution
Dextran sulfate	Assists formation of probe network
DTT	Inhibition of Rnase activity
yeast t-RNA	Blocking solution
Deionised formamide	Ensure optimum binding temperature
salmon sperm DNA	Blocking solution
probe conc.	Bnsure optimum binding
Post-hybridization	
Sodium Chloride, Sodium citrate (SSC washes)	Clean up step, ensures no non-specific binding
Imaging	
Blocking buffer (Triton X-100 and sheep serum)	Blocking solution
Fast green	Counterstain
Anti-Digoxigenin antibody	Bind to Digoxigenin

Table 3.2: Digoxigenin labeled oligonucleotide probe sequences. Two oligonucleotide probes were designed for pituitary adenylate cyclase polypeptide (PACAP) messenger ribonucleic acid (mRNA). An antisense complementary to PACAP mRNA and a sense probe with the same sequence of PACAP mRNA was designed for each set of probes. Probe 1 targeted the Cryptic peptide (NM_009625.3, 648 – 696). Probe 2 was targeted to PACAP -elated peptide (NM_00962.3; 697 – 746) (NCBI, Blast: Basic Local Alignment Search tool), within the PACAP mRNA.

Probe	Target region in mRNA	Sequence (5' – 3')
Probe 1	Cryptic Peptide	as: CTCTCCTGTCCGCTGGATAGTAAAGGGCGTAAGCGTCACGCAGCGCGGAG s: CTC CGCGCTGCGTGACGCTTACGCCCTTTACTATCCAGCGGACAGGAGAG
Probe 2	PACAP related Peptide	as: TGGTCCAAGAACTTTTCGATAGGCTTCGTTAAGGATCGTGGGCGACATC s: GATGTCGCCCACGA AATCCTTAACGAAGCCTATCGAAAAGTCTTGGACCA

glycine (100 mM) twice for 5 mins. The sections were permeabilized using 0.3% Triton X-100 for 15 min followed by 2 washes twice in PBS for 5 min, using gentle agitation. The sections were then further permeabilized using Proteinase K (attempted at various concentrations, see Table 3.3) at 37°C for 30 min. The tissues were fixed with 4% paraformaldehyde for 5 mins, followed 2- 5 mins washes in 1X PBS.

To reduce non-specific binding due to the negatively charged oligonucleotide probes binding to positively charged amine, acetylation was conducted by bathing sections in 100 µl of 0.1 M triethanolamine (TEA) buffer, pH 8.0, containing 0.25% acetic anhydride twice, for 5 mins.

Pre-hybridization buffer (40 ul) was prepared using; 2X sodium chloride, sodium citrate (SSC), 10% dextran sulfate, 1× Denhardt's solution [0.02% Ficoll, 0.02% polyvinylpyrrolidone, 0.2 mg/ml RNase free bovine serum albumin], 50 mM phosphate buffer saline (PBS), 50 mM DTT, 250 µg/ml yeast t-RNA, 5 µg/ml polydeoxyadenylic acid, 100 µg/ml polyadenylic acid, 47% deionized formamide and 500 µg/ml denatured and sheared salmon sperm DNA. Brain sections were incubated in pre-hybridization buffer for 2 hrs at between 30°C - 40°C (attempted at various temperatures, see Table 3.3). The pre-hybridization temperature was identical to the hybridization temperature used for each run.

Hybridization

After equilibrating the tissue sample in 30 µl of hybridization buffer (identical to pre-hybridization buffer), antisense (30 ng – 100 ng) and sense probes (30 ng – 100 ng) were added to PACAP wild type brain sections and incubated overnight in a humidity chamber at between 30 - 40°C (see Table 3.3). The temperature and concentration of probes along with reagents in

Table 3.3: *In situ* hybridization (ISH) protocol development using oligonucleotide probes. Digoxigenin (DIG) labeled oligonucleotide probes were used to detect pituitary adenylate cyclase polypeptide (PACAP) messenger ribonucleic acid (mRNA) expression. Critical steps in the ISH protocol were modified to achieve specific binding of the probes. Two antisense oligonucleotide probes were designed, targeting cryptic peptide (CRP) and PACAP related peptide (PRP) within the PACAP mRNA. Sense probe was used as an experimental control to decipher specific binding. The highlighted steps were modified in each run.

Experimental condition	Run 1	Run 2	Run 3	Run 4	Run 5	Run 6	Run 7	Run 8	Run 9	Run 10	Run 11	Run 12	Run 13	Run 14
Pre-Hybridization														
Proteinase K conc.	1 µg/ml	0.05 µg/ml	0.05 µg/ml	0.5 µg/ml	0.5 µg/ml	0.5 µg/ml	0.5 µg/ml	0.5 µg/ml	0.5 µg/ml	0.5 µg/ml	0.5 µg/ml	0.5 µg/ml	0.5 µg/ml	0.5 µg/ml
Hybridization														
Probe concentration	30 ng	30 ng	60 ng	60 ng CRP only	60 ng CRP only	60 ng CRP only antisense only	60 ng CRP only antisense only	60 ng CRP only antisense only	60 ng CRP only antisense only	60 ng PRP only	60 ng both probes	100 ng both probes	100 ng both probes	100 ng both probes
Salmon sperm DNA	500µg/ml	500µg/ml	500µg/ml	500µg/ml	500µg/ml	500µg/ml	500µg/ml	500µg/ml	500µg/ml	500µg/ml	500µg/ml	500µg/ml	500µg/ml	100µg/ml
Temperature	37°C	37°C	30°C	37°C	40°C	40°C	37°C	37°C	37°C	37°C	37°C	37°C	37°C	37°C
Post-Hybridization														
Temperature	37°C	37°C	30°C	37°C	40°C	40°C	37°C	37°C	37°C	37°C	37°C	37°C	37°C	37°C
Imaging														
Blocking buffer (Triton X-100 and sheep serum)	0.1 % triton. 2% normal sheep serum	0.1 % tritonX with 2% normal sheep serum	0.1 % tritonX with 2% normal sheep serum	0.1 % tritonX with 2% normal sheep serum	0.1 % tritonX with 2% normal sheep serum	0.1 % tritonX with 2% normal sheep serum	0.1 % tritonX with 2% normal sheep serum	0.1 % tritonX with 2% normal sheep serum	0.1 % tritonX with 2% normal sheep serum	0.1 % tritonX with 2% normal sheep serum	0.1 % tritonX with 2% normal sheep serum	0.1 % tritonX with 2% normal sheep serum	0.1 % tritonX with 1% normal sheep serum	0.1 % tritonX with 1% normal sheep serum
Fast green	0.02%	0.10%	0.10%	0.10%	0.10%	no counterstain	no counterstain	no counterstain	no counterstain	no counterstain	no counterstain	no counterstain	no counterstain	no counterstain
anti-Dig	1:100	1:100	1:100	1:100	1:100	1:1000	1:500	1:250	1:100	1:250	1:250	1:250	1:250	1:250

the master mix were manipulated in pursuit of specific binding of probe to PACAP mRNA (Table 3.2).

Post-hybridization

To remove non-specific binding, the slides were exposed to a series of wash steps of decreasing SSC concentrations (2X SSC, 1X SSC, 0.25X SSC) for 15 mins in a water bath with gentle agitation at the hybridization temp.

Imaging

The slides were washed twice for 10 mins with washing buffer (100 mM Tris-HCl (pH 7.5), 150 mM NaCl) to equilibrate the slides for the labelling reaction. The samples were incubated at RT in blocking buffer (100 µl) containing 0.1% Triton X-100 and normal sheep serum, were added to brain tissues. The sections were then incubated at RT for 30 mins. Various concentrations of anti-digoxigenin antibody (1:100 – 1:1000, Table 3.3), diluted in blocking buffer (100 µl) were added to brain sections and incubated for 2 hrs. The sections were washed twice for 10 mins using washing buffer, with gentle agitation at RT. Next, the tissues were equilibrated for 10 min with 100 µl of detection buffer [100 mM Tris-HCl (pH 9.5), 100 mM NaCl, 50 mM $MgCl_2$] before applying 200 µl of detection buffer containing, 9.4 mg/ml nitroblue tetrazolium/ 0.188 mg/ml 5-bromo-4-chloro-3-indolyl-phosphate (NBT/BCIP) and incubating sections overnight at RT in a humidity chamber. The color reaction was stopped using buffer, 10 mM Tris-HCl (pH 8.1), 1 mM EDTA, the slides were rinsed in distilled water and mounted using Immounomount mounting media (Fisher scientific, Canada). The sections were analyzed using bright field microscopy (BX61 Olympus microscope, Richmond Hill, ON, Canada).

Riboprobe synthesis

The mRNA sequences for the PACAP probe was previously cloned into pGEM-T (pGEM-PACAP) by an undergrad student in the Gray lab. The plasmid designed consisted of; the ampicillin resistant gene and a 701bp fragment of the PACAP gene required for riboprobe synthesis (reference sequence: NM_001315503.1, region 303 – 1004) situated between a T7 and an SP6 promoter (Figure 3.3) (Figure 3.4).

Transformation

pGEM-PACAP plasmid was transformed into XL-1 blue cells (100ul, thawed right before transformation). The cells were incubated for 10 mins on ice, while mixing them every 2 mins. pGEM-PACAP (50 ng) DNA was added to the cells and 1.7 µl of β-mercapthoethanol (1:10). The sample was kept on ice for 30 mins, following by heat shocking the cells at 42°C for 45 sec. The cells were then immediately transferred on ice for 2 mins. The cells were recovered in 0.9 ml of Super Optimal broth with catabolite repression (SOC) media (bacto-tryptone, bacto-yeast extract, NaCl, glucose, $MgCl_2$, $MgSO_4$, pH 7.0) at 37°C for an hr, with gentle shaking at 250 RPM. The cells were pelleted at 1000 RPM and suspended in 200 µl of fresh SOC media.

The cells were transferred into Lysogeny broth (LB) (bacto-tryptone, bacto-yeast extract, NaCl, pH 7.0) agar plates containing 100 µg/ml ampicillin. In order to conduct blue white screening 100 µl IPTG (10mM), 100 µl (2% X-gal) were added to the LB plates prior to adding the cell suspended in SOC. The cells were incubated overnight at 37°C. Transformed colonies, containing pGEM-PACAP insert were selected, as transformed colonies appear white in contrast to blue colonies, that don't undergo transformation. Non-transformed plasmid contains LacZ gene which is induced by IPTG to produces β galactosidase enzyme, the β-galactosidase hydrolyzes X-gal to produce a blue pigment. If the LacZ gene is disrupted due to transformation

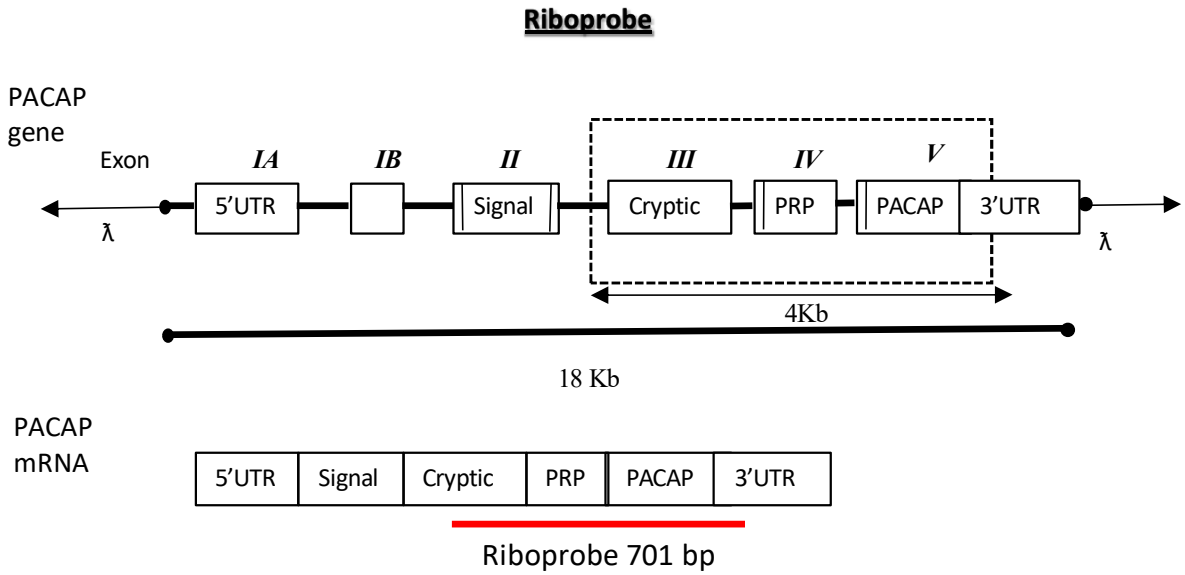

Figure 3.3: Digoxigenin labeled riboprobe was designed complementary to pituitary adenylate cyclase-activating polypeptide (PACAP) messenger ribonucleic acid (mRNA) (reference sequence: NM_001315503.1, region 303 – 1004) (NCBI, Blast: Basic Local Alignment Search tool). The PACAP gene consists of 5 exons, including a 5' untranslated region (5'UTR), signal peptide, cryptic peptide, PACAP related peptide (PRP), PACAP and a 3'UTR. The riboprobe designed for *in situ* hybridization targeted the region of PACAP mRNA consisting of the cryptic peptide, PACAP related peptide (PRP), PACAP, and the 3'UTR.

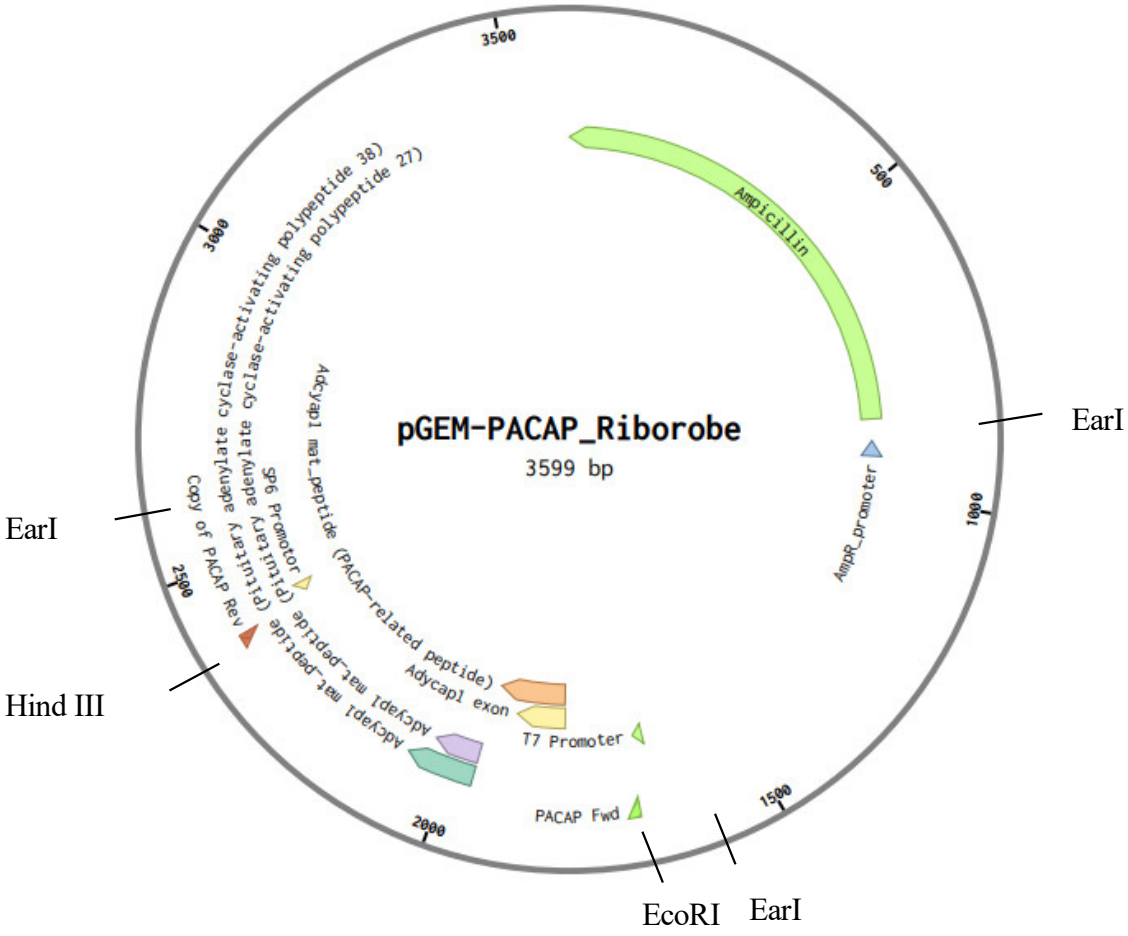

Figure 3.4: pGEM-PACAP was isolated from XL-1 blue cells using Ampicillin selection. The plasmid included the portion of the coding sequence of pituitary adenylate cyclase-activating polypeptide (PACAP) cDNA designed to generate riboprobe (reference sequence: NM_001315503.1, region 303 – 1004)(NCBI, Blast: Basic Local Alignment Search Tool). An SP6 promoter upstream of the PACAP sequence was utilized to generate antisense probe complementary to the PACAP messenger ribonucleic acid (mRNA). A T7 promoter was present to generate a sense probe. Restriction enzyme cut sites for EarI, EcoRI, and Hind III are shown in the figure. The plasmid was constructed using, Benchling [Sequence map]. (2019). Retrieved from: benchling.com

of the plasmid, this reaction doesn't occur and the colonies appear white (Blue-White Screening & Protocols for Colony Selection | Sigma-Aldrich n.d).

Transformed cells were grown in LB media containing 100 µg/ml of ampicillin. pGEM-PACAP was isolated from XL-1 blue cells using DNA extraction midiprep kit (QIAGEN-tip 100, Ontario, Canada). The protocol was followed as per the manufacturer's guidelines. The integrity of the PACAP sequence was confirmed through sequencing (University of British Columbia's Sequencing and bioinformatics consortium).

Linearizing plasmid

The plasmid was linearized using double restriction enzyme digests. A linearized plasmid used to generate the antisense probe using SP6 polymerase was generated by digesting the plasmid with EcoRI-HF and EarI (5 µl 10X CutSmart buffer, 1 µl EcorRI-HF (20 U), 1µl EarI (20U) to ~ 25µg of plasmid DNA). A linearized plasmid used to generate the sense probe using T7 pGEM PACAP was generated by digesting the plasmid with HindIII--HF and EarI (5 µl 10X CutSmart buffer, 1 µl HindIII-HF (20 U), 1µl EarI (20U) to ~ 25µg of plasmid DNA) (Figure 3.5). Restriction enzyme digests were conducted at 37^{o}C for 3 hr and enzymes were inactivated after the reaction by heating the sample at 80^{o}C for 20 mins. Linearized plasmids containing SP6 polymerase (antisense, 720 bp) or T7 polymerase (sense, 712 bp) were selected by running the sample on 1.5 % agarose gel at 100 V for 45 mins and excised from the gel using a bench top UV box and the Gene Jet extraction kit (Thermo scientific, California, USA) as per the manufacturer's guidelines (Figure 3.5).

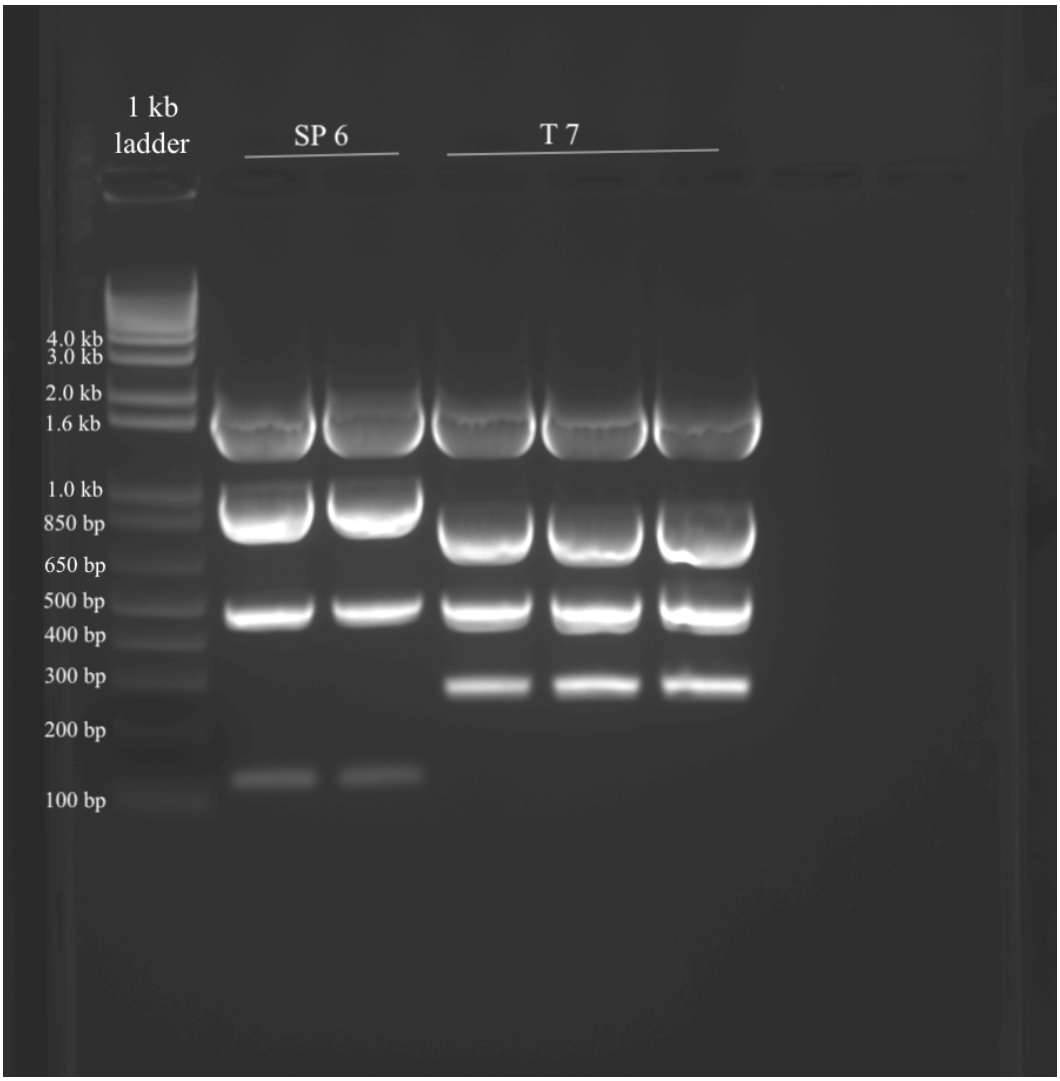

Figure 3.5: Restriction enzyme digestion was conducted to isolate Sp6 promoter (Antisense probe) and T7 promote (sense probe). The following restriction enzymes were used; EcoRI and EarI, and HindIII and Ear I. To generate respective strands. The antisense strand consisting of 721 base pairs and sense strand consisting of 712 base pairs was isolated using GeneJet extraction (Thermo scientific).

Transcription and Labelling of riboprobe with Digoxigenin

Antisense and sense riboprobes were transcribed from the isolated DNA fragment using SP6/T7 DIG RNA labelling kit (Millipore Sigma, Manheim, Germany). To generate antisense riboprobe complementary to PACAP mRNA; NTP labeling mixture (2 µl, 10 X), transcription buffer (2 µl, 10 X), SP6 RNA polymerase (2 µl), and protector RNase inhibitor (1 µl) was added to 1 µg of single stranded stand of DNA containing SP6 promoter upstream of PACAP sequence. Transcription was conducted at 37°C for 2 hrs. DNase I inhibitor (2 µl) was used to degrade genomic DNA; the reaction was conducted at 37°C for 15 mins. The transcription reaction was stopped using 2 µl of 0.2 M EDTA (pH 8.0).

The sense probe was transcribed and labelled in a similar manner using single stranded of DNA consisting of T7 promoter upstream of sequence complementary to PACAP sequence. The T7 promoter is required for the synthesis of the sense strand that has the same sequence as PACAP. The labelling efficiency was confirmed using dot blot analysis.

Dot Blot analysis of riboprobe concentration

Antisense or sense probes (1ul) at different concentrations; stock, 1:2, 1:4, 1:10 (dilution were made using DEPC treated water, 20X SSC and formaldehyde, in a ratio of 5:3:2) were dotted onto a positively charged nylon membrane in a grid pattern. A DIG labelled Neomycin (Millipore Sigma, Manheim, Germany) was run alongside the samples as a standard for determining the unknown concentration of the labelled antisense and sense probes. The concentrations of the standard controls were 100 ng/µl, 10 ng/µl, 1 ng/µl, and 0.1 ng/µl.

The probes and standards were baked onto the membrane by incubating the membrane at 80°C for 2 hrs. The nylon membrane was washed in 1X wash buffer (0.1 M maleic acid, 0.15 M

NaCl; pH 7.5; 0.3% Tween 20) for 2 mins, with gentle shaking, followed by incubation in 1X blocking buffer (Millipore Sigma) for 30 mins. The membrane was then transferred into blocking buffer containing 1:5000 anti-dig antibody (Millipore Sigma, Manheim, Germany), for 30 mins at RT. The membrane was washed twice for 10 mins in 1X wash buffer. The membrane was then equilibrated in 1X detection buffer (0.1 M Tris-HCl, 0.1 M NaCl, pH 9.5) for 5 mins, at RT, and incubated overnight in 2 ml 1X detection buffer with NBT/BCIP (0.375mg/ml NBT/9.4 mg/ml BCIP). The color reaction was stopped by soaking the membrane for 5 mins in distilled water. The intensity of the antisense and sense riboprobe "dots" were compared to the intensity of the standard controls to qualitatively deduce the concentration of the riboprobes.

The total (labeled and unlabeled) concentration of the antisense and sense probe was quantified using Nanodrop OneC microvolume UV-Vis spectrophotometer (Thermofisher scientific, Burlington, Ontario, Canada). The percentage of the labelled probe as observed from the dot blot, relative to the total concentration of the probes was used to deduce the labeling efficiency of the probes.

Riboprobe: *In situ* hybridization

. The protocol for *in situ* hybridization to detect PACAP mRNA expression using the above described riboprobe was adapted from DIG Application Manual for Nonradioactive *in situ* Hybridization (SIGMA-ALDRICH, 2008), the approach is described in Table 3.4. The protocol for *in situ* hybridization using riboprobe includes the same 4 key steps as used for the oligonucleotide probes; pre-hybridization, hybridization, post-hybridization and imaging. Antisense and sense probes were tested on PACAP +/+ brain samples during each run, with the sense probe acting as a control for non-specific binding. PACAP -/- brain samples provided a negative control, to assess specific binding of the antisense probe, as PACAP -/- mice do not

express PACAP mRNA. *In situ* hybridization was conducted using the riboprobes in a similar manner to the oligonucleotide probes. Key modifications in the protocol are detailed below.

Pre-hybridization

The samples were prepped for hybridization as before, with the Proteinase K concentration manipulated to allow the probes to penetrate the cell (0.25 µg/ml - 0.5 µg/ml) (Table 3.4). Pre-hybridization buffer (40 ul, 4XSSC in 50% deionized formamide) was added to the brain tissue and incubated at 37°C for 10 mins.

Hybridization

Hybridization buffer (30 µl) was prepared with; 40% deionized formamide, 10% dextran sulfate, 1× Denhardt's solution, 4× SSC, 10 mM DTT, 1 mg/ml yeast t-RNA, and 0 – 1 mg/ml of denatured and sheared salmon sperm DNA (see Table 3.4). The hybridization reaction was conducted at 42°C overnight in a humidity chamber. Antisense (10 ng) and sense probe (10 ng) were run on PACAP +/+ samples. When binding of the probes was observed in the PACAP +/+ sample, the experiment was repeated on a PACAP +/+ sample and on a PACAP -/- sample to confirm results with a biological negative control.

Post-hybridization

Following hybridization, the sections were washed in decreasing concentrations of SSC buffer (2X SSC (50 % formamide), 1X SSC, 0.1 X SSC) for 15 mins with gentle shaking 37°C to 60°C (Table 3.4) to remove non-specific binding. The slides were treated with or without RNase A at various concentrations (30 ng/ml – 20 µg/ml) (see Table 3.4), for 30 mins at 37°C, to eradicate background signals due to unbound riboprobe.

Table 3.4: *In situ* hybridization protocol development using a riboprobe. A digoxigenin labeled riboprobe was used to detect pituitary adenylate cyclase activating polypeptide (PACAP) messenger ribonucleic acid (mRNA) expression in the hypothalamus. Coronal brain section,from a wildtype mouse, inclusive of the hypothalamus, were used to test for detection of PACAP mRNA. Brain sections from PACAP knockout mice were used as negative controls to discern specific binding of probe to PACAP. Antisense riboprobe, complementary to PACAP mRNA and a control sense probe were used in each experiment. Various experimental conditions were manipulated in attempt to achieve specific binding of PACAP mRNA. The highlighted conditions were manipulated in each of the given runs. Runs marked in an asterisk (*) were rerun to confirm the results.

Experimental condition	Run 1	Run 2	Run 3	Run 4	Run 5	Run 6*	Run 7	Run 8
				Pre-Hybridization				
Proteinase K conc.	0.5 µg/ml	0.25 µg/ml	0.25 µg/ml	0.25 µg/ml	0.25 µg/ml	0.25 µg/ml	0.25 µg/ml	0.25 µg/ml
				Hybridization				
Salmon sperm DNA	1mg/ml	1mg/ml	1mg/ml	1mg/ml	1mg/ml	1mg/ml	No salmon sperm DNA added	1mg/ml
				Post-Hybridization				
RNase A	No RNase A	20µg/ml	20 µg/ml	20 µg/ml	30ng/ml	No RNase A	No RNase A	No RNase A
Temperature	37°C	60°C	52°C	37°C	52°C	52°C	52°C	52°C
Results	Non-specific binding was present. Tissue was damaged	Probe did not bind to PACAP mRNA.	Probe did not bind to PACAP mRNA.	Probe did not bind to PACAP mRNA.	Probe did not bind to PACAP mRNA.	The sense probe was binding to PACAP +/+. No binding was seen in the antisense probe.	Probe did not bind to PACAP mRNA.	The sense probe was binding to both the wild type and knockout sample. Antisense probe did not bind to PACAP mRNA.
Analysis of the run	1.Proteinase K concentration was too high 2. Unbound RNA might be resulting in high background. 3. Low temperature might be resulting in non-specific binding	Stringency might be too high due to the increase in temperature.	Post-hybridization temperature was still too high.	1.RNase A concentration might have been high resulting in degradation of all the RNA. 2. Based on results from Run 1, post-hybridization temperature might be high.	RNase A regardless of the concentration used was resulting in degradation in riboprobe.	Salmon sperm DNA might have been binding to antisense riboprobe.	1. Salmon sperm DNA was not the issue. 2. PACAP -/- sample was needed to ensure that sense probe was binding non-specifically.	Labelling efficiency of antisense probe might have been low. The probes need to be synthesized again.

Imaging

Slide preparation for detection of DIG label was done using DIG nucleic acid detection kit (Millipore Sigma, Manheim, Germany). The slides were rinsed in 1X wash buffer (0.1 M maleic acid, 0.15 M NaCl; pH 7.5; 0.3% Tween 20) for 10 min, twice, with gentle agitation. To reduce non-specific binding brain sections were incubated for 30 mins in a humidity chamber with 1X blocking buffer (100 µl), followed by a 2 hr incubation in 1:250 anti-dig antibody (Millipore Sigma, Manheim, Germany) (diluted in 1X blocking buffer) at RT. The slides were washed in wash buffer for 10 mins, twice (with gentle agitation at rt) followed by equilibration in 1X detection buffer (0.1 M Tris-HCl, 0.1 M NaCl, pH 9.5) for 10 mins at RT. The slides were then incubated o/n at RT with, color reaction consisting of NBT/BCIP (200 µl) (0.375mg/ml NBT/9.4 mg/ml BCIP) in detection buffer. The color reaction was stopped using 10 mM Tris-HCl (pH 8.1), 1 mM EDTA, the slides were rinsed in distilled water and mounted using Immunomount mounting media (Fisher scientific, Ontario, Canada). Visualization of label, was performed using brightfield microscopy (BX61 Olympus microscope, Richmond Hill, ON, Canada).

3.3 Results

After repeated attempts, using two different strategies for probe development, we were unable to develop an *in situ* hybridization protocol that specifically detected PACAP mRNA in mouse brain sections. My experimental approach to troubleshooting did however make significant progress towards development of a PACAP specific *in situ* hybridization protocol, by confirming experimental criteria for several key steps within the 5 stages of *in situ* hybridization discussed above.

Results from Strategy 1, Oligonucleotide probes

A combination of factors was changed in each run (Table 3.3) (Figure 3.6). Key modifications were made in the 4 stages of *in situ* hybridization as detailed below:

Pre-hybridization: Permeabilization

Starting concentrations of Proteinase K (1 µg/ml) as per recommendation (Sigma-Aldrich, 2008) for tissue permeabilization resulted in tissue sections that were severely over digested, and no probe binding was detected (Table 3.3). The Proteinase K concentration was therefore decreased to 0.5 µg/ml (Figure 3.6 E), and 0.05 µg/ml (figure 3.6 D) which improved tissue morphology (Figure 8 D, E) as noted by clearly identifiable anatomical landmarks within in the hypothalamus; the 3rd ventricle, the VMN, and the arcuate nuclei (Figure 3.6 A – E). A Proteinase K concentration of 0.5 µg/ml, resulted in a positive colorimetric reaction (Figure 3.6 E), suggesting an appropriate stringency for probe penetration while maintaining tissue morphology, and was therefore used in subsequent *in situ* hybridization runs.

Hybridization: Temperature, Blocking, Probe concentration

A starting hybridization reaction temperature of 37°C as recommended (Sigma-Aldrich, 2008) resulted in no probe binding (Table 3.3). As such, in subsequent runs, hybridization temperature was reduced to 30°C to facilitate binding, however, no probe binding was detected (Table 3.3, 3.5). An increase in hybridization temperature to 40°C did not promote binding either (Table 3.5, Figure 3.6). In further attempt to encourage probe binding, oligoprobe concentration was increased from 30 ng to 100 ng (Table 3.3), and the concentration of blocking reagent; salmon sperm DNA, was decreased from 500 µg/ml to 100 µg/ml (Table 3.3). Despite these

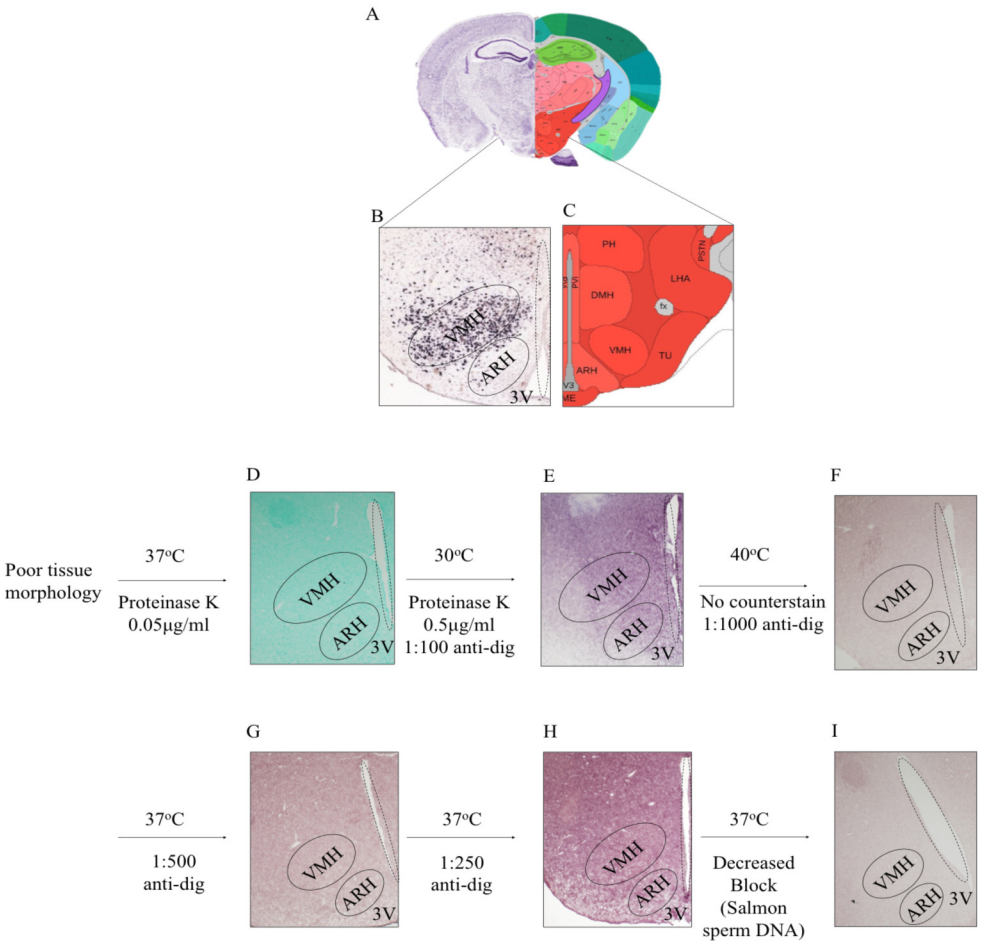
A
B
C
VMH
ARH
3V
PH
LHA
DMH
fx
VMH
TU
ARH
PSTN
Poor tissue morphology
37°C
Proteinase K 0.05µg/ml
D
30°C
Proteinase K 0.5µg/ml 1:100 anti-dig
E
40°C
No counterstain 1:1000 anti-dig
F
37°C
1:500 anti-dig
G
37°C
1:250 anti-dig
H
37°C
Decreased Block (Salmon sperm DNA)
I

Figure 3.6: Results of *in situ* hybridization (ISH) for Pituitary adenylate cyclase activating polypeptide (PACAP) using oligonucleotide probes. *In situ* hybridization was conducted on brain samples obtained from a C57Bl6 wildtype mouse (n=1). Image (**A**) obtained from Allen Brain Atlas (Image 71), depicts the spatial context of the coronal section of the hypothalamus. Image (**B**) from the Allen Brain Atlas represents the known expression of PACAP mRNA in the hypothalamus of mice, as deduced using *in situ* hybridization. Image(**C**) represents a diagram of anatomical landmarks of the hypothalamus; the 3rd ventricle (3V), ventromedial nucleus (VMN), and the arcuate nucleus (ARC). ISH was conducted using 50bp oligonucleotide probes designed to target cryptic peptide and PACAP-related peptide, labelled with Digoxigenin (Dig). Images **D – I** are representative images of *in situ* hybridization runs conducted under 4X magnification using brightfield microscopy. Critical experimental conditions were modified. The various nuclei in the images are not to scale.

Allen Institute.© [2004] Allen Institute for Brain Science. Allen Mouse Brain Atlas, Coronal. Available from: atlas.brain-map.org/atlas

Allen Institute.© [2004] Allen Institute for Brain Science. Allen Mouse Brain ISH Atlas, Coronal. Available from: mouse.brain-map.org/gene/show/1103.

Table 3.5: Analysis of *in situ* hybridization (ISH) protocol using oligonucleotide probes. Digoxigenin (DIG) labeled oligonucleotide probes were designed. The probes (2) targeted the cryptic peptide (CRP) and PACAP-related peptide (PRP) within the pituitary adenylate cyclase activating polypeptide (PACAP) messenger ribonucleic acid (mRNA) sequence. Binding of the probes was detected using anti-digoxigenin (anti-dig) antibody. Various modifications were made (Run1 – Run 14) in the protocol to achieve specific binding of oligonucleotide probes to PACAP mRNA. The results of each run were analyzed in order to develop a strategy for the subsequent run.

	Run 1	Run 2	Run 3	Run 4	Run 5	Run 6	Run 7
Results	Tissue morphology was disrupted	Probe did not bind to PACAP mRNA.	Probe did not bind to PACAP mRNA.	Probe did not bind to PACAP mRNA.	• Probe did not bind to PACAP mRNA. • High background	• Probe did not bind to PACAP mRNA. • Low background	• Probe did not bind to PACAP mRNA. • Low background
Analysis	Proteinase K concentration was too high	• Hybridization temperature might have been high. • Probe concentration could have been low	• Probes were potentially not penetrating the cell. • Low hybridization temperature was not promoting binding	Hybridization temperature might have been low.	• The two probes might be inhibiting the binding to PACAP mRNA. • Anti-Digoxigenin concentration was too high.	• Anti-dig concentration might have been too low. • High temperature might be causing stringent conditions for binging.	Anti-dig concentration might have been too low.

Table 3.5: Continued.

	Run 8	Run 9	Run 10	Run 11	Run 12	Run 13	Run 14
Results	Probe did not bind to PACAP mRNA.	• Probe did not bind to PACAP mRNA. • High background	• Probe did not bind to PACAP mRNA. • Low background	Probe did not bind to PACAP mRNA.	Probe did not bind to PACAP mRNA.	Probe did not bind to PACAP mRNA.	Probe did not bind to PACAP mRNA.
Analysis	Anti-dig concentration seemed sufficient. Since it is critical Run 9 was conducted to ensure 1:100 too high a concentration.	• Anti-dig concentration was too high. • Oligonucleotide probe targeting cryptic peptide within PACAP mRNA might be not be binding to PACAP mRNA	• Using probes separately might be resulting in low sensitivity. • Probe concentration might have been too low.	Probe concentration might have been too low.	The concentration of blocking reagents might be inhibiting binding of probes to PACAP mRNA.	The concentration of blocking reagents might be inhibiting binding of probes to PACAP mRNA.	Oligonucleotide probes were not a successful tool in detection of PACAP mRNA.

modifications to the protocol, examining the tissues revealed no decipherable binding of the probe (Figure 3.6).

Post-hybridization and Imaging: Antibody concentration, blocking

The anti-dig antibody concentration initially used was, 1:100 as per recommendation (SIGMA-ALDRICH, 2008). This resulted in high background staining in both the antisense and sense treated tissue section, with no specific binding in the antisense section (Figure 3.6 E). In order to equilibrate the color reaction, the anti-dig antibody concentration was tittered between 1:100 -1:1000, an anti-dig concentration of 1:250 resulted in a successful equilibration of the color reaction (Figure 3.6 H). Neither of the anti-dig concentrations however were successful in detecting probe hybridization (Figure 3.6 G - H). The concentration of blocking reagent, normal sheep serum, was reduced to 1%, instead of 2% in blocking buffer (Table 3.3), the concentration of the blocking reagent did not promote probe binding (Figure 3.6 I).

The combination of variables in the experiment showed that the oligonucleotide probes did not successfully bind to PACAP mRNA (Figure 3.6).

Results from Strategy 2, Ribonucleotide probe (riboprobe)

Riboprobes were alternatively used to increase the sensitivity of the *in situ* hybridization reaction. The labeled concentration of both (antisense, sense) probes was approximately 10 ng/µl each (Figure 3.7). The labeling efficiency of the antisense probe was 4.85%, and the sense probe was 33.3%.

Critical modifications in the protocol were made in attempts to detect specific expression of PACAP mRNA (Table 3.4). As with the oligonucleotide probe, we approached key steps in the pre-hybridization, hybridization, post-hybridization, and imaging conditions.

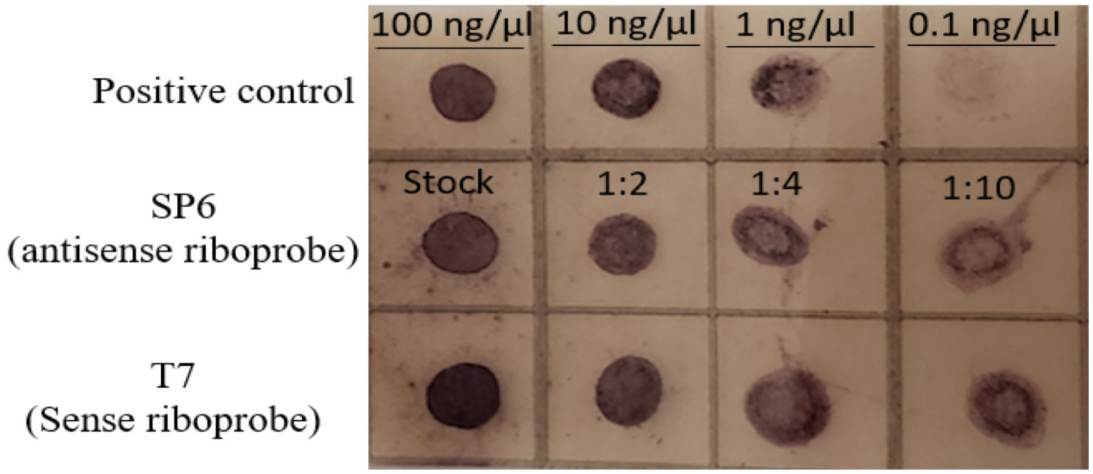

Figure 3.7: Colorimetric dot blot analysis of Digoxigenin (DIG) labelled antisense and sense probe. The binding efficiency of antisense and sense strand of the riboprobe was assessed using dot blot analysis. DIG-labelled Neomycin RNA of known concentration (Cat. No. 11 175 025 910) was run as a positive control, at various different concentrations (100, 10, 1 , 0.1 ng/µl). Antisense and sense riboprobe were tittered (stock, 1:2, 1:4, 1:10) to qualitatively assess labelling efficiency as deduced by intensity of the Dot Blot in comparison to controls. The analysis was run twice and same results were obtained.

Pre-hybridization: Permeabilization

The initial run was done with a Proteinase K concentration of 0.5 µg/ml, the tissue however appeared over digested (Table 3.4). A decrease in Proteinase K concentration to 0.25 µg/ml, rescued the morphology of the tissue, and was therefore used for subsequent runs (Table 3.4).

Hybridization: Blocking reagent

To promote binding of the probes the concentration of the blocking reagent, salmon sperm DNA was reduced from an initial concentration of 1 mg/ml to 0 mg/ml (Table 3.4). The concentration of the salmon sperm DNA did not influence probe binding.

Post-hybridization and Imaging: Temperature, RNase A concentration

Primarily post-hybridization was conducted at 37°C, this resulted in non-specific binding of the antisense probe and the sense probe (Table 3.4). To promote specific binding of the antisense probe to PACAP mRNA, the temperature was increased to 60°C (Table 3.4). This resulted in the loss of binding of both the antisense and the sense probes. At a post-hybridization temperature of 52°C, we were able to recover probe binding, however only non-specific binding of the sense probe was detected (Figure 3.8). Parallel to the post-hybridization temperature, the RNase A concentration was manipulated (0 – 20 µg/ml). In the presence of RNase A, we failed to see any distinctive probe binding (Table 3.4).

3.4 Discussion

I present here a significant body of work towards the development of an *in situ* hybridization protocol to detect PACAP mRNA in mouse hypothalamus, troubleshooting both

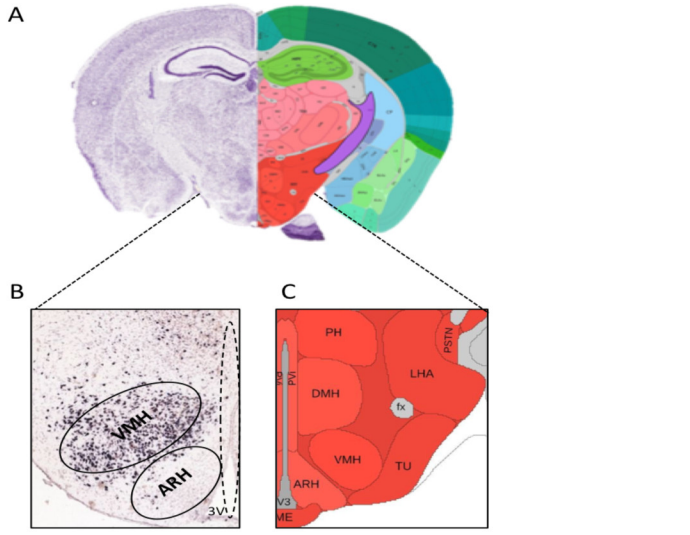
A
B
C
VMH
ARH
3V
PH
PSTN
LHA
DMH
fx
VMH
TU
ARH

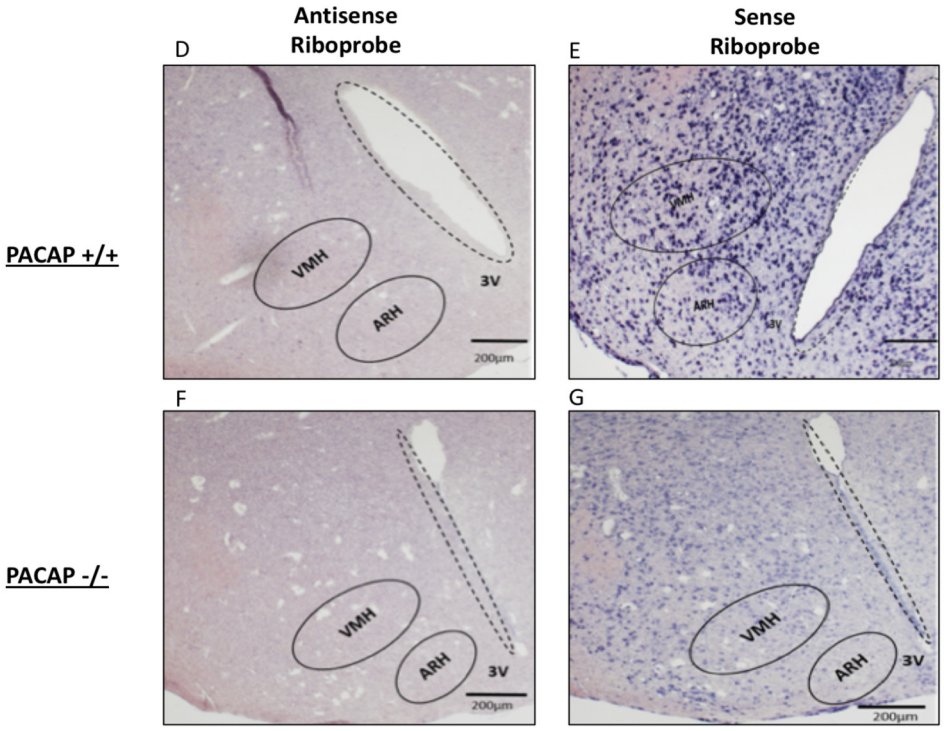
Antisense Riboprobe
Sense Riboprobe
D
E
PACAP +/+
VMH
ARH
3V
200μm
F
G
PACAP -/-
VMH
ARH
3V
200μm

Figure 3.8: Results of *in situ* hybridization (ISH) targeting PACAP mRNA using ribonucleic acid probes (riboprobe). Images on the left-hand panel (**A – C**) were obtained from the Allen Brain Atlas. Image **A** is a spatial orientation of the mouse brain (image 71 on the Allen Brain Atlas). Image (**B**) is the expected expression of PACAP mRNA in the hypothalamus. Image (C) is a diagram representing the anatomical landmarks in the hypothalamus such as; the 3rd ventricle, ventromedial nucleus (VMN), arcuate nucleus (ARH). Images (**D-G**) are representative images from run 8 of the *in situ* hybridization protocol conducted at 4X mag using brightfield microscopy. *In situ* hybridization was conducted using brain tissues isolated from a PACAP wildtype (+/+) mouse (n = 1) **(D – E),** and a PACAP knockout (-/-) mouse (n = 1) **(F- G)**. On both the PACAP +/+ and PACAP -/- samples, an antisense probe was used **(D) (F),** a sense probe was used as a technical negative control (**E**) (**G**).

Allen Institute.© [2004] Allen Institute for Brain Science. Allen Mouse Brain Atlas, Coronal. Available from: atlas.brain-map.org/atlas

Allen Institute.© [2004] Allen Institute for Brain Science. Allen Mouse Brain ISH Atlas, Coronal. Available from: mouse.brain-map.org/gene/show/1103.

the use of oligonucleotide probes and a riboprobe. While we were not able to develop a complete protocol, the results presented here suggest the following key recommendations for further work towards establishing this protocol.

We were successful in getting the riboprobe to penetrate the cells, as demonstrated through non-specific binding of the probes (Figure 3.8). However, further work needs to be done to attain specific binding. After significant troubleshooting, we concluded oligonucleotide probes used in our experimental design were not a reliable tool in detecting PACAP mRNA expression. After manipulating multiple key factors and thoroughly analyzing the results, we saw no indication of probe binding in our experiment, to suggest the oligonucleotide probes were binding to PACAP mRNA. Oligonucleotide probes are short in length (around 50 bp) the probes incorporate a single label, which could decrease the sensitivity of *in situ* hybridization reaction using oligonucleotide probes. Since the oligonucleotide probes did not work, a further investment of time and resources in pursuit of getting the oligonucleotide probes to bind was not feasible.

We were successfully able to determine the Proteinase K concentration required for probe permeabilization. Proteinase K is a broad-spectrum protease commonly used to prepare tissue for *in situ* hybridization (Gerard J, 2013). The permeabilization step is one of the most critical steps in, *in situ* hybridization (SIGMA-ALDRICH, 2008). The concentration of Proteinase K used and the duration of exposure to Proteinase K is not only integral to maintaining tissue morphology but has been shown to influence the sensitivity of the in the *in situ* hybridization reaction (Gerard J, 2013). Over-digestion of tissues could compromise the availability of mRNA, whereas a low concentration of Proteinase K interferes with probe penetration. We had initially used 1 µg/ml of Proteinase K. Brain tissues are fatty in nature, and do not require stringent Proteinase K

treatment, additionally thin sections of the tissue were mounted on the slides (10 µm) due to which the high concentration of Proteinase K resulted in distortion of the tissue. (Young, Jackson, & Wyeth, 2020).We therefore found that a concentration of 1 µg/ml was too stringent for brain tissues, a concentration of 0.25 µg/ml was sufficient to permeabilize tissue sections and maintain tissue integrity (Table 3.4).

Once we had optimized tissue penetration, critical modifications were made in the hybridization, post-hybridization and imaging stages of the *in situ* hybridization protocol in attempts to improve the specificity of probe binding for both oligonucleotide probes and the riboprobe. In the hybridization reaction, we first manipulated probe concentration. While it has been suggested that a low concentration of probe can lead to low signals, high concentrations of probe may result in high background signal (Gerard J, 2013). In troubleshooting the oligonucleotide probes, concentrations from 30 ng – 100 ng (Table 3.3), we did not observe an influence on probe binding. Based on this result, we did not manipulate the concentration of the riboprobes and instead used a concentration of 10 ng/µl that was easily observed on the dot blot.

Since hybridization temperature is critical to ensure specific bond formation between the target mRNA and the probe hybridization temperature affects the specificity of probe binding, with higher temperatures increasing the stringency of the reaction. Long probes (riboprobes -701 nt) have a higher GC content and therefore require a higher hybridization temperature, as compared to shorter probes (oligonucleotide – 50 nt)("Hybridization Conditions and Melting Temperature – Lablogatory," n.d.). We, therefore, started our approach by conducting hybridization reactions using oligonucleotide probes at 37°C, and riboprobes at 42°C. Since attempts resulted in no probe binding, hybridization was lowered to 30°C (Table 3.3) with the goal of reducing the stringency of the reaction and promoting probe binding. Unfortunately,

decreasing the hybridization temperature did not promote specific probe binding in our reaction, and we, therefore, pursued our experiment with the original hybridization temperatures of 42°C for riboprobes and 37°C for oligonucleotide probes. Finally, in an attempt to support probe binding, the concentration of the blocking reagent was decreased (Table 3.3, 3.4), however, none of these modifications resulted in binding of the probes to PACAP mRNA in the brain samples.

The post-hybridization temperature did not influence probe binding using oligonucleotide probes. However, the binding of the riboprobes was highly influenced by the post-hybridization temperature (Figure 3.8). To ensure probe binding was not being lost with high stringency post hybridization washes, we lowered post-hybridization washes to occur at 37°C, which increased non-specific probe binding, but not specific binding of the riboprobe. Instead, PACAP+/+ and PACAP-/- brain samples with both antisense and sense probes, showed probe binding suggesting non-specific binding of riboprobe to the brain tissue. Once non-specific binding had been achieved, we then increased the stringency of post hybridization washes by increasing the post-hybridization temperature to 52°C. This resulted in the sense probe (control) binding in the brain, but no antisense probe binding (Table 3.4) (Figure 3.8). The binding of the sense probe was present in the PACAP +/+ and PACAP -/- brain sample (Figure 3.8). The binding was therefore attributed to non-specific binding.

While this pattern of binding was unexpected it led us to suspect that there was discrepancy in the labelling efficiency of the antisense and sense probe. In order to confirm this, we measured the concentration of antisense and sense riboprobe. The percentage of the labelled probe relative to total probe concentration was used to deduce labelling efficiency. The labelling efficiency of the antisense probe was 4.85%, which was lower than the sense probe 33.3%. This

was a great indication that relabeling of the probes, with a higher labelling efficiency could potentially assist in riboprobe hybridization to PACAP mRNA.

Future directions

The riboprobes are a promising tool to detect PACAP mRNA. The work we have invested into troubleshooting the *in situ* hybridization protocol has allowed me to suggest the following next steps:

1. Re-synthesize and label the riboprobes: Prior to proceeding with further troubleshooting with the hybridization reaction, I suggest that more antisense and sense riboprobe is synthesized and labelled. The labelling efficiency is extremely critical, as a low labelling efficiency would greatly reduce the sensitivity of the *in situ* hybridization reaction. Results from analysing the results suggest the antisense probe had low labelling efficiency which may have contributed to the unexpected results shown in Figure 3.8.

2. Secondary Structure of the probe: Another critical factor that could potentially affect probe binding is the conformation of the probes. Intramolecular base pairing could occur, resulting in decreased binding efficiency (Farrell Jr, 2005). To counteract this, prior to conducting the hybridization reaction, riboprobes could be briefly heated to 80°C to disrupt the intramolecular bonds, followed by cooling the probes immediately on ice to maintain the riboprobes in an open conformation suitable for binding.

3. Post hybridization temperature: The post-hybridization temperature is critical in regulating the stringency of post-hybridization conditions. The antisense probe bound non-specifically at 37°C (Table 3.4), however increasing the stringency with a post-hybridization temperature of 52°C, resulted in loss of binding of the antisense probe (Figure 3.8). The post-hybridization

temperature could be decreased to 42°C to decrease stringency, so that specific binding of the probe to the target sequence isn't loss.

In situ hybridization is the gold standard to measure mRNA *in situ,* but is known as a challenging protocol to optimize and design. A robust *in situ* hybridization protocol is critical to validating the efficiency of the AAV9-SF1-PACAP, as a tool inducing PACAP expression exclusively in the VMN as it allows visualization of PACAP mRNA in specific neurons of the hypothalamus and therefore will allow us to identify specific neurons that are expressing PACAP which will allow neuroanatomical localization of the PACAP expressing cells and allow us to assess the number of cells expressing PACAP in the various nuclei of the hypothalamus. An alternate approach that is used to localize expression, is immunohistochemistry. Immunohistochemistry analysis involves using antibodies, that target a specific epitope on a protein. However, as aforementioned PACAP peptide shares high structural homology with other peptide in PACAP/VIP superfamily (McRory et al., 2000), therefore an antibody that specifically detects the PACAP peptide is challenging to design and the results would likely be questioned, and require additional confirmation through detection of nucleic acid .

Additionally, having an optimized *in situ* hybridization protocol for PACAP mRNA would be an asset in the Gray lab as they are leading research in PACAP physiology and energy metabolism, and the ability to detect PACAP mRNA expression in brain tissue and other tissue involved in regulating energy metabolism, such as ganglia of the autonomic nervous system and adipose tissue, will be critical for various other projects currently being initiated in the lab.

Chapter 4

Concluding Remarks

4.1 Summary

The overarching goal for the work completed in this thesis was to (**A**) Develop a protocol using adeno associated virus for transgenic overexpression of PACAP in the VMN, and (**B**) Develop a sensitive and specific protocol for *in situ* hybridization to detect PACAP mRNA expression to confirm the expression of PACAP in the VMN upon transgenic overexpression. As such, the goals of our research were as following:

1. Develop a stereotaxic surgery protocol to deliver the control virus scAAV9-SF1-eGFP into the VMN of the hypothalamus.
2. Confirm the expression of AAV9-SF1-eGFP plasmid in the VMN to elucidate the specific expression of eGFP in the VMN using morphological assessment of the brain.
3. Develop an immunohistochemistry protocol to detect SF1 immunoreactivity, using commercially available SF1 antibodies to confirm an overlap in eGFP expression and SF1 immunoreactivity using a molecular technique.
4. Develop a protocol for *in situ* hybridization to detect PACAP mRNA expression in the hypothalamus.

Chapter 2 focused on the first three aims of our research. Previous work done in the Gray lab had shown that the scAAV9-SF1-eGFP virus is a great tool to deliver the virus to the hypothalamus (Cline, 2020). However, the expression of the vector was 0.025 mm superior to VMN; additionally, the administration of a high viral dose resulted in leakiness of the virus (Cline, 2020). We, therefore, adjusted the coordinates of the stereotaxic surgery to deliver the virus at an increased depth, and we decreased the concentration of the viral dose. Combining the

two factors resulted in the successful delivery of scAAV9-SF1-eGFP in the VMN as determined by the morphological assessment of the hypothalamus (Figure 2.4).

To confirm our results using a molecular technique, we developed an immunohistochemistry protocol using commercially available SF1 antibody. The antibody was not specific for SF1 protein, as was confirmed by Western blot analysis (Figure 2.5, 2.6). We tested three commercial antibodies' integrity using Western blot analysis to ensure specific binding of the antibodies to SF1 protein. Neither of the antibodies SF1 were specific. Due to the sparsity of commercially available SF1 antibodies specific for SF1 protein, I have suggested either collaborating with an independent lab that has synthesized an SF1 antibody (Yokoyama et al., 2009) or use a neuroanatomical dye to confirm the expression of eGFP in the VMN.

In chapter 3, we focused on our aim 4. *In situ* hybridization is a complex protocol to design and optimize. To establish an *in situ* hybridization protocol to detect PACAP mRNA, we designed two different Digoxigenin labeled probes, an oligonucleotide probe and a riboprobe. We thoroughly troubleshooted the *in situ* hybridization protocol; while we were unable to establish a complete protocol for *in situ* hybridization, we could conclude that the oligonucleotide probes were not a reliable tool to detect PACAP mRNA expression (Figure 3.6). The riboprobes, on the other hand, did generate a signal. However, the signal was detected in the negative control (sense probe) (Figure 3.8). Upon analysis of the riboprobes' labeling efficiency, we found that the antisense probe complementary to PACAP mRNA had a low labeling efficiency compared to sense probe (control). Therefore, I recommend re-labeling the riboprobes before proceeding with *in situ* hybridization.

4.2 Significance

Obesity is a growing health concern globally. The development of obesity is associated with various health conditions (Van Gaal et al., 2006). Obesity is caused by an imbalance in energy homeostasis, whereby the energy input exceeds exergy expenditure occurring through basal metabolic rate, physical activity, and thermogenesis. While it is essential to maintain a healthy lifestyle by consuming a balanced diet and staying physically active, the development of obesity is more complicated. To develop a therapeutic target to overcome obesity and its comorbidities it is essential to understand the pathophysiology of the development of obesity. Endocrine factors play a critical role in regulating energy metabolism. A crucial endocrine factor regulating energy expenditure is PACAP. PACAP is a neuroendocrine factor required for regulating adaptive thermogenesis (Diané et al., 2014; Gray et al., 2002). Research on animal models has shown that PACAP expression's absence results in a cold-sensitive phenotype (Diané et al., 2014; Gray et al., 2002). PACAP regulates thermogenesis through the SNS. In our research, we focused on the role of the central expression of PACAP, precisely in the VMN, on the regulation of thermogenesis. Our work aims to develop a transgenic line of mice that express PACAP only in the VMN to rescue the cold-sensitive phenotype of the PACAP -/- mice.

Pharmacological studies show strong evidence that PACAP expressed in the VMN, at pharmacological doses has a significant effect on regulation of adaptive thermogenesis (Banki et al., 2014; Resch et al., 2011). However, to understand the neurocirculatory effect of PACAP that is endogenously expressed in the VMN, a genetic approach is more robust. In order to develop a protocol to deliver AAV9-SF1-PACAP in the VMN to the transgenic animal, we conducted preliminary stereotaxic surgeries using a control AAV9-SF1-eGFP plasmid in order to develop an injection protocol to deliver

virus specifically in the VMN. A precise injection protocol for AAV mediated therapy is essential, for all future physiological experiments that will be run in the Gray lab on transgenic mice. Based on the morphological assessment we were successful in delivering the AA9-SF1-eGFP virus specifically in the VMN. Stereotaxic surgeries are challenging to perform due to the complexity of delivering a viral dose in a small region of the hypothalamus, an *in situ* hybridization protocol to detect PACAP mRNA will be critical to confirm accurate delivery of vector. Upon administration of AAV9-SF1-PACAP, it will be crucial to ensure specific expression of PACAP mRNA in the VMN, using *in situ* hybridization. We have made great progress to develop a sensitive and specific *in situ* hybridization protocol using riboprobes to detect PACAP mRNA expression in the hypothalamus.

With the work done in this thesis to establish a protocol to overexpress eGFP and PACAP in the VMN of the hypothalamus, preliminary physiological experiments could be conducted using the established coordinates for stereotaxic surgery. The AAV9-SF1-eGFP virus will need to be administered in the VMN in C57Bl6 mice. Additionally, sham experiments will need to be done using saline to confirm that the delivery of the virus and/or stereotaxic surgery has no significant effect on thermogenesis. This will allow us to make robust comparisons once AAV9-SF1-PACAP is administered into the VMN to confirm that PACAP expressed in the VMN is required for adaptive thermogenesis.

In conclusion, while historically lesioning studies of the VMN have been done to understand the role of VMN in energy expenditure (Nishizawa & Bray, 1978), and recent work has been done using a pharmacological approach to study and establish the crucial

role of PACAP in energy metabolism (Banki et al., 2014; Resch et al., 2011, 2013). As per my knowledge there has been no recovery studies conducted using a genetic approach to induce PACAP expression in the VMN in a PACAP -/- to observe a rescue in cold sensitive phenotype in the -/- mice. The development of a transgenic mice which expresses PACAP in the VMN will be of immense value to the current literature and our understanding of the effect of PACAP expression in the VMN on thermogenesis. The findings from our physiological studies on transgenic mice expressing PACAP in the VMN, could be used in the future to design therapeutic targets to combat obesity.

References

Banki, E., Pakai, E., Gaszner, B., Zsiboras, C., Czett, A., Bhuddi, P. R. P., … Garami, A. (2014). Characterization of the Thermoregulatory Response to Pituitary Adenylate Cyclase-Activating Polypeptide in Rodents. *Journal of Molecular Neuroscience*, *54*(3), 543–554. https://doi.org/10.1007/s12031-014-0361-0

Bechtold, D. a, Luckman, S. M., Hawke, Z., Ivanov, T. R., Dhillon, H., & Lowell, B. B. (2006). PACAP neurons in the hypothalamic ventromedial nucleus are targets of central leptin signaling. *The Journal of Neuroscience : The Official Journal of the Society for Neuroscience*, *147*(47), 14828–14835. https://doi.org/10.1210/en.2006-0753

Bingham, N. C., Anderson, K. K., Reuter, A. L., Stallings, N. R., & Parker, K. L. (2008). Selective loss of leptin receptors in the ventromedial hypothalamic nucleus results in increased adiposity and a metabolic syndrome. *Endocrinology*, *149*(5), 2138–2148. https://doi.org/10.1210/en.2007-1200

Bishop, R. (2010, March 1). Applications of fluorescence in situ hybridization (FISH) in detecting genetic aberrations of medical significance. *Bioscience Horizons*. Oxford Academic. https://doi.org/10.1093/biohorizons/hzq009

BLAST: Basic Local Alignment Search Tool. (n.d.). Retrieved June 12, 2019, from https://blast.ncbi.nlm.nih.gov/Blast.cgi

Blue-White Screening & Protocols for Colony Selection | Sigma-Aldrich. (n.d.). Retrieved October 26, 2020, from https://www.sigmaaldrich.com/technical-documents/articles/biology/blue-white-screening.html

Cannon, B., & Nedergaard, J. (2004). Brown Adipose Tissue: Function and Physiological Significance. *Physiological Reviews*, *84*(1), 277–359. https://doi.org/10.1152/physrev.00015.2003

Carter, M., & Shieh, J. (2015). Stereotaxic Surgeries and In Vivo Techniques. In *Guide to Research Techniques in Neuroscience* (pp. 73–88). Elsevier. https://doi.org/10.1016/b978-0-12-800511-8.00003-4

Chevalier, J., Yi, J., Michel, O., & Tang, X.-M. (1997). *Biotin and Digoxigenin as Labels for Light and Electron Microscopy in Situ Hybridization Probes: Where Do We Stand? The Journal of Histochemistry & Cytochemistry* (Vol. 45). Retrieved from https://journals.sagepub.com/doi/pdf/10.1177/002215549704500401

Choi, S., Sparks, R., Clay, M., & Dallman, M. F. (1999). Rats with hypothalamic obesity are insensitive to central leptin injections. *Endocrinology*, *140*(10), 4426–4433. https://doi.org/10.1210/endo.140.10.7064

Choi, Sujean, & Dallman, M. F. (1999). *Hypothalamic Obesity: Multiple Routes Mediated by Loss of Function in Medial Cell Groups**. Retrieved from https://academic.oup.com/endo/article-abstract/140/9/4081/2990720

Cline, D. L. (2020). *Role of pituitary adenylate cyclase-activating polypeptide in energy*

expenditure including the thermogenic response | University of Northern British Columbia Institutional Repository. Retrieved from https://unbc.arcabc.ca/islandora/object/unbc%3A59035?solr_nav%5Bid%5D=c41c24644b0d12191a18&solr_nav%5Bpage%5D=0&solr_nav%5Boffset%5D=0

Cohen, P., Zhao, C., Cai, X., Montez, J. M., Rohani, S. C., Feinstein, P., … Friedman, J. M. (2001). Selective deletion of leptin receptor in neurons leads to obesity. *Journal of Clinical Investigation*, *108*(8), 1113–1121. https://doi.org/10.1172/JCI200113914

Cone, R. D. (2005, May 26). Anatomy and regulation of the central melanocortin system. *Nature Neuroscience*. Nature Publishing Group. https://doi.org/10.1038/nn1455

Cypess, A. M., Lehman, S., Williams, G., Tal, I., Rodman, D., Goldfine, A. B., … Kahn, C. R. (2009). Identification and importance of brown adipose tissue in adult humans. *The New England Journal of Medicine*, *360*(15), 1509–1517. https://doi.org/10.1056/NEJMoa0810780

Dayton, R. D., Wang, D. B., & Klein, R. L. (2012, June). The advent of AAV9 expands applications for brain and spinal cord gene delivery. *Expert Opinion on Biological Therapy*. Expert Opin Biol Ther. https://doi.org/10.1517/14712598.2012.681463

Dhillon, H., Zigman, J. M., Ye, C., Lee, C. E., McGovern, R. A., Tang, V., … Lowell, B. B. (2006). Leptin directly activates SF1 neurons in the VMH, and this action by leptin is required for normal body-weight homeostasis. *Neuron*, *49*(2), 191–203. https://doi.org/10.1016/j.neuron.2005.12.021

Diané, A., Nikolic, N., Rudecki, A. P., King, S. M., Bowie, D. J., & Gray, S. L. (2014). PACAP is essential for the adaptive thermogenic response of brown adipose tissue to cold exposure. *Journal of Endocrinology*, *222*(3), 327–339. https://doi.org/10.1530/JOE-14-0316

Dickson, L., & Finlayson, K. (2009, March). VPAC and PAC receptors: From ligands to function. *Pharmacology and Therapeutics*. Pharmacol Ther. https://doi.org/10.1016/j.pharmthera.2008.11.006

Farrell Jr, R. E. (2005). *RNA Methodologies* (3rd ed.). Retrieved from https://www-sciencedirect-com.ezproxy.library.ubc.ca/book/9780122496967/rna-methodologies

Fenzl, A., & Kiefer, F. W. (2014). Brown adipose tissue and thermogenesis. *Horm Mol Biol Clin Invest*, *19*(1), 25–37. https://doi.org/10.1515/hmbci-2014-0022

Filatov, E., Short, L. I., Forster, M. A. M., Harris, S. S., Schien, E. N., Hughes, M. C., … Gray, S. L. (2020). Contribution of thermogenic mechanisms by male and female mice lacking Pituitary Adenylate Cyclase-Activating Polypeptide in response to cold acclimation. *American Journal of Physiology-Endocrinology and Metabolism*. https://doi.org/10.1152/ajpendo.00205.2020

Flotte, T., & CARTER, B. (1999). 6 Adeno-Associated Viral Vectors.

Furness, S. G. B., Wootten, D., Christopoulos, A., & Sexton, P. M. (2012, May). Consequences of splice variation on Secretin family G protein-coupled receptor function. *British Journal of Pharmacology*. Wiley-Blackwell. https://doi.org/10.1111/j.1476-5381.2011.01571.x

Gabriela Pop, M., Crivii, C., & Opincariu, I. (2018). Anatomy and Function of the Hypothalamus. In *Hypothalamus in Health and Diseases*. IntechOpen. https://doi.org/10.5772/intechopen.80728

Gall, J. G., & Pardue, M. L. (1969). Formation and detection of RNA-DNA hybrid molecules in cytological preparations. *Proceedings of the National Academy of Sciences of the United States of America*, *63*(2), 378–383. https://doi.org/10.1073/pnas.63.2.378

Gerard J, N. (2013). The Basics of In Situ Hybridization. In *In Situ Molecular Pathology and Co-Expression Analyses* (pp. 81–131). Elsevier. https://doi.org/10.1016/b978-0-12-415944-0.00004-8

Gray, S. L., & Cline, D. L. (2019). PACAP: Regulator of the stress response. In *Stress: Physiology, Biochemistry, and Pathology Handbook of Stress Series, Volume 3* (pp. 279–291). Elsevier. https://doi.org/10.1016/B978-0-12-813146-6.00021-7

Gray, S. L., Cummings, K. J., Jirik, F. R., & Sherwood, N. M. (2001). Targeted Disruption of the Pituitary Adenylate Cyclase-Activating Polypeptide Gene Results in Early Postnatal Death Associated with Dysfunction of Lipid and Carbohydrate Metabolism. *Molecular Endocrinology*, *15*(10), 1739–1747. https://doi.org/10.1210/mend.15.10.0705

Gray, S. L., Yamaguchi, N., Vencová, P., & Sherwood, N. M. (2002). Temperature-Sensitive Phenotype in Mice Lacking Pituitary Adenylate Cyclase-Activating Polypeptide. *Endocrinology*, *143*(10), 3946–3954. https://doi.org/10.1210/en.2002-220401

Grigorev, I. ., & Korzhevskii, D. . (2018). Current Technologies for Fixation of Biological Material for Immunohistochemical Analysis (Review), *10*(2). https://doi.org/10.17691/stm2018.10.2.19

Hannibal, J., Mikkelsen, J. D., Clausen, H., Holst, J. J., Wulff, B. S., & Fahrenkrug, J. (1995). Gene expression of pituitary adenylate cyclase activating polypeptide (PACAP) in the rat hypothalamus. *Regulatory Peptides*, *55*(2), 133–148. https://doi.org/10.1016/0167-0115(94)00099-J

Hannibal, Jens. (2002). Pituitary adenylate cyclase-activating peptide in the rat central nervous system: an immunohistochemical and in situ hybridization study. *The Journal of Comparative Neurology*, *453*(4), 389–417. https://doi.org/10.1002/cne.10418

Harmar, A. J., Fahrenkrug, J., Gozes, I., Laburthe, M., May, V., Pisegna, J. R., … Said, S. I. (2012, May). Pharmacology and functions of receptors for vasoactive intestinal peptide and pituitary adenylate cyclase-activating polypeptide: IUPHAR Review 1. *British Journal of Pharmacology*. Wiley-Blackwell. https://doi.org/10.1111/j.1476-5381.2012.01871.x

Hashimoto, Hitoshi; Nogi, Hiroyuki; Mori, Kensaku; Ohishi, Hitoshi; Shigemoto, Yamamoto, Kyohei; Matsuda, Toshio; Mizuno, Noboru; Nagata, Shigekazu; Baba, A. (1996). Distribution of the mRNA for a Pituitary Adenylate Cyclase-Activating Polypeptide Receptor in the Rat Brain: An in Situ Hybridization Study. *The Journal of Comparative Neurology*, *371*(4). https://doi.org/10.1002/(SICI)1096-9861(19960805)371:4<567::AID-CNE6>3.0.CO;2-2

Hawke, Z., Ivanov, T. R., Bechtold, D. A., Dhillon, H., Lowell, B. B., & Luckman, S. M. (2009).

PACAP neurons in the hypothalamic ventromedial nucleus are targets of central leptin signaling. *Journal of Neuroscience*, *29*(47), 14828–14835. https://doi.org/10.1523/JNEUROSCI.1526-09.2009

Hirabayashi, T., Nakamachi, T., & Shioda, S. (2018). Discovery of PACAP and its receptors in the brain. *The Journal of Headache and Pain*, *19*(1), 28. https://doi.org/10.1186/s10194-018-0855-1

Hraton, G. M., Wagenvoord, R. J., Kemp, A., & Nicholls, D. G. (1978). Brown-Adipose-Tissue Mitochondria: Photoaffinity Labelling of the Regulatory Site of Energy Dissipation. *European Journal of Biochemistry*, *82*(2), 515–521. https://doi.org/10.1111/j.1432-1033.1978.tb12045.x

Hu, S., Wang, L., Yang, D., Li, L., Togo, J., Wu, Y., … Speakman, J. R. (2018). Dietary Fat, but Not Protein or Carbohydrate, Regulates Energy Intake and Causes Adiposity in Mice. *Cell Metabolism*, *28*(3), 415-431.e4. https://doi.org/10.1016/j.cmet.2018.06.010

Hybridization Conditions and Melting Temperature – Lablogatory. (n.d.). Retrieved November 2, 2020, from https://labmedicineblog.com/2016/06/06/hybridization-conditions-and-melting-temperature/

Ikeda, Y., Luo, X., Abbud, R., Nilson, J. H., & Parker, K. L. (1995a). *The Nuclear Receptor Steroidogenic Factor 1 Is Essential for the Formation of the Ventromedial Hypothalamic Nucleus*. Retrieved from https://academic.oup.com/mend/article/9/4/478/2715148

Ikeda, Y., Luo, X., Abbud, R., Nilson, J. H., & Parker, K. L. (1995b). *The Nuclear Receptor Steroidogenic Factor 1 Is Essential for the Formation of the Ventromedial Hypothalamic Nucleus*. Retrieved from https://academic.oup.com/mend/article-abstract/9/4/478/2715148

Klok, M. D., Jakobsdottir, S., & Drent, M. L. (2007, January 1). The role of leptin and ghrelin in the regulation of food intake and body weight in humans: A review. *Obesity Reviews*. John Wiley & Sons, Ltd. https://doi.org/10.1111/j.1467-789X.2006.00270.x

Kumar, A. (2009). In situ Hybridization, *44*(1), 30–34. Retrieved from www.ijabpt.com

Lander, E. S., Linton, L. M., Birren, B., Nusbaum, C., Zody, M. C., Baldwin, J., … Morgan, M. J. (2001). Initial sequencing and analysis of the human genome. *Nature*, *409*(6822), 860–921. https://doi.org/10.1038/35057062

Lee, P., Swarbrick, M. M., & Ho, K. K. Y. (2013). Brown Adipose Tissue in Adult Humans: A Metabolic Renaissance. *Endocrine Reviews*, *34*(3), 413–438. https://doi.org/10.1210/er.2012-1081

Lewis, M. E., Sherman, T. G., & Watson, S. J. (1985). In situ hybridization histochemistry with synthetic oligonucleotides: Strategies and methods. *Peptides*, *6*, 75–87. https://doi.org/10.1016/0196-9781(85)90138-X

Lowell, B. B., & Spiegelman, B. M. (2000a). Towards a molecular understanding of adaptive thermogenesis. *Nature*, *404*(6778), 652–660. https://doi.org/10.1038/35007527

Lowell, B. B., & Spiegelman, B. M. (2000b). Towards a molecular understanding of adaptive thermogenesis. *Nature*, *404*(6778), 652–660. https://doi.org/10.1038/35007527

Lukashchuk, V., Lewis, K. E., Coldicott, I., Grierson, A. J., & Azzouz, M. (2016). AAV9-mediated central nervous system–targeted gene delivery via cisterna magna route in mice. *Molecular Therapy - Methods and Clinical Development*, *3*, 15055. https://doi.org/10.1038/mtm.2015.55

Luxol® fast blue solution 1% | Sigma-Aldrich. (n.d.). Retrieved February 4, 2021, from https://www.sigmaaldrich.com/catalog/product/sigma/l0294?lang=en&region=CA&gclid=EAIaIQobChMI8afKkuzR7gIVtSCtBh313QGuEAAYAiAAEgKhYPD_BwE

Majdic, G., Young, M., Gomez-Sanchez, E., Anderson, P., Szczepaniak, L. S., Dobbins, R. L., … Parker, K. L. (2002). Knockout Mice Lacking Steroidogenic Factor 1 Are a Novel Genetic Model of Hypothalamic Obesity. *Endocrinology*, *143*(2), 607–614. https://doi.org/10.1210/endo.143.2.8652

Masuo, Y., Noguchi, J., Morita, S., & Matsumoto, Y. (1995). Effects of intracerebroventricular administration of pituitary adenylate cyclase-activating polypeptide (PACAP) on the motor activity and reserpine-induced hypothermia in murines. *Brain Research*, *700*(1–2), 219–226. https://doi.org/10.1016/0006-8993(95)00978-Y

McMillan, T. (2017). *The role of pituitary adenylate cyclase-activating polypeptide (PACAP) in the ventromedial nucleus and its association with the melanocortin system in regulating adaptive thermogenesis*. University of Northern British Columbia. Retrieved from https://unbc.arcabc.ca/islandora/object/unbc%3A54746/

McRory, J. E., Krueckl, S. L., & Sherwood, N. M. (2000). The Origin and Function of the Pituitary Adenylate Cyclase-Activating Polypeptide (PACAP)/Glucagon Superfamily*. *Endocrine Reviews*, *21*(6), 619–670. https://doi.org/10.1210/edrv.21.6.0414

Min, L., Shuto, Y., Somogyvári-Vigh, A., & Arimura, A. (1999). Prohormone convertases 1 and 2 process ProPACAP and generate matured, bioactive PACAP38 and PACAP27 in transfected rat pituitary GH4C1 cells. *Neuroendocrinology*, *69*(3), 217–226. https://doi.org/10.1159/000054422

Miyata, A., Arimura, A., Dahl, R. R., Minamino, N., Uehara, A., Jiang, L., … Coy, D. H. (1989). Isolation of a novel 38 residue-hypothalamic polypeptide which stimulates adenylate cyclase in pituitary cells. *Biochemical and Biophysical Research Communications*, *164*(1), 567–574. https://doi.org/10.1016/0006-291X(89)91757-9

Miyata, A., Jiang, L., Dahl, R. D., Kitada, C., Kubo, K., Fujino, M., … Arimura, A. (1990). Isolation of a neuropeptide corresponding to the N-terminal 27 residues of the pituitary adenylate cyclase activating polypeptide with 38 residues (PACAP38). *Biochemical and Biophysical Research Communications*, *170*(2), 643–648. https://doi.org/10.1016/0006-291X(90)92140-U

Monda, M., Sullo, A., & De Luca, B. (1997). Lesions of the ventromedial hypothalamus reduce postingestional thermogenesis. *Physiology and Behavior*, *61*(5), 687–691. https://doi.org/10.1016/S0031-9384(96)00520-3

Mouse Brain Atlas. (n.d.). Retrieved January 27, 2021, from http://labs.gaidi.ca/mouse-brain-atlas/?ml=2.5&ap=-.4&dv=3.2

Murlidharan, G., Samulski, R. J., & Asokan, A. (2014, September 19). Biology of adeno-associated viral vectors in the central nervous system. *Frontiers in Molecular Neuroscience*. Frontiers Research Foundation. https://doi.org/10.3389/fnmol.2014.00076

Naso, M. F., Tomkowicz, B., Perry, W. L., & Strohl, W. R. (2017, August 1). Adeno-Associated Virus (AAV) as a Vector for Gene Therapy. *BioDrugs*. Springer International Publishing. https://doi.org/10.1007/s40259-017-0234-5

Nguyen, T. T., Kambe, Y., Kurihara, T., Nakamachi, T., Shintani, N., Hashimoto, H., & Miyata, A. (2020). Pituitary Adenylate Cyclase-Activating Polypeptide in the Ventromedial Hypothalamus Is Responsible for Food Intake Behavior by Modulating the Expression of Agouti-Related Peptide in Mice. https://doi.org/10.1007/s12035-019-01864-7

Nishizawa, Y., & Bray, G. A. (1978). Ventromedial hypothalamic lesions and the mobilization of fatty acids. *The Journal of Clinical Investigation*, *61*(3), 714–721. https://doi.org/10.1172/JCI108984

NR5A1 Antibody (434200). (n.d.). Retrieved January 29, 2021, from https://www.thermofisher.com/antibody/product/NR5A1-Antibody-clone-N1665-Monoclonal/434200

Obesity and overweight. (n.d.). Retrieved April 26, 2020, from https://www.who.int/news-room/fact-sheets/detail/obesity-and-overweight

Okazaki, K., Itoh, Y., Ogi, K., Ohkubo, S., & Onda, H. (1995). Characterization of murine PACAP mRNA. *Peptides*, *16*(7), 1295–1299. https://doi.org/10.1016/0196-9781(95)02018-R

Oride, A., Kanasaki, H., & Kyo, S. (2018). Role of pituitary adenylate cyclase-activating polypeptide in modulating hypothalamic-pituitary system. *Reproductive Medicine and Biology*, *17*(3), 234–241. https://doi.org/10.1002/rmb2.12094

Overweight and obese adults, 2018. (2019). Retrieved August 14, 2020, from www.statcan.gc.ca

Overweight and obese adults (self-reported), 2014. (n.d.). Retrieved August 14, 2020, from https://www150.statcan.gc.ca/n1/pub/82-625-x/2015001/article/14185-eng.htm

Pataki, I., Adamik, Á., Jászberényi, M., MácSai, M., & Telegdy, G. (2000). Pituitary adenylate cyclase-activating polypeptide induces hyperthermia in the rat. *Neuropharmacology*, *39*(7), 1303–1308. https://doi.org/10.1016/S0028-3908(99)00209-9

Pelleymounter, M. A., Cullen, M. J., Baker, M. B., Hecht, R., Winters, D., Boone, T., & Collins, F. (1995). Effects of the obese gene product on body weight regulation in ob/ob mice. *Science*, *269*(5223), 540–543. https://doi.org/10.1126/science.7624776

Perkins, M. N., Rothwell, N. J., Stock, M. J., & Stone, T. W. (1981). Activation of brown adipose tissue thermogenesis by the ventromedial hypothalamus. *Nature*, *289*(5796), 401–402. https://doi.org/10.1038/289401a0

Protein BLAST: Align two or more sequences using BLAST. (n.d.). Retrieved January 28, 2021, from https://blast.ncbi.nlm.nih.gov/BlastAlign.cgi

Qian, X., & Lloyd, R. V. (2002). 3 Target and signal amplification to increase the sensitivity of in situ hybridization. In *Handbook of Immunohistochemistry and in Situ Hybridization of Human Carcinomas* (Vol. 1, pp. 27–42). Elsevier Inc. https://doi.org/10.1016/S1874-5784(04)80013-8

Radinsky, R., Bucana, C. D., Ellis, L. M., Sanchez, R., Cleary, K. R., Brigati, D. J., & Fidler, I. J. (1993). A Rapid Colorimetric in Situ Messenger RNA Hybridization Technique for Analysis of Epidermal Growth Factor Receptor in Paraffin-embedded Surgical Specimens of Human Colon Carcinomas. *Cancer Research*, *53*(5).

Resch, J. M., Boisvert, J. P., Hourigan, A. E., Mueller, C. R., Yi, S. S., & Choi, S. (2011). Stimulation of the hypothalamic ventromedial nuclei by pituitary adenylate cyclase-activating polypeptide induces hypophagia and thermogenesis. *American Journal of Physiology. Regulatory, Integrative and Comparative Physiology*, *301*(6), R1625-34. https://doi.org/10.1152/ajpregu.00334.2011

Resch, J. M., Maunze, B., Gerhardt, A. K., Magnuson, S. K., Phillips, K. A., & Choi, S. (2013). Intrahypothalamic pituitary adenylate cyclase-activating polypeptide regulates energy balance via site-specific actions on feeding and metabolism. *American Journal of Physiology - Endocrinology and Metabolism*, *305*(12), E1452. https://doi.org/10.1152/ajpendo.00293.2013

Robert E.FArrell, J. (2010). RNA methodologies A Laboratory Guide for Isolation and Charecterization. In *RNA methodologies A Laboratory Guide for Isolation and Charecterization* (4th ed., pp. 264–280). Elsevier.

Samulski, R. J., & Muzyczka, N. (2014). AAV-mediated gene therapy for research and therapeutic purposes. *Annual Review of Virology*, *1*(1), 427–451. https://doi.org/10.1146/annurev-virology-031413-085355

Scarpace, P. J., & Matheny, M. (1998). Leptin induction of UCP1 gene expression is dependent on sympathetic innervation. *American Journal of Physiology - Endocrinology and Metabolism*, *275*(2 38-2). https://doi.org/10.1152/ajpendo.1998.275.2.e259

Schaeren-Wiemers, N., & Gerfin-Moser, A. (1994). *A single protocol to detect transcripts of various types and expression levels in neural tissue and cultured cells: in situ hybridization using digoxigenin-labelled cRNA probes*. *Histochemistry* (Vol. 100).

Segal, J. P., Stallings, N. R., Lee, C. E., Zhao, L., Socci, N., Viale, A., … Friedman, J. M. (2005). Use of laser-capture microdissection for the identification of marker genes for the ventromedial hypothalamic nucleus. *The Journal of Neuroscience : The Official Journal of the Society for Neuroscience*, *25*(16), 4181–4188. https://doi.org/10.1523/JNEUROSCI.0158-05.2005

SIGMA-ALDRICH. (2008). *DIG Application Manual for Nonradioactive In Situ Hybridization* (4th ed.). SIGMA-ALDRICH. Retrieved from https://www.sigmaaldrich.com/content/dam/sigma-aldrich/docs/Roche/General_Information/1/dig-application-manual-for-nonradioactive-in-situ-hybridisation-iris.pdf

Stahl, W. L., Eakin, T. J., & Baskin, D. G. (1993). *The Journal of Histochemistry and*

Cytochemistry Selection of Oligonucleotide Probes for Detection of mRNA Isoformd (Vol. 41). Retrieved from https://journals.sagepub.com/doi/pdf/10.1177/41.12.8245420

Tanida, M., Hayata, A., Shintani, N., Yamamoto, N., Kurata, Y., Shibamoto, T., … Hashimoto, H. (2013). Central PACAP mediates the sympathetic effects of leptin in a tissue-specific manner. *Neuroscience*, *238*, 297–304. https://doi.org/10.1016/j.neuroscience.2013.02.016

The Pros and Cons of FFPE vs Frozen Tissue Samples. (n.d.). Retrieved April 10, 2019, from https://www.geneticistinc.com/blog/the-pros-and-cons-of-ffpe-vs-frozen-tissue-samples

Trayhurn, P., & James, W. P. T. (1978). Thermoregulation and non-shivering thermogenesis in the genetically obese (ob/ob) mouse. *Pflügers Archiv European Journal of Physiology*, *373*(2), 189–193. https://doi.org/10.1007/BF00584859

Van Gaal, L. F., Mertens, I. L., & De Block, C. E. (2006, December 14). Mechanisms linking obesity with cardiovascular disease. *Nature*. Nature Publishing Group. https://doi.org/10.1038/nature05487

Vázquez-Vela, M. E. F., Torres, N., & Tovar, A. R. (2008, November). White Adipose Tissue as Endocrine Organ and Its Role in Obesity. *Archives of Medical Research*. Arch Med Res. https://doi.org/10.1016/j.arcmed.2008.09.005

Virtue, S., & Vidal-Puig, A. (2013). Assessment of brown adipose tissue function. *Frontiers in Physiology*, *4*, 128. https://doi.org/10.3389/fphys.2013.00128

Wang, D., Tai, P. W. L., & Gao, G. (2019, May 1). Adeno-associated virus vector as a platform for gene therapy delivery. *Nature Reviews Drug Discovery*. Nature Publishing Group. https://doi.org/10.1038/s41573-019-0012-9

Wilson, M. J., Jeyasuria, P., Parker, K. L., & Koopman, P. (2005). The transcription factors steroidogenic factor-1 and SOX9 regulate expression of Vanin-1 during mouse testis development. *Journal of Biological Chemistry*, *280*(7), 5917–5923. https://doi.org/10.1074/jbc.M412806200

Yokoyama, C., Komatsu, T., Ogawa, H., Morohashi, K., Azuma, M., & Tachibana, T. (2009). Generation of rat monoclonal antibodies specific for Ad4BP/SF-1. *Hybridoma*, *28*(2), 113–120. Retrieved from https://go-gale-com.ezproxy.library.ubc.ca/ps/i.do?p=HRCA&sw=w&issn=15540014&v=2.1&it=r&id=GALE%7CA205568310&sid=googleScholar&linkaccess=fulltext

Young, A. P., Jackson, D. J., & Wyeth, R. C. (2020). A technical review and guide to RNA fluorescence in situ hybridization. *PeerJ*, *8*. https://doi.org/10.7717/peerj.8806

Zhu, L., Tamvakopoulos, C., Xie, D., Dragovic, J., Shen, X., Fenyk-Melody, J. E., … Roy, R. S. (2003). The role of dipeptidyl peptidase IV in the cleavage of glucagon family peptides: In vivo metabolism of pituitary adenylate cyclase-activating polypeptide-(1-38). *Journal of Biological Chemistry*, *278*(25), 22418–22423. https://doi.org/10.1074/jbc.M212355200

Zimmerman, S. G., Peters, N. C., Altaras, A. E., & Berg, C. A. (2013). Optimized RNA ISH, RNA FISH and protein-RNA double labeling (IF/FISH) in Drosophila ovaries. *Nature Protocols*, *8*(11), 2158–2179. https://doi.org/10.1038/nprot.2013.136